Running-in control and creation of super low friction interface in water for tribological system using double network gel

Laura Jay

N°d'ordre NNT : 2021LYSEC12

THESE de DOCTORAT DE L'UNIVERSITE DE LYON
opérée conjointement
au sein de l'Ecole centrale de Lyon et de Tohoku University

Ecole Doctorale N° 488
Sciences Ingénierie Santé

Spécialité de doctorat :
Mécanique et Ingénierie

Soutenue publiquement le 31/03/2021, par :
Laura Jay

CONTROLE DU PROCESSUS PERMETTANT LA CREATION D'UNE INTERFACE DE FROTTEMENT EXTREMEMENT FAIBLE POUR UN SYSTEME TRIBOLOGIQUE UTILISANT UN DN GEL

Devant le jury composé de :

Richard, Caroline	Professeure	Université de Tours	Présidente
Chabrand, Patrick	Professeur	Aix Marseille Université	Rapporteur
Bou-said, Benyebka	Professeur	INSA Lyon	Rapporteur
Vico-Pouget, Laurence	Professeure	Université Jean Monnet	Examinatrice
Donnet, Christophe	Professeur	Université Jean Monnet	Examinateur

Zahouani, Hassan	HDR/Pr	Ecole Centrale de Lyon	Directeur de thèse
Adachi, Koshi	HDR/Pr	Tohoku University	Co-directeur de thèse
Kapsa, Philippe	HDR/Pr	Ecole Centrale de Lyon	Co-encadrant de thèse

During this Ph.D. period, the following scientific contents were produced:

- **Journal paper**

Laura Jay, Koki Kanda, Philippe Kapsa, Hassan Zahouani and Koshi Adachi, Effect of double network hydrogel film thickness on the run-in tribological properties of a friction system using DN gel, Wear of Materials, published on January 2021

- **Poster and oral presentation**

Laura Jay, Koki Kanda, Philippe Kapsa, Hassan Zahouani and Koshi Adachi, *Wear evaluation of a soft material for an artificial cartilage application: a Double Network hydrogel*, Rencontres du LTDS, Chateau de Goutelas, France, 10/2017

Laura Jay, Francis Canon, Carole Tournier, Roberto Vargiolu and Hassan Zahouani, *Astringency comprehension via mechanical and tribological properties of the tongue: an ex vivo study*, 4th International Conference of BioTribology, Montreal, Canada, 26-29/09/2018

Laura Jay, Koki Kanda, Philippe Kapsa, Hassan Zahouani and Koshi Adachi, *Multi-scale surface texturing and effect on the tribological behavior for artificial cartilage*, ELyT workshop, Satilleux, France, 6-8/03/2018

Laura Jay, Koki Kanda, Philippe Kapsa, Hassan Zahouani and Koshi Adachi, *Tribological characterization of a new soft matter: Double Network hydrogel (DN gel)*, 5th International Conference of Biotribology, Online, 26-28/04/2021

Laura Jay, Koki Kanda, Philippe Kapsa, Hassan Zahouani and Koshi Adachi, *Control of the tribological properties by thickness change of a Double Network hydrogel (DN gel)*, 23rd International Conference on Wear of Materials, Online, 25-29/04/2021

Abstract

Over the past 20 years, hydrogels have been widely studied. Hydrogel has a large range of application due to its different properties and capacities compared to conventional hard materials, such as metals or ceramics. Hydrogels, thanks to their high water content (almost 90%), have unique reservoirs or absorbent capacities and wettability. However, their mechanical resistance has been lacking. Recently a new generation of hydrogels is making them much tougher. This technology consists of two interpenetrating polymers networks. It is called double network (DN gel). This double network realizes great shear, compressive and tensile stress resistance compared to conventional single network hydrogel. Then, this material is expected to fit to more various applications. Thus far, studies focused on the mechanical properties of DN gel, however, depending on the different applications, tribological properties of this material must be investigated. Then, this Ph.D. work investigates the potential of DN gel as a covering film for a low friction system application. The DN gel and SiC friction interface is understood and the cells support capacity of DN gel is also clarified.

The first chapter brings introduction about hydrogels by divided two parts. The first one is about classical mechanical application, especially the behavior of a soft material sliding on a hard material. The second part is a state of the art of cartilage diseases and actual solutions, how to get inspired from the cartilage structure and how the DN gel can be a solution to recover damage at human natural cartilage.

The second chapter, introduces the fundamental mechanical properties of the DN gel obtained by indentation tests. Next, it focused on the basics DN gel friction properties and the purpose was to find out the ideal configuration to use DN gel in a tribological system. By using a ball-on-disc rotational tribometer, three configurations were tested using Silicon Carbide (SiC) as hard material counter surface. Configuration are the following: migrating contact (SiC as a ball against DN gel disc); gemini contact (DN gel film covering SiC ball against DN gel disc); and stationary contact (DN gel film covering SiC ball). Results shows the ability of DN gel film as a material to create a super low friction interface ($\mu < 0.01$) through a run-in period. Thus, this run-in process during friction is found to be the key to generate super low friction.

The third chapter aims to understand the influence of DN gel film thickness on fundamental friction property and wear property in the tribological system. Three thicknesses are used: 1.5 mm, 3 mm and 6 mm thick DN gel film. Even though sliding speed and applied load are important parameters in the resulting friction coefficient, the thickness of the DN gel film also revealed to be a key property in the friction coefficient understanding. Finally, a positive effect is highlighted by using a thick (6 mm) and a thin (1.5 mm) thick DN gel. Although both DN gel film result in low friction, process until low friction is achieved are different. In case of 6 mm thick DN gel, friction coefficient suddenly decreases from the beginning of friction test and running-in period is not seen. On the other hand, in case of 1.5 mm thick DN gel, friction coefficient shows unique running-in period twice, then super low friction coefficient (μ<0.01) is achieved. These typical friction behaviors have been classified into three different friction modes: stable is friction mode 1, suddenly decreasing is friction mode 2 and double decreasing is friction mode 3.

The fourth chapter focuses the investigations on the fundamental wear property. In order to allow detailed observation of DN gel surface in SEM, nano-suit and t-butanol were employed. As a result, three typical wear types were determined. This damage characteristic has been successfully linked with the previously determined friction mode. The wear scar after a friction mode 1 is severe and presents scale like shape, the wear after friction mode 2 is barely detectable traduced by only a few linear scar. Finally, the wear after friction mode 3 is atypical and has linear scar along the sliding direction.

As a summary of the previous three chapters, the fifth chapter, brings an explanation to the mechanisms of friction. An *in-situ* observation technic using a glass plate and a camera clarifies the different friction mechanisms in friction modes. Especially, in case of friction mode 3 where super low friction coefficient occurs, water is absorbed into internal damaged layer of DN gel surface gradually, thus thin water film is formed and super low friction is realized due to unique damage property of DN gel. Indeed, from previous study a tensile stress on the DN gel implies a density change due to sacrificial bonds principle. Finally, it explained the unique double decreasing friction coefficient.

The sixth chapter, is split in two parts: the first one resulting from previous findings. It was understood that a controlled damage layer on DN gel is benefic to change its structures and thus improve the friction properties. In order to reproduce it a pre-texture was applied on DN gel. Finally for a same DN gel film thickness, the textured DN gel generates super low friction coefficient and lowers range of friction coefficient; the second part emphasized the similar properties of DN gel and cartilage. Also, the quality of cartilage cells growth was improved in

the purpose to use DN gel as a support for cartilage self-regeneration. This enhancement was possible by managing its elastic modulus and its surface texture.

In the final chapter, general conclusions based on summary of previous chapters are stated.

Flow chart

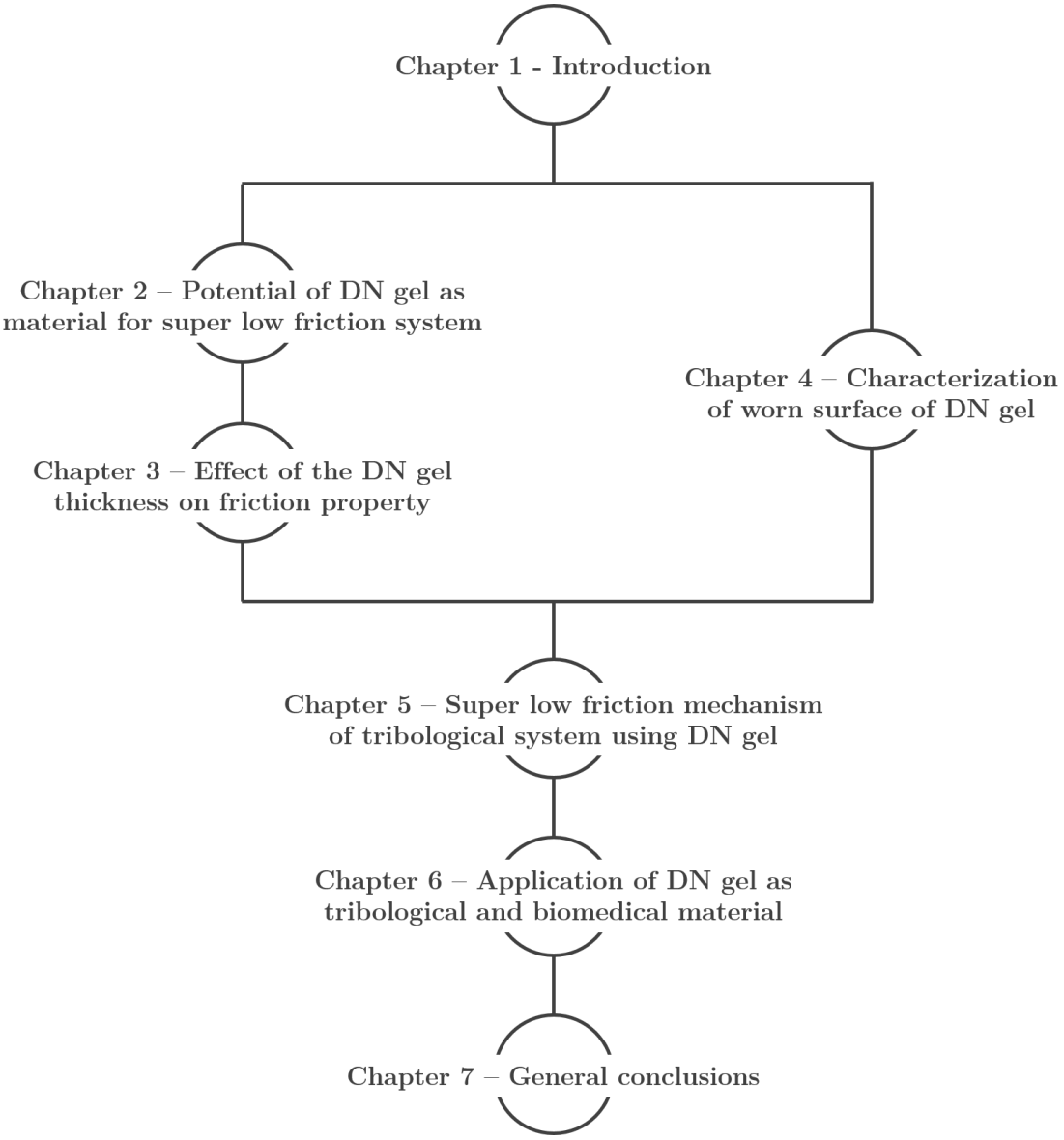
Chapter 1 - Introduction
Chapter 2 – Potential of DN gel as material for super low friction system
Chapter 3 – Effect of the DN gel thickness on friction property
Chapter 4 – Characterization of worn surface of DN gel
Chapter 5 – Super low friction mechanism of tribological system using DN gel
Chapter 6 – Application of DN gel as tribological and biomedical material
Chapter 7 – General conclusions

Table of contents

Figure list

Table list

Symbol list

α-keto

2-Oxoglutaric acid (α-ketoglutaric acid)

Co-Cr

Cobalt-Chromium

HA

Hydroxyapatite

MBAA

N,N'- Methylenebisacrylamide

PAAm

Poly-Acrylamide

PAMPS

Poly2-Acrylamido-2-Methyl-1-PropaneSulfonic acid

PDMAAm

Poly N,N-Dimethylacrylamide

PE

Polyethylene

PEEK

Polyetheretherketone

PEG

Polyethyleneglycol

pHEMA

Polyhydroxyethylmethacrylate

PMMA

Polymethylmethacrylate

pNIPAAm

Poly N-Isopropylacrylamide

PTFE

Polytetrafluroethylene

PVA

Polyvinyl Alcohol

SiC

Silicon Carbide

UHMWPE

Ultra-High Molecular Weight Polyethylene

Chapter 1 – Introduction

1.1. Objectives

The double network hydrogel (DN gel) which mainly consists of Poly2-Acrylamido-2-Methyl-1-PropaneSulfonic acid (PAMPS) and Poly N,N-Dimethylacrylamide (PDMAAm) is a new and promising material. The purpose of this study is to highlight its fundamental friction and wear properties in order to consider potential of application. Different aspects from general mechanical properties of this material to its fundamental wear property have been studied. Also, its behavior in interaction with human cells must be clarified because this material seems promising for bio applications, in that way experiments are performed on the DN gel in order to anticipate most of the needs for these bio applications. Among bio application, the cartilage replacement is one of the most promising way to use this new DN gel.

1.2. Introduction on hydrogels

1.2.1. Conventional hydrogel

1.2.1.1. Generality about structure and polymerization

Hydrogel are, generally, defined as a water-swollen “hydro”, and cross-linked polymeric networks produced by the reaction of monomers “gel” [1]. All types of hydrogel are made of a polymer network highly hydrophilic. This non common polymer has polymeric chains that can be connected in two different ways to create either physical gel or chemical gel. These chain connections can be reversible (Van der Waals bounds) or irreversible (covalent bound). Then the type of hydrogel can be identified by their structure or their composition. The polymer network always consists of a monomer, a cross linker, and an initiator. The synthesis method, the type (natural or synthetic), the properties (pH or thermo-responsive) are groups to classify the different hydrogels.

1.2.1.1.1. Natural or synthetic hydrogels

A natural network include natural proteins and polysaccharides [2]. Among proteins are hydrogels made of hyaluronic acid, collagen, gelatin, or fibrin. Among polysaccharides they consist of chitosan, hyaluronan, agarose or alginate. The networks polymers can also be synthetics, for instance, PVA, pHEMA [3], pNIPAAm [4] or PEG [5]. There are also combinations of natural and synthetic polymers, for drug delivery [6] or for cartilage regeneration by joining alginate and hyaluronic acid [7]. For now, most of the polymers used are synthetics because they are stiffer than natural ones and have a better wear resistance. The advantage of natural hydrogel type is its better biocompatibility.

1.2.1.1.2. Structure of hydrogels

First generation, around 1960s, and first use in the biomedical field [3] are Hydroxyethyl methacrylate (HEMA), polyvinyl alcohol (PVA) and polyethylene glycol (PEG) [8]. These are the most famous and used hydrogel.

Then, more recently, temperature and pH sensitive hydrogels have been created. These transformations are based on a mixture of different polymers for example PEG with PCL combining the polymer as an ABA or BAB structures. These second generation types are called copolymers [9], their advantage is higher strength without breaking their chains. I can also find multi-polymers with more than two polymers in the structure.

Another category including double networks or triple networks hydrogel is different from “co” or “multi” polymers because the networks are not only held by others, but they are completely intertwined and practically form a full-blown new polymer. They also have a higher fracture strength due to their interpenetrated and independent crosslinked networks [10].

1.2.1.2. Applications

Due to their high biocompatibility and their mechanical behavior (viscosity) close to living tissue, hydrogels are typically used for medical applications. Indeed, contact lenses [11] are the first example of hydrogels as a biomaterial. However, hydrogels are also used for drug delivery [6], wound dressing [12], hygienic solutions with SAP (Super Absorbent Polymer) or SPH (Super Porous Hydrogel)

[13] or model for surgery training [14]. Finally, the most recent and developing application is in tissue engineering field [15].

For tissue engineering applications the hydrogel is used as a matrix or a support to let the patient's repair cells grow. For now, hydrogels have a really low mechanical resistance and is suitable for the seeding of keratinocytes, fibroblasts cells to mimic natural tissues such as the skin.

Nevertheless, whatever the application, the weak mechanical resistance is its main drawback. Indeed, they are not considered for tissues such as bones, cartilage, blood vessels or muscles, because these tissues are placed in areas under heavy mechanical stress [16].

1.2.2. DN gel

1.2.2.1. Structure of DN gel

Hydrogels have been commonly used since the 70s for their biocompatibility, these biomaterials are being developed in different fields as previously mentioned. Only their mechanical resistance was often lacking. In the 90's this problem is solved by the discovery and creation of a double network which brought a high resistance to the hydrogel [8]. One of the most studied DN gels, developed in 2003 by Pr. Gong [17], consists of two interpenetrating networks PAMPS stands for poly(2-acrylamido-2-methylpropanesulfonic acid) and PAAm for poly(acrylamide). The high-strength DN gel has shown good reproducibility and excellent tensile, compressive and shear strength [9],[18],[19]. Often complementary, the networks are completed with about 80 to 90% of water. Regarding double networks hydrogels, several combinations of polymers as for co/multi polymers exists. However, scheme is same for each DN gel. First lattice as the shield (highly resistant) and the other mimics the behavior of collagen (elastic). The association can be a mixture with natural and synthetic polymers networks, for example. Finally, with its different structural parameters the DN gel is located between conventional rubbers and simple networks hydrogels in a stress-strain map (cf. Fig. 1-1) [20]. This new structure (DN gel) has same advantages than simple hydrogel with a higher tensile fracture strength. Then, by this innovative structure DN gel can reach fracture strength around 0.1 to 1 kJ/m^2 which is highly more than conventional hydrogel materials. Its elastic modulus investigated in the following chapter 2 is also not comparable with simple network hydrogel (~ 10 to 100 kPa) because it is about 50 time higher for DN gel (~ 400 to 2 000 kPa).

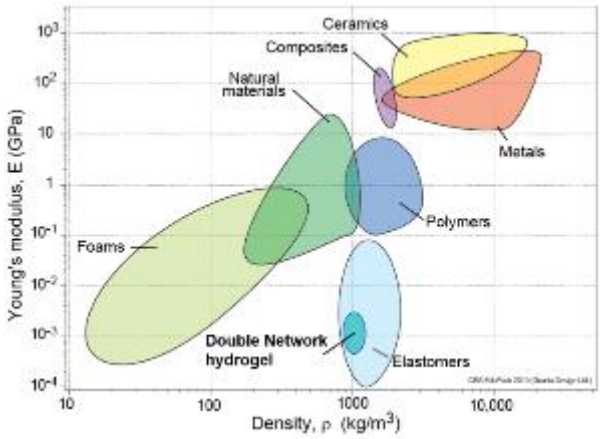

(a) DN gel on a Granta graphic representation (Chart created using CES EduPack 2019, ANSYS Granta © 2020 Granta Design)

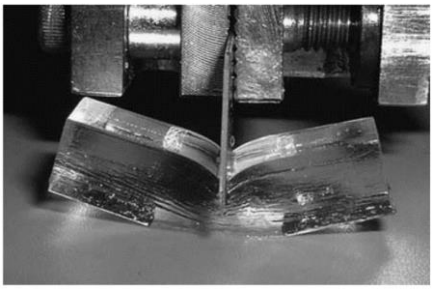

(b) Photo of tough PAMPS/PAAm DN gel against deformation

Fig. 1-1 – DN gel mechanical strength capacities exposed on this study [20] ***(a) DN gel on Ashby's representation and (b) resistance of DN gel***

The combination that has already proven its effectiveness in the cartilage replacement (direct implanted support for cartilage self-regeneration) is PAMPS, for poly(2-acrylamido-2-methyl-1-propanesulfonic acid), and PDMAAm, for poly(N,N-dimethyl acrylamide). In the following study our interest is on this combination of DN gel shortly called: PAMPS/PDMAAm.

1.2.2.2. PAMPS/PDMAAm

1.2.2.2.1. Composition

The PAMPS/PDMAAm DN gel is a structure composed of two polymers (cf. Fig. 1-2). The first network is the brittle part, the shield of the gel. It consists of the AMPS monomer (15%) and of N,N'-Methylene bis acrylamide (MBAA) as a cross linking agent (0.55%), the initiator is α-ketoglutaric acid (0.175%), and the solvent is water (83.8%). The second network is the flexible part. Interpenetrating the first network, the PDMAAm is a polymer made of the DMAAm monomer (20.7%) with the same cross linker (MBAA) (0.005%), initiator (α-keto) (0.0328%) and solvent (water) (79.23%) as the first network.

This double network « PAMPS/PDMAAm » will be widely investigated in this study. Indeed, created in 2003 in Japan, it has been the subject of studies mainly about its mechanical properties and for its bio application. As a fact,

previous studies have already proved its biocompatibility by using this gel directly implanted into the body [21],[22]. However, almost no works covered its tribological properties.

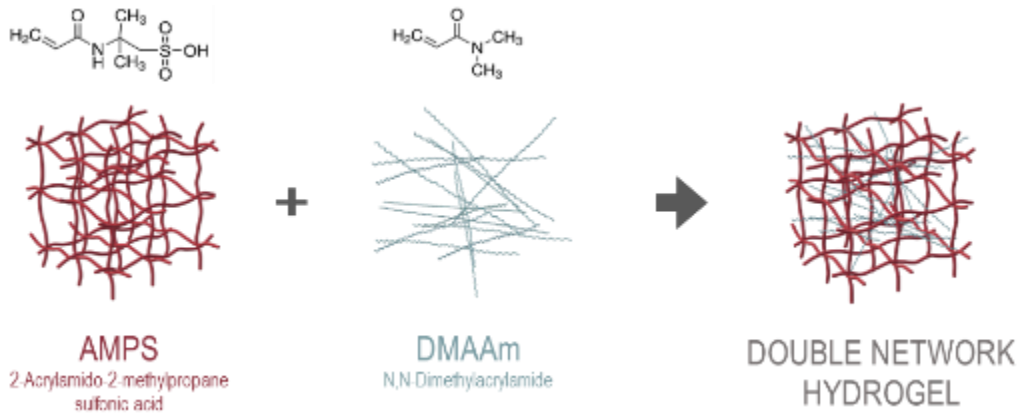

Fig. 1-2 – DN gel composition

1.2.2.2.2. Synthesis

The synthesis of the DN gel consists of three main steps, the first one is the creation and polymerization of the first mesh, the second one is creation of second and the third one is the polymerization of both intertwined networks detailed in Fig. 1-3. The total synthesis times is approximately one week. First of all, polymerization of the first polymer network (PAMPS) takes 18 hours. Then, this polymer network is immersed in a bath, consisting of the second polymer (PDMAAm), for 48 hours. To finish, the first network soaked by the second network is polymerized in order to fix the interpenetrated network, this final polymerization of the DN gel also takes 18 hours. Each step is performed at 30 degrees Celsius control environment. During each steps, plastic film or aluminum foil is necessary to prevent from a chemical reaction between the gel and external air or light. The polymerization process is performed under UV black light with a wavelength of 354 nm, the UV type used is part of UV group A. During the polymerization process, the gel was always at the exact same distance from the light in order to obtain a similar chemical structure between the different samples.

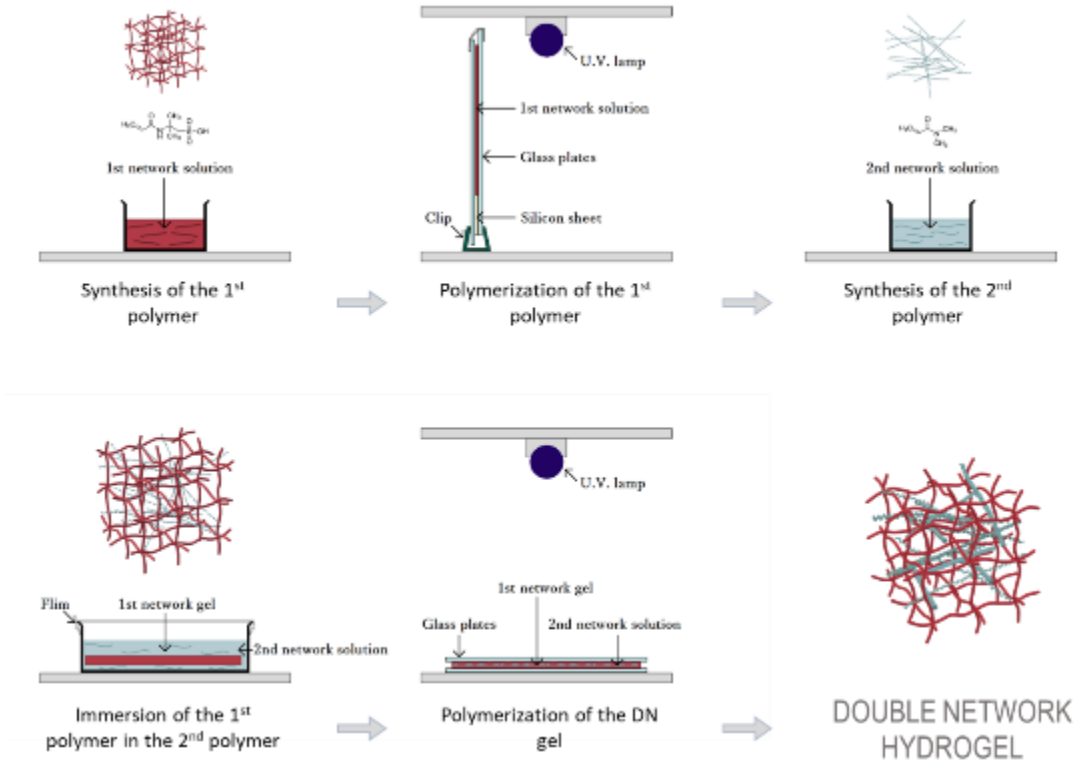

Fig. 1-3 – DN gel synthesis

1.3. Mechanical application

As this DN gel is a recent material, there is not enough data to classify it and choose its optimal application. Regarding the situation, further investigation of the DN gel is necessary. The wear and friction mechanisms are essential to understand to predict ideal parameters and to find out the best way to use it.

1.3.1. Tribology on soft matters

First, DN gel is part of the soft materials category. Soft matters are a widely studied area. However, it has a wide range of studies from which different materials categories can be differentiated, indeed, these materials can have viscosity, stiffness, or elastic modulus in the opposite range.

The most popular soft matters are polymer like: PVA, PMMA, and Polystyrene. Then, rubbers and elastomers softer material are present in seal, joint or used for tires. And finally, the hydrogels: Among them, simple or double networks, pH sensitive or not, the particularity of these lasts is their amount of water.

Whatever soft matter is a polymer, rubber or hydrogel, the three most influential parameters on the friction properties and deterioration of soft matters are: pressure, velocity of friction, temperature and visco-elastic properties of the material. About the counter hard surface, the most influent parameter is roughness. Finally, DN gel is in a halfway between flexible polymers and block copolymers (cf. Fig. 1-4).

Fig. 1-4 – Components of modern Soft matter systems arranged in a triangle [23]

The most widely used and studied flexible material for its friction and wear is rubber. Indeed, this material can be used for wheels but also for joints in mechanical torque. The most famous application remains the tire sliding on the road. These rubbers mostly slide against hard material. This is why most studies report the behavior of rubbers against hard materials such as metal or ceramic.

The first observation of rubber against hard materials was about the relationship between sliding speeds and friction coefficient. Rubbers have a

negative relationship between their friction coefficient and sliding speed at low speed and a positive relation at higher speeds [24]. Then, the scientists found a dependence of the friction coefficient with the velocity and the temperature [25]. Also, the visco-elastic property of the rubber has a major role in its behavior [26]. Finally, the roughness of the counter material during friction has an essential role. Indeed, it is the main responsible for creating scratches, therefore the amount of wear highly depends on the surface shape of the hard material [27].

About the temperature dependence, it has been reported and it is assumed that adhesion force of the highly elastic material, to the metal increases as the temperature decreases. Regarding the rubber like polymers, there is a linear dependence of decreasing temperature with the decreasing friction force. This observation can only be made at high temperature, in fact, the temperature must be higher than the glass-transition temperature [26].

Finally, the friction of soft material cannot be resumed in a conventional comportment. But it is known now that the friction coefficient of DN gel will greatly depends on the sliding speed and load. On the temperature applied during friction and on the roughness of the counter material. Also, it relies on the visco-elastic properties of DN gel.

1.3.2. Wear behavior characteristics

Usually, the rubber or polymer like material exhibits a typical behavior when it slides against a hard material. Most of the time, studies use rubber as the flat counter face and the hard material is the ball sliding on it [26], [28], [29].

Pr. Schallamach widely studied polymer and rubber materials [28]. Indeed, the shape of the damage observed on the polymer material waves-like is called Schallamach waves. Many variations of this wear have been observed since. However, this can be a general definition of the wear on polymer. Therefore, these shapes are probably the ones expected on the DN gel wear observation. Then, the propagation of the solicitation, observed on Fig. 1-5 is extremely deep due to the low elastic modulus of the material. The elastic property of the material should be considered because there is a difference in propagation depending on it.

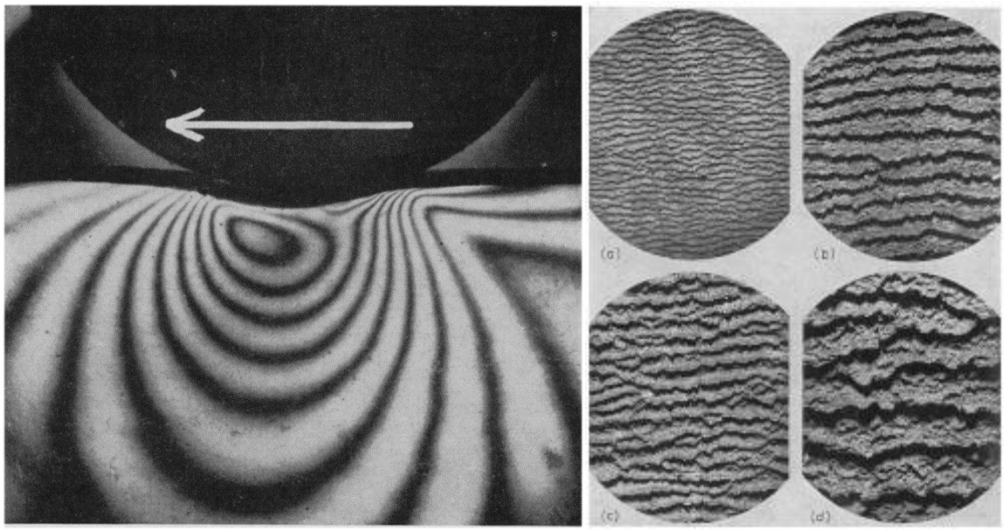

***Fig. 1-5** – Photo elastic picture of a hard ball sliding on rubber. Typical wear on polymeric materials* [28]

1.3.3. Hydrogel tribology

1.3.3.1. Simple hydrogels

The surface properties of the hydrogel have been investigating mainly for biological applications. Indeed, the hydrogel can be used for lenses [30], for drug delivery [31] or as a biological model for surgical training [32]. This material is well known for its biocompatibility but also for its low mechanical resistance. This is why it has never been envisaged to use it for various mechanical applications.

From there, the main hydrogel used in these studies is PVA for biological models, p-HEMA and PMAA for lenses. Since it is extremely difficult to quantify the wear of a soft material, most of the studies have focused on the friction properties of these hydrogels. For instance, the lenses material is highly studied for its reaction because of the rubbing with the eyelid.

These studies [33],[34] focused on simple hydrogel friction such as PVA for instance. Also, researchers used either low load or slow sliding speed. Finally, the configuration does not seem applicable for a mechanical device. In fact, these studies are favorable about the low friction coefficient of DN gel and highlight the importance in the friction of other parameter than load and sliding speed. In hydrogel friction parameter such as chemical structure (water content), visco-elasticity, and roughness of hydrogel or counter surface material properties are influent on the friction coefficient.

1.3.3.2. DN gel as a bulk

Most of the existing studies investigated the DN gel friction using DN gel as a bulk and flat material.

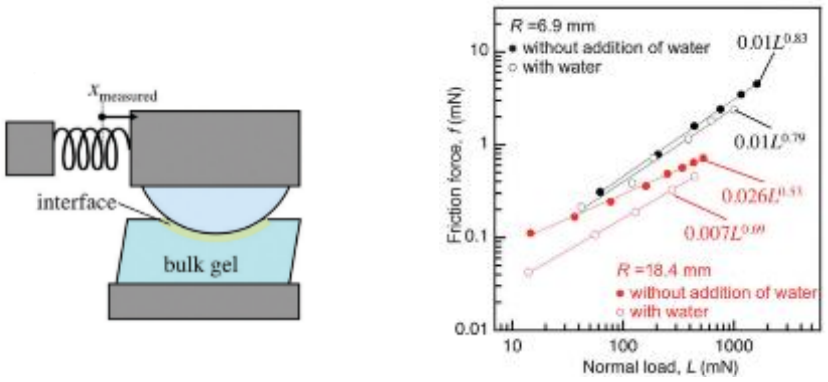

(a) Measurement of friction by resonance shear apparatus

(b) Friction force obtained by resonance shear

Fig. 1-6 – Apparatus and results from a study using resonance shear measurement to determine friction properties of DN gel [35]

For example, this study, [35] (cf. Fig. 1-6), focus on the friction obtained by DN gel using resonance shear measurements. Researchers allows to understand the influence and importance of elastic component in the hydrogel structure. However, this study as most of the others focused on the DN gel as a bulk and it is difficult to imagine application with this configuration. Moreover, normal loads are quite low and do not exceed 2 N. Another study using the DN gel PAMPS/PAAM, underline a promising low friction coefficient of this material even under high pressure [10].

1.3.3.3. Wear on DN gel

The deterioration of hydrogel has been weakly studied due to their lack of wear resistance. However, a recent study about DN gels highlighted the ability of the DN gel to resist to the friction [36]. After 50 km of sliding stress the damage depth of the DN gel PAMPS/PDMAAm was similar to the one of the UHMWPE. Thus, this DN gel is promising for its low friction and low wear.

1.4. Biological application

The PTFE is the first biopolymer used in the application of the prosthesis. Due to its high wear, it was quickly replaced by Ultra High Molecular Weight PolyEthylene (UHMWPE). The amount of the wear is even higher than expected but the particles are less dangerous for health. Then scientists developed a crosslinked UHMWPE which made this material much stronger and less wearable, it is commonly referred to as Cross Linked PolyEthylene (XLPE) [37]. Nowadays, progress is coming for news biopolymers and especially hydrogels. Indeed, among the polymeric materials, hydrogels are the most biocompatible. Indeed, these polymers networks often consists in 80 to 90% of water, the same main consistence of our body. This hydrophilic material acts like a sponge with the water and literally swell from twice to multiple times their size. Also, hydrogels present a good friction capacity, with an extremely low friction coefficient it has the potential to mimic the cartilage.

1.4.1. General introduction about cartilage

From generation to generation, cartilage issues are ubiquitous. Indeed, due to aging or intense sporting activity, the natural solution that protects the bones is highly strained. Besides, this tissue does not regenerate easily. It is, nevertheless, essential for the proper functioning of the articulation joint.

1.4.1.1. Anatomic structure

Three types of cartilage can be found in the human body: fibrous, elastic and hyaline. This last category is the cartilage located between the bones in natural joints (cf. Fig. 1-7). Also called articular cartilage, the function of this tissue is to protect the bone from friction during the articulation motion. Moreover, it enables an excellent sliding between the bones, protecting them. This part of the natural tribological triplet is sought a lot along people's life [38]. Unfortunately, it does not regenerate easily, and its wear does not become painful until bone is affected, which means it is often too late.

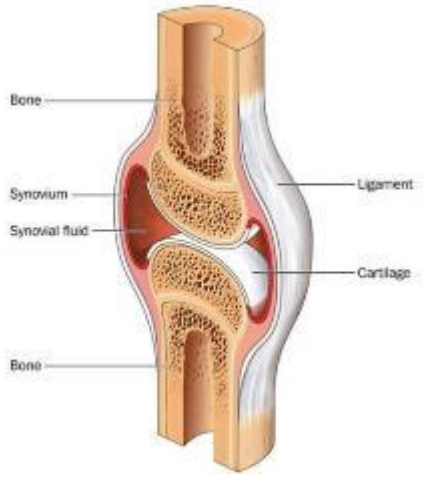

Fig. 1-7 - Hyaline cartilage scheme [39]

White and vitreous in appearance, the hyaline cartilage is constantly submerged in the synovial fluid, inside the joint capsule. This natural lubricant doubles its properties with the lubricin present locally on the surface of the cartilage. This combination offers one of the lowest friction coefficients in our body. Composed of several elements, cartilage consists of a complex multi-layer structure. This natural material has no nerves, no blood vessels and no lymphatic network [40]. It is made up of a unique type of cell: chondrocytes. The latter are supplied by synovial liquid and subchondral bone diffusion, which is why the cartilage must be sufficiently porous [41].

For the human, the total thickness of the femoral condylar cartilage (thickest cartilaginous part of the knee joint) is approximately 2 – 3 mm [42]. Cartilage is mainly composed of water, proteoglycan and type II collagen [43]. For better understanding, the cartilage can be divided into two matrices: the aqueous and the macromolecular:

1. The aqueous part of cartilage represents the liquid phase consisting of water, gas, proteins, metabolites, equilibrating cations and proteoglycans. The main division of extracellular proteoglycans present in cartilage is aggrecans (PG-H), this type consists of large proteoglycans capable of creating a supramolecular edifice with hyaluronic acid. The role of the extracellular matrix (ECM) is to transport lubricant into the joint. Furthermore, it withstands pressure and deformation.

2. The macromolecular is the rigid part mainly made up of collagen. The main component is the type II collagen. By itself, this type of collagen

represents 95% of normal cartilage collagens. However, other types of "minor" collagens have been described in cartilage (III, VI, IX, X, XI, XII and XIV), they are also present during maturation. When the matrix is mature the main network is a mixture of three types of collagens II, IX, XI (heteropolymer structure) [44],[45].

These two phases, presented above, have different evolutionary behaviors depending on the depth. Indeed, the natural cartilage can be divided into four layers, detailed later. The elements are not present in the same quantities depending on the depth, for instance the water concentration is higher on the surface (80 %) and lower deeper (65%). But considering the total volume; the amount of water represents 70 to 80%, the cells 3%, the collagens 15% (including 80% type II) and the aggrecans 9% [46]. Its closely remind the structure of the DN gel, with an 80 % of water in its composition.

1.4.1.2. Biomechanical properties

All these layers form the osteochondral unit, naturally organized to respond to the different mechanical solicitations in the joint. General properties of the cartilage are its high stress, shear resistance and its extremely low friction coefficient.

Depending on the different layers, elements are arranged in order to respond and to be useful in their role. The cartilage is then highly anisotropic [47]. The amount of water is different depending on the depth; indeed, the higher amount of water is on the gliding surface because the water affords a better lubrication locally at the surface of the cartilage. In addition to its biomechanical role, water is also involved in the transport of solutes, contributing to joint lubrication [43]. However, the lubrication of the cartilage is ensuring by the synovial fluid thanks to the viscoelastic property of the hyaluronic acid.

In another hand, proteoglycans give a higher compressive resistance to the cartilage because of their high elasticity and their compressive properties. Moreover, proteoglycans are hydrophilic material because of their high sulfur content. This allows the proteoglycans to capture water, and then, to be more elastic. The latter are located in a higher number on the center of the cartilage structure [48]. The hydrostatic pressure effective on the cartilage is needed because it compresses proteoglycans and it affords water on at the interface.

Then, collagens fibers also help for the pressure resistance when they are parallel to the surface. Like the proteoglycans, their orientation change depending

on their location. Indeed, in the surface fiber and proteoglycan are oriented parallel. The deeper the fibers are, the more they are oriented perpendicularly to the surface. This is in order to regulate the mechanical forces distribution and to absorb shocks in a better way [49].

Thanks to the collagen and proteoglycans the cartilage has a high resistance. Thanks to the water it has a high elasticity. By its zone arrangement the extracellular matrix manage the stress distribution [50],[51].

The extracellular matrix contains a lot of cells, the chondrocytes. These cells are fundamental for the homeostasis of the cartilage tissue.

Natural tissue is most of the time viscoelastic material. That signify there is two phases: the solid, to afford the elasticity to cartilage and the liquid to afford the viscosity. This viscoelastic property is useful for the stress/ strain resistance and for low friction; DN gel is based on the same structure.

1.4.2. Alteration

Cartilage is severely damaged mainly due to age and physical condition. The thickness of the joint also decreases due to non-use of the articulation. Moreover, some diseases are responsible for premature degeneration, the most known is osteoarthrosis with 4.6 million cases per year in France. This degenerative disease is not the only pathology, in addition rheumatoid arthritis, atrophic polychondritis or chondrodysplasia can also affect this connective tissue.

Cartilaginous elements have different lifespans. In fact, type II collagen have a lifespan of one hundred to four hundred years. Aggrecan, the main type of proteoglycan in cartilage has a lifespan of about twenty years [41]. The loss of aggrecan is probably the reason for defective cartilage. In addition, repeated movements apply high loads on the cartilage. These charges cause a change in the shape of the chondrocytes. When chondrocytes are constrained, the metabolic activity of the cytoskeletal cells is altered.

Over time, the cartilage becomes too defective and bones start to touch and rub against each other. At this point, it is often too late and the joint is painful due to the nerves located in the bones. Indeed, the damage to the cartilage cannot be felt because it is not innervated however when the bones touch each other, the joint is already non-viable.

1.4.2.1. Actual solutions

There are several solutions for replacing cartilage, depending on the stage of the defect. For partial or not completely defective cartilage, it is possible to repair local lesions of the cartilage by gene therapy with a cell autograft or by tissue engineering with a cell culture in a biomaterial. The last solution is still in progress depending on the knowledge of the chondrocyte, macromolecules and the physiology of the extra-cellular matrix. The actual development provides a three-dimensional structure for chondrocytes regrowth. These biomaterials are either natural, absorbable synthetic, non-absorbable synthetic or composite materials. These materials are used as a support for natural regeneration.

For large cartilage diseases, the last resort is often a prosthetic surgery (total hip or knee prostheses). Before made of metallic material but increasingly composed of ceramics and polyethylene. Even though these types of prostheses are widely used as a quick and efficient solution, this solution nevertheless has significant drawbacks regarding the resulting particles.

Unfortunately, for large cartilage diseases, an effective solution is to replace the articulation joint. Therefore, the joint is completely removed with the defect and replaced by a partial or total prosthesis implanted in the bone. This is the broadest solution for cartilage deficiency, it is widely used for hip cartilage replacement, around 143 000 implants in 2018 [52], the second in the ranking is the knee prosthesis.

1.4.2.1.1. Artificial joint prosthesis

The main material of prosthesis pair for knee or hips, Fig. 1-8, is divided into two groups, hard on hard and soft on hard. In all cases, the main materials are metals, ceramics or polymers [53]. Among the biocompatible ceramics there are Zirconia, Alumina or Hydroxyapatite (HA), for the metal, alloys of Cobalt-Chromium (Co-Cr) and Titanium, and for the polymer a lot of type have been used such as Polyethylene (PE), ultra-high molecular weight Polyethylene (UHMWPE), Polytetrafluoroethylene (PTFE), Polymethylmethacrylate (PMMA) or Polyetheretherketone (PEEK) [54]. The material of the friction couple is widely studied, especially in this biocompatible system. Indeed, a multitude of coating have been tested to find the best couple to mimic the tribological triplet of the natural joint. This ideal pair is, therefore, also highly coveted by every other friction systems.

Fig. 1-8 – Knee and hip joint prostheses

1.4.2.1.2. Wear rates

The main drawback of the total prosthesis is the lifetime of the material and how it is damaged. Indeed, the friction on hard materials begets wear and releases particles which are dangerous for the body. The impact of particles on the body had been studied *in vitro* [55] on a rat model, which had the same body reaction as human against the released particles.

Among the two materials mainly used for joint replacement, the most to the least wearable are, in general, first: metal on polymer (MoP), second, ceramic on polymer (CoP), third, metal on metal (MoM) and finally, ceramic on ceramic (CoC) [56]. For instance, detailed wear rates are exposed in Fig. 1-9, [57].

Wear particles of metal alloys have a toxic impact on the body. Only polymeric material are non-toxic but involve the intervention of bone-resorbing mediators on the loosening polymeric parts, which can cause inflammation of the joint [58],[59],[60]. Thus, even though metal on metal or ceramic on ceramic artificial joint release less wear particles, they are more toxic than polymeric particles [60],[61].

Ceramic has also been used due to its biocompatibility and low roughness. This is one of the reasons the couple ceramic on ceramic create less particles than metal on metal. For our study on the DN gel, the damage criterion is probably the most important in such a characterization of a material. Thus, in order to determine and understand deterioration mechanisms on the DN gel, several experiments will be performed by using mainly the hydrogel couple with ceramic. The ceramic used is the silicon carbide (SiC), because this material has a low roughness and is already used for several medical applications.

Soft Bearings	Paired Materials *	Overall Wear Rate (mm^3/Mc)
MoP	CoCr—XLPE	6.71 ± 1.03
	Biolox®Delta—XLPE	2.0 ± 0.3 **
CoP	CoCrMo—XLPE	$4.09 + 0.64$
	Alumina—XLPE	3.35 ± 0.29
	Alumina—PE	34
	ZTA—PE	80

Hard Bearings	Paired Materials *	Overall Wear Rate (mm^3/Mc)
CoM	CoMplete	0.129 ± 0.096
	Biolox®Delta - CoCrMo	0.02 ± 0.01
	Biolox®Delta-CoCrMo	0.87
CoC	Biolox®Forte-Biolox®Forte	0.052
	Alumina-Alumina	0.03
	ATZ-ATZ	0.024
	ATZ-ATZ	$0.06 + 0.004$
	ZTA-ZTA	0.14 ± 0.10
	ATZ-ZTA	0.18
	ATZ-Alumina	0.20
	Alumina-Alumina	0.74 ± 1.73
	Biolox®Delta-Biolox®Delta	0.10
MoM	CoCrMo-CoCrMo	0.60 ± 0.18
	CoCrMo-CoCrMo	0.11 ± 0.055

Fig. 1-9 - Wear rates of couple of friction used for artificial joint [57]

1.4.2.2. Future solutions

The solution to a partial flawed cartilage is chondroplasty, autologous or allogeneic transplantation [63]. These methods allow a fibrous cartilage creation. It completes the lack of cartilage in the joint. Nowadays, a lot of research work is being carried out on biomaterial as a support for cartilage regeneration and these works are really promising.

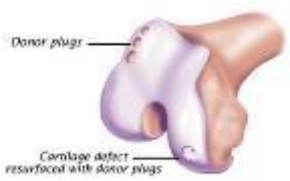

Fig. 1-10 - Autograft principle and implantation

The principle of abrasive chondroplasty is to make micro fractures in the cartilage which will induce activation of chondrocytes. Cartilage cells will colonize and produce fibrous cartilage. Basically, spongalization involves removing the defective part of the cartilage in order to prevent the spread of the disease. Allograft is a direct implantation of small pieces of cartilage supplied by another person and implanted in the defective patient's joint in order to aid in the self-regeneration of the cartilage [64]. Close to the principle of allograft, the autograft (cf. Fig. 1-10) is based on the same idea but the healthy cartilage is from the patient itself. Indeed, the principle of autograft is to remove parts of the healthy cartilaginous region in order to place it in the healing zone [65], this mosaic of cartilage is safer than allograft. Coming from the patient's own cartilage, it drastically reduces the rejection of the graft. The main disavantage of allograft is the risk of implant refection. Because the autograft conists in defecting another part of the patient's cartilage.

The solution called autologous chondrocytes transplantation is also envisaged. It consists of removing the chondrocytes from patients, allowing them to grow, and replacing the flawed cartilage part with the new one. It was firstly used without support [66],[67], then with a scaffold colonized by cells [67]. The biomaterial matrix is often bio-absorbable or biodegradable. This advance in the field of tissue engineering has, for the moment, some points to study. First, the chondrocytes culture, then, and the most important: the matrix. This cell growth support, which should also serve as an implant, is the subject of much research in the tissue engineering field.

Finally, directly implanted material to let cartilage self-regenerate are now being studied. This could be an application for the DN gel which has already proved its efficiency [21],[69],[70].

Nowadays, bioengineering is developing with biomimicry. Indeed, if to solve the joint replacement issue, by using a biomimetic approach, the investigation of the natural cartilage properties is needed, in order to copy them. Then, a soft material might be the ideal candidate for cartilage substitution. This approach is also true for classical tribological material, as the natural cartilage is one of the most efficient natural tribological system it is needed to be inspire from its composition and evolution for example.

1.5. Chapter conclusions

This first chapter focused on the background about the hydrogel potential applications. In the following work, the friction and wear should be deeply investigated because it can be the real advantage of this material. Also, if the DN gel is used as a support for cartilage replacement, the culture cell and surface change to improve it should also be studied. By using the DN gel material (PAMPS/PDMAAm) as a solution to the cartilage issue, there are two mains ways of thinking in this study:

First of all, DN gel is a material with excellent friction property. The aim is to improve this faculty and especially understand, in order to use the gel into prostheses or for other mechanical systems applications. The first objective is to clarify the potential of DN gel to achieve low friction (chapter 2). Then, it is needed to understand the role of the DN gel film thickness on the friction for mechanical applications, because in this work DN gel is used as a covering film (chapter 3). The objective of the next part is to highlight the wear on the DN gel to determine its role in the interface and link it with friction behavior (chapter 4). Also, arising from previous chapters, a low friction mechanism will be explained based on the friction and wear results (chapter 5). Finally, the consideration of DN gel application as first tribological material and second, biomedical material is explored (chapter 6). By using chondrocyte cells culture, the best conditions for cells growth on this biomaterial with or without texture will be determine (chapter 2). Indeed, in one hand, many studies used it as a support to help the regrowth of the cartilage [21], [68]–[70]. In another hand, a lot of studies already implies the positive influence of the texture on the cell culture [71]. Our principal idea is to combine theses fact to create a better support for the chondrocyte's regeneration.

Finally this work purpose is to find out and create design technology of tribological system using DN gel which realizes super low friction in water environment.

1.6. Bibliography

[1] E. M. Ahmed, "Hydrogel: Preparation, characterization, and applications: A review," *Journal of Advanced Research*, vol. 6, no. 2, pp. 105–121, Mar. 2015.

[2] W. Zhao, X. Jin, Y. Cong, Y. Liu, and J. Fu, "Degradable natural polymer hydrogels for articular cartilage tissue engineering," *Journal of Chemical Technology & Biotechnology*, vol. 88, no. 3, pp. 327–339, Mar. 2013.

[3] O. Wichterle and D. Lím, "Hydrophilic Gels for Biological Use," *Nature*, vol. 185, no. 4706, pp. 117–118, Jan. 1960.

[4] M. Heskins and J. E. Guillet, "Solution Properties of Poly(N-isopropylacrylamide)," *Journal of Macromolecular Science: Part A - Chemistry*, vol. 2, no. 8, pp. 1441–1455, 1968.

[5] P. A. King and J. A. Ward, "Radiation chemistry of aqueous poly(ethylene oxide) solutions. I," *Journal of Polymer Science Part A-1: Polymer Chemistry*, vol. 8, no. 1, pp. 253–262, 1970.

[6] B. Jeong, Y. H. Bae, D. S. Lee, and S. W. Kim, "Biodegradable block copolymers as injectable drug-delivery systems," *Nature*, vol. 388, no. 6645, pp. 860–862, Aug. 1997.

[7] L. Keller, Q. Wagner, P. Schwinté, and N. Benkirane-Jessel, "Double compartmented and hybrid implant outfitted with well-organized 3D stem cells for osteochondral regenerative nanomedicine," *Nanomedicine*, vol. 10, no. 18, pp. 2833–2845, 2015.

[8] S. J. Buwalda, K. W. M. Boere, P. J. Dijkstra, J. Feijen, T. Vermonden, and W. E. Hennink, "Hydrogels in a historical perspective: From simple networks to smart materials," *Journal of Controlled Release*, vol. 190, pp. 254–273, Sep. 2014.

[9] J.-Y. Sun *et al.*, "Highly stretchable and tough hydrogels," *Nature*, vol. 489, no. 7414, pp. 133–136, Sep. 2012.

[10] D. Kaneko, T. Tada, T. Kurokawa, J. P. Gong, and Y. Osada, "Mechanically Strong Hydrogels with Ultra-Low Frictional Coefficients," *Advanced Materials*, vol. 17, no. 5, pp. 535–538, Mar. 2005.

[11] A. A. Pitenis *et al.*, "Biotribology Corneal cell friction : Survival , lubricity , tear films , and mucin production over extended duration in vitro studies," *Biotribology*, vol. 11, no. May, pp. 77–83, 2017.

[12] B. Balakrishnan, M. Mohanty, P. Umashankar, and A. Jayakrishnan, "Evaluation of an in situ forming hydrogel wound dressing based on oxidized alginate and gelatin," *Biomaterials*, vol. 26, no. 32, pp. 6335–6342, Nov. 2005.

[13] H. Omidian, J. G. Rocca, and K. Park, "Advances in superporous hydrogels," *Journal of Controlled Release*, vol. 102, no. 1, pp. 3–12, 2005.

[14] H. Kosukegawa, "Development of Blood Vessel Biomodel with Realistic Mechanical Properties and Geometrical Structures," Tohoku University, 2011.

[15] J. L. Drury and D. J. Mooney, "Hydrogels for tissue engineering: scaffold design variables and applications," *Biomaterials*, vol. 24, no. 24, pp. 4337–4351, Nov. 2003.

[16] E. Caló and V. V. Khutoryanskiy, "Biomedical applications of hydrogels: A review of patents and commercial products," *European Polymer Journal*, vol. 65, pp. 252–267, 2015.

[17] J. P. Gong, Y. Katsuyama, T. Kurokawa, and Y. Osada, "Double-Network Hydrogels with Extremely High Mechanical Strength," *Advanced Materials*, vol. 15, no. 14, pp. 1155–1158, Jul. 2003.

[18] W. Zhang *et al.*, "Fatigue of double-network hydrogels," *Engineering Fracture Mechanics*, vol. 187, pp. 74–93, 2018.

[19] W. Yang, H. Furukawa, and J. P. Gong, "Highly extensible double-network gels with self-assembling anisotropic structure," *Advanced Materials*, vol. 20, no. 23, pp. 4499–4503, 2008.

[20] J. P. Gong, "Why are double network hydrogels so tough?," *Soft Matter*, vol. 6, no. 12, pp. 2583–2590, 2010.

[21] K. Arakaki *et al.*, "Artificial cartilage made from a novel double-network hydrogel: In vivo effects on the normal cartilage and ex vivo evaluation of the friction property," *Journal of Biomedical Materials Research Part A*, no. 3, 2009.

[22] N. Kitamura *et al.*, "Induction of spontaneous hyaline cartilage regeneration using a double-network gel: Efficacy of a novel therapeutic strategy for an articular cartilage defect," *American Journal of Sports Medicine*, vol. 39, no. 6, pp. 1160–1169, 2011.

[23] T. Osswald and N. Rudolph, *Polymer Rheology*, vol. 37. München: Hanser Publications, Cincinnati, 2014.

[24] F. L. Roth, R. L. Driscoll, and W. L. Holt, "Frictional Properties of Rubber," *Rubber Chemistry and Technology*, vol. 16, no. 1, pp. 155–177, Mar. 1943.

[25] A. Schallamach, "Abrasion Pattern on Rubber," *Rubber Chemistry and Technology*, vol. 26, no. 1, pp. 230–241, Mar. 1953.

[26] G. M. Bartenev and A. I. El'kin, "Friction properties of high elastic materials," *Wear*, vol. 8, no. 1, pp. 8–21, Jan. 1965.

[27] N. Amino and Y. Uchiyama, "Relationships Between the Friction and Viscoelastic Properties of Rubber," *Tire Science and Technology*, vol. 28, no. 3, pp. 178–195, Jul. 2000.

[28] A. Schallamach, "Friction and abrasion of rubber," *Wear*, vol. 1, no. 5, pp. 384–417, Apr. 1958.

[29] N. K. Myshkin, M. I. Petrokovets, and A. V. Kovalev, "Tribology of polymers: Adhesion, friction, wear, and mass-transfer," *Tribology International*, vol. 38, no. 11–12, pp. 910–921, Nov. 2005.

[30] A. C. Rennie, P. L. Dickrell, and W. G. Sawyer, "Friction coefficient of soft contact lenses: measurements and modeling," *Tribology Letters*, vol. 18, no. 4, pp. 499–504, Apr. 2005.

[31] S. Garg, A. Garg, and V. Singh, "Hydrogels : effectiveness extension for drug delivery and biomedical application Review Article Hydrogels : effectiveness extension for drug delivery and biomedical application," *Asian Journal of Biomaterial Research*, vol. 5, no. 2, pp. 142–151, 2016.

[32] H. Kosukegawa, V. Fridrici, E. Laurenceau, P. Kapsa, and M. Ohta, "Friction of 316L stainless steel on soft-tissue-like poly(vinyl alcohol) hydrogel in physiological liquid," *Tribology International*, vol. 82, pp. 407–414, Feb. 2015.

[33] J. P. Gong, "Friction and lubrication of hydrogels—its richness and

complexity," *Soft Matter*, vol. 2, no. 7, pp. 544–552, 2006.

[34] S. Yashima, N. Takase, T. Kurokawa, and J. P. Gong, "Friction of hydrogels with controlled surface roughness on solid flat substrates," *Soft Matter*, vol. 10, no. 18, pp. 3192–3199, Mar. 2014.

[35] H.-Y. Ren, M. Mizukami, T. Tanabe, H. Furukawa, and K. Kurihara, "Friction of polymer hydrogels studied by resonance shear measurements," *Soft Matter*, vol. 11, no. 31, pp. 6192–6200, 2015.

[36] K. Yasuda *et al.*, "Biomechanical properties of high-toughness double network hydrogels," *Biomaterials*, vol. 26, no. 21, pp. 4468–4475, Jul. 2005.

[37] T. Joyce, "Biopolymer Tribology," in *Polymer Tribology*, Imperial College Press, 2009, pp. 227–266.

[38] M. A. Lafortune, P. R. Cavanagh, H. J. Sommer, and A. Kalenak, "Three-dimensional kinematics of the human knee during walking," *Journal of Biomechanics*, vol. 25, no. 4, pp. 347–357, 1992.

[39] Blamb/Shutterstock, "Cross section through a typical synovial joint." [Online]. Available: https://www.news-medical.net/health/What-is-Cartilage.aspx.

[40] J. M. Mansour, "Biomechanics of Cartilage," *Kinesiology: the mechanics and pathomechanics of human movement*, pp. 66–79, 2009.

[41] X. Chevalier and P. Richette, "Cartilage articulaire normal: Anatomie, physiologie, métabolisme, vieillissement," *EMC-Rhumatologie-Orthopedie*, vol. 2, no. 1, pp. 41–58, 2005.

[42] K. E. Jensen, H. Lerche, A. U. Kontakt, and C. M. Savery, "In Vitro Chondrogenesis of Bone Marrow-Derived Mesenchymal Progenitor Cells Brian," *Tidsskriftet Dansk Musikterapi*, vol. 7, no. 2, pp. 3–8, 2010.

[43] A. J. Sophia Fox, A. Bedi, and S. A. Rodeo, "The Basic Science of Articular Cartilage: Structure, Composition, and Function," *Sports Health: A Multidisciplinary Approach*, vol. 1, no. 6, pp. 461–468, Nov. 2009.

[44] P. S. Erbach, D. A. Gregory, and J. B. Hammock, "Collagen of articular cartilage," *BioMed Central Ltd*, vol. 35, no. 17, pp. 3091–3096, 2002.

[45] Y. Wang, Y. Yuan, Y. Liu, X. Chang, and C. Academy, "Geophysical data

oriented curvelet-like transform," *Sciences-New York*, vol. 1, pp. 3663–3667, 2011.

[46] L. Sandell and T. Aigner, "Articular cartilage and changes in artritis An introduction: Cell biology of osteoarthritis.," *Arthritis Res*, vol. 3, pp. 107–113, 2001.

[47] N. D. Broom, "Further insights into the structural principles governing the function of articular cartilage.," *Journal of Anatomy*, vol. 139, no. 2, pp. 275–294, 1984.

[48] M. Wong and D. R. Carter, "Articular cartilage functional histomorphology and mechanobiology: A research perspective," *Bone*, vol. 33, no. 1, pp. 1–13, 2003.

[49] J. A. Roberts, D. F. Finlayson, and P. A. Freeman, "The long-term results of the Howse total hip arthroplasty. With particular reference to those requiring revision," *Journal of Bone and Joint Surgery. British Volume*, vol. 69, no. 4, pp. 545–550, 1987.

[50] K. B. L. Lee, J. H. P. Hui, I. C. Song, L. Ardany, and E. H. Lee, "Injectable Mesenchymal Stem Cell Therapy for Large Cartilage Defects-A Porcine Model," *Stem Cells*, vol. 25, no. 11, pp. 2964–2971, 2007.

[51] M. Jung *et al.*, "Enhanced early tissue regeneration after matrix-assisted autologous mesenchymal stem cell transplantation in full thickness chondral defects in a minipig model," *Cell Transplantation*, vol. 18, no. 8, pp. 923–932, 2009.

[52] PMSI, "Chiffres clés Médecine, chirurgie, obstétrique," 2018. [Online]. Available: https://www.atih.sante.fr/sites/default/files/public/content/2554/atih_chiffres_cles_mco_2018_1.pdf.

[53] A. Dambreville and J. Hummer, "Friction couples and total hip prostheses," *European Journal of Orthopaedic Surgery & Traumatology*, vol. 9, no. 4, pp. 237–240, Dec. 1999.

[54] S. Ramakrishna, J. Mayer, E. Wintermantel, and K. W. Leong, "Biomedical applications of polymer-composite materials: a review," *Composites Science and Technology*, vol. 61, no. 9, pp. 1189–1224, Jul. 2001.

[55] S. D. Rogers, D. W. Howie, S. E. Graves, M. J. Pearcy, and D. R. Haynes, "In Vitro Human Monocyte Response To Wear Particles Of Titanium Alloy Containing Vanadium Or Niobium," *The Journal of Bone and Joint Surgery*, vol. 79, no. 2, pp. 311–315, 1997.

[56] C. R. Schwartsmann, L. C. Boschin, R. Z. Gonçalves, A. K. Yépez, and L. De Freitas Spinelli, "New bearing surfaces in total hip replacement," *Revista Brasileira de Ortopedia*, vol. 47, no. 2, pp. 154–159, 2012.

[57] M. Merola and S. Affatato, "Materials for Hip Prostheses: A Review of Wear and Loading Considerations," *Materials*, vol. 12, no. 3, p. 495, Feb. 2019.

[58] D. R. Haynes and B. Vernon-Roberts, "Potential pharmacological treatments of prosthetic joint loosening," *Inflammopharmacology*, vol. 3, no. 3, pp. 213–219, Sep. 1995.

[59] M. A. McGee, D. W. Howie, S. D. Neale, D. R. Haynes, and M. J. Pearcy, "The role of polyethylene wear in joint replacement failure," *Proceedings of the Institution of Mechanical Engineers, Part H: Journal of Engineering in Medicine*, vol. 211, no. 1, pp. 65–72, 1997.

[60] J. Charnley and Z. Cupic, "The nine and ten year results of the low-friction arthroplasty of the hip.," *Clinical orthopaedics and related research*, vol. 11, no. 95, pp. 9–25, Sep. 1973.

[61] C. Brown, J. Fisher, and E. Ingham, "Biological effects of clinically relevant wear particles from metal-on-metal hip prostheses," *Proceedings of the Institution of Mechanical Engineers, Part H: Journal of Engineering in Medicine*, vol. 220, no. 2, pp. 355–369, Feb. 2006.

[62] M. Endo, J. L. Tipper, D. C. Barton, M. H. Stone, E. Ingham, and J. Fisher, "Comparison of wear, wear debris and functional biological activity of moderately crosslinked and non-crosslinked polyethylenes in hip prostheses," *Journal of Engineering in Medicine*, vol. 216, no. 2, pp. 111–122, Feb. 2002.

[63] E. B. Hunziker, "Articular cartilage repair: Basic science and clinical progress. A review of the current status and prospects," *Osteoarthritis and Cartilage*, vol. 10, no. 6, pp. 432–463, 2002.

[64] A. Bakay, L. Csönge, G. Papp, and L. Fekete, "Osteochondral resurfacing of the knee joint with allograft. Clinical analysis of 33 cases," *International Orthopaedics*, vol. 22, no. 5, pp. 277–281, 1998.

[65] V. Bobić, "Arthroscopic osteochondral autograft transplantation in anterior cruciate ligament reconstruction: A preliminary clinical study," *Knee Surgery, Sports Traumatology, Arthroscopy*, vol. 3, no. 4, pp. 262–264, Mar. 1996.

[66] D. A. Grande, M. I. Pitman, L. Peterson, D. Menche, and M. Klein, "The repair of experimentally produced defects in rabbit articular cartilage by autologous chondrocyte transplantation," *Journal of Orthopaedic Research*, vol. 7, no. 2, pp. 208–218, 1989.

[67] M. Brittberg, A. Lindahl, A. Nilsson, C. Ohlsson, O. Isaksson, and L. Peterson, "Treatment of Deep Cartilage Defects in the Knee with Autologous Chondrocyte Transplantation," *New England Journal of Medicine*, vol. 331, no. 14, pp. 889–895, Oct. 1994.

[68] N. Kitamura, M. Yokota, T. Kurokawa, J. P. Gong, and K. Yasuda, "In vivo cartilage regeneration induced by a double-network hydrogel: Evaluation of a novel therapeutic strategy for femoral articular cartilage defects in a sheep model," *Journal of Biomedical Materials Research Part A*, vol. 104, no. 9, pp. 2159–2165, Sep. 2016.

[69] C. Azuma *et al.*, "Biodegradation of high-toughness double network hydrogels as potential materials for artificial cartilage," *Journal of Biomedical Materials Research Part A*, vol. 81A, no. 2, pp. 373–380, May 2007.

[70] K. Yasuda *et al.*, "A Novel Double-Network Hydrogel Induces Spontaneous Articular Cartilage Regeneration in vivo in a Large Osteochondral Defect," *Macromolecular Bioscience*, vol. 9, no. 4, pp. 307–316, Apr. 2009.

[71] V. Dumas *et al.*, "Multiscale grooved titanium processed with femtosecond laser influences mesenchymal stem cell morphology, adhesion, and matrix organization," *Journal of Biomedical Materials Research Part A*, vol. 100A, no. 11, pp. 3108–3116, Nov. 2012.

Chapter 2 – Potential of DN gel as tribological material

From previous introduction it was needed to understand the DN gel tribological behavior. The apprehension of its friction properties is absolutely necessary for a better usage of this soft matter. Then, in this chapter deeply focus on the DN gel as a tribological material. By a first investigation about the role of the water in this material and the function of the applied load and speed on its different friction behaviors and run-in process.

2.1. DN gel mechanical properties

2.1.1. Experimental apparatus & calculation method

2.1.1.1. Indentation

In order to highlight the elastic modulus, which is an essential parameter to define a material, indentation test was performed. This test consists in applying a normal load on the material surface, then the displacement of the probe in the material is recorded. By plotting the indentation curve the reduced elastic modulus of the material is calculated. Also, the water film thickness at the surface and the adhesion force of the material with the probe are investigated.

In order to measure properly the Young's modulus, the maximum depth indentation has to be less than 1/6 of the material measured thickness. Indeed, in the other case there are a risk of the substrate influence on the elastic modulus measurement.

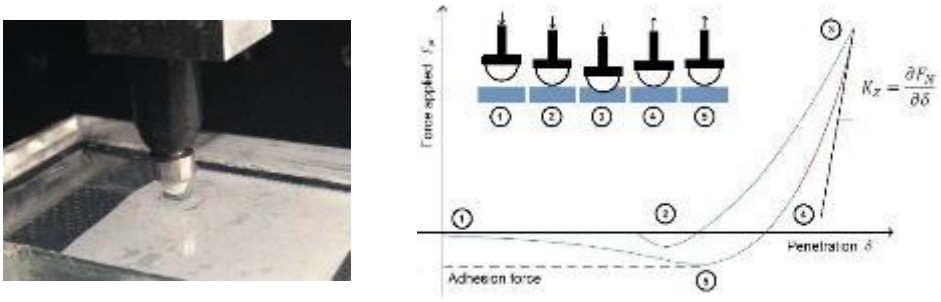

(a) Picture of indentation (b) Resulting curve after indentation

Fig. 2-1 – (a) Indentation with Teflon probe on DN gel (b) Typical indentation curve

A thick DN gel is used to avoid any influence of the substrate and I indent the surface with a Teflon probe, much harder than DN gel as shown in Fig. 2-1 (a).

The micro indentation test is an apparatus already used in several studies, especially for low stiffness material and biological materials. The indentation test on soft matter is interesting for elastic modulus determination but also viscosity and adhesion properties [1],[2]. Elastic modulus can be calculated from two methods the Hertzian (E^*_{Hz}) and the Johnson, Kendall and Roberts (JKR) method (E^*_{JKR}). This last one, considers the adhesion force. If the adhesion force is null, then, $E^*_{Hz} = E^*_{JKR}$.

From conventional elastic modulus equation, it is possible to obtain the reduce elastic modulus (E^*) [3],[4]. Using the contact stiffness, defined from the decreasing indentation curve (cf. Fig. 2-1 (b)):

$$K_Z = \frac{\partial F_N}{\partial \delta} \qquad (2\text{-}1)$$

And the Hertzian contact area (a) for a spherical indenter is determined from the probe radius (R) and indentation depth (δ_{max}):

$$a = \sqrt{R * \delta_{max}} \qquad (2\text{-}2)$$

The reduced elastic modulus is the following:

$$E^* = \frac{K_Z}{2 * a} \qquad (2\text{-}3)$$

This reduced elastic modulus, is famously describe as:

$$\frac{1}{E^*} = \frac{1-{\upsilon_1}^2}{E_1} - \frac{1-{\upsilon_2}^2}{E_2} \qquad (2\text{-}4)$$

With E_1 and υ_1, the elastic modulus and the Poisson coefficient of the Teflon probe respectively. E_2 and υ_2, the elastic modulus and Poisson coefficient of the DN gel respectively. In our case, $E_1 \gg E_2$, then, $\frac{1}{E^*} = \frac{1-\upsilon^2}{E_1}$ because the DN gel elastic modulus is much lower than the elastic modulus of the Teflon probe.

In this case Johnson, Kendall and Roberts model (JKR) is employed, because of adhesion phenomenon. For example, from the indentation curve shown on Fig. 2-1, interaction forces can be observed, the number 2 and 5 clearly indicate an attractive force and an adhesive force respectively between the probe and the sample surface. The reduced elastic modulus, from the JKR model is calculated as follow:

$$E^*_{JKR} = \sqrt{\frac{K_z^3}{6R * (F_{max} - 2F_{adh} - 2\sqrt{F_{adh} * (F_{max} - F_{adh})}}} \qquad (2\text{-}5)$$

With K_Z the contact stiffness determined by the slop of the indentation curve, R the probe radius, F_{max} the maximum force applied and F_{adh} the adhesion force (from the minimum value of the indentation curve).

$$K_Z = \frac{\partial F_N}{\partial \delta} \qquad (2\text{-}6)$$

2.1.1.2. Relaxation

The relaxation is close to the indentation method. However, this test enables to evaluate the viscosity of the material. Indeed, the apparatus is similar, the probe indents the surface with a given load. Then, the probe maintains the load for a long duration. While the load remains, a sensor captures the resulted force released from the material tested. This is the relaxation, the response of a material under an applied and maintained displacement (δ). Parameters such as relaxation time or viscosity can be determined from this test and resulting curve.

The fundamental purpose of relaxation test is to highlight the viscosity parameters of the material. The principle is by applying a strain $G(t)$ and a small stress γ_0 depending on the time $\tau(t)$

$$G(t) = {}^{\tau_{xy}(t)}/_{\gamma_0} \qquad (2\text{-}7)$$

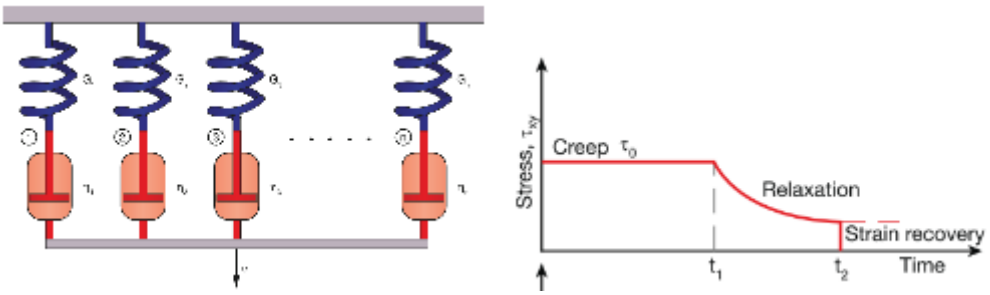

Fig. 2-2 - Stress relaxation measurement method [5]

From previous researches, information such as the relaxation time (τ_{eq}) or viscosity of the DN gel (η_{eq}) [6] can be obtained. Indeed, based on the generalized Maxwell model with n branches (cf. Fig. 2-2), the following equation was proposed:

$$G(t) = \sum_{i=1}^{n} G_i \, e^{-\left({}^{1}/_{\lambda_i}\right)t} \qquad (2\text{-}8)$$

With $\lambda_i = {}^{\eta_i}/_{G_i}$. Then, by supposition of Poisson ratio it is possible to determine G depending on E. From this technic E_{inst}, E_{inf} the relaxation time and the viscosity of the material are calculated.

In our case the 3 branches, generalized Maxell model is selected to determine these parameters. These tests were performed on bulk DN gel with a Teflon ball. By maintaining the indentation, it is possible to record the resulting force. Following Fig. 2-3, is an example of the material response to an imposed displacement.

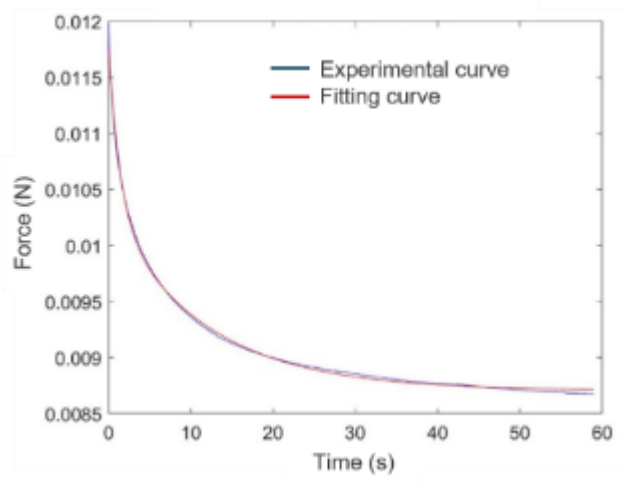

Fig. 2-3 - Fitting curve of stress relaxation of DN gel, generalized Maxell model 3 branches

2.1.2. Experimental results depending on DN gel thickness

DN gel can be process into different thicknesses, depending on the initial mold thickness. Then, in this "bulk" material study it is interesting to focus on the classical viscoelastic properties change depending on the bulk thickness. The load / displacement chosen are extremely low and the probe ball is very small, to avoid the environment influence.

2.1.2.1. Elastic modulus

The reduced elastic modulus of DN gel E^* as a bulk is measured in 2 thicknesses conditions.

The first one is 2 mm, the second is 18 mm thick, presented in

Fig. 2-4.

(a) 2 mm thick DN gel (b) 18 mm thick DN gel

Fig. 2-4 – DN gel synthesis (PAMPS/PDMAAm)

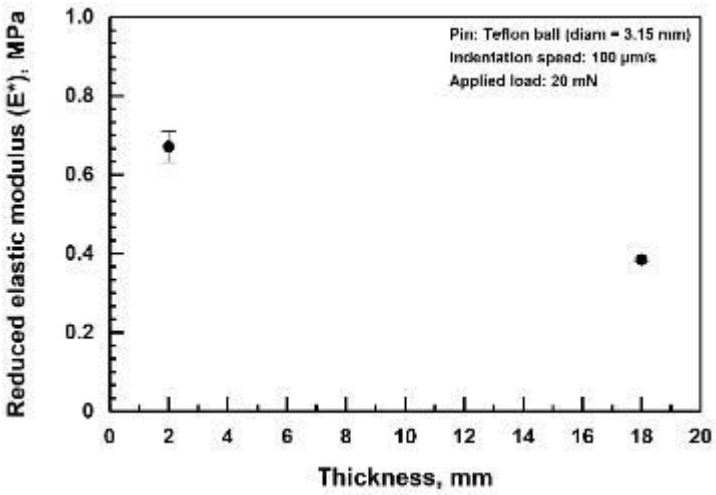

Fig. 2-5 – Elastic modulus of DN gel calculated by JKR method, depending on the applied load and thickness (a) is about 2 mm thick, (b) is about 18 mm thick

Loads chosen for the indentation (20 mN) is extremely low in order to not have the substrate influence in these measurements. Indeed, the maximum depth indentation in these loads cases are up to 100 µm, this is anyway lower than 1/6 of the total thickness of these samples. From Fig. 2-5, for a 2 mm thickness gel the average value of reduced elastic modulus is 0.62 MPa. For the 18 mm thickness the elastic modulus average is about 0.39 MPa. There is a difference between both thicknesses, the material is harder in the case of a thin sample. As it is a micro indentation, the substrate cannot be influent because the material is indent at less than 1/10 of the total thickness. Then, this slight difference is coming from

the fabrication process, inevitably due to the difference of thickness. Same UV radiation time have been used however a thicker DN gel probably required more time for a complete polymerization. Thus, as a wide range, the elastic modulus can be estimated as 0.39 – 0.62 MPa, this range is encapsulated into typical DN gels elastic modulus values. Resulting data are compared to other material values found in literature, the elastic modulus is extremely higher for DN gel rather conventional hydrogels (cf. Table 2-1).

Table 2-1 - DN gel elastic modulus comparison with other hydrogels

DN gel (literature)	**DN gel (PAMPS/PDMAAm) (18 mm – 2 mm thick)**	**Standard hydrogels**
0.5 – 2 MPa	0.39 – 0.62 MPa	~10 kPa

2.1.2.2. Viscosity

Chosen displacement for the relaxation were determined in order not to exceed 1/6 of the total thickness. Then, as the minimum thickness is 2 mm the maximal enforcement was 100 µm (1/20 of the thickness). Fig. 2-6 does not shows a noticeable difference between the η global of both thicknesses.

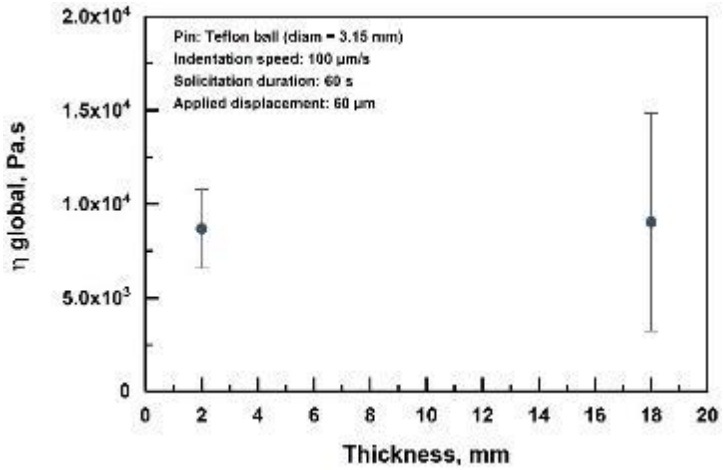

Fig. 2-6 - Global viscosity of the material depending on the thickness

2.2. Water content, influence on mechanical parameters

Water behavior of the DN gel was studied in order to understand fundamental DN gel property.

2.2.1. Hydration and dehydration property

First, the basic process of DN gel allows the production of a film with a thickness of 3 mm. From this process and following the proportion of synthesis. The proportion of water is, for the first network: 6.704 mL for 8 mL in total. And for the second network: 396.178 mL for 500 mL. Thereby, the amount of water is about 80 % according to the process.

Then, from experimental tests, by measuring the size and weight during evaporation and hydration, the amount of water is about 80%. This means that the UV radiation process does not influence the final amount of water.

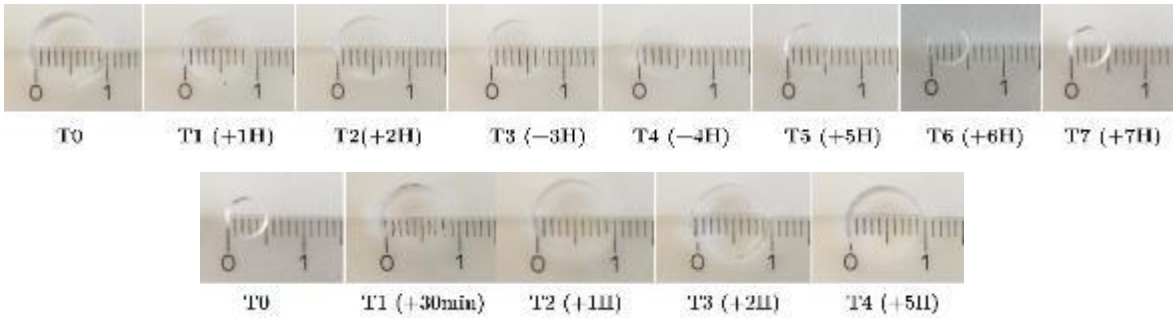

Fig. 2-7 - Pictures of dehydrating and hydrating DN gel

The size and weight of the samples were measured every 30 minute or 1 hour. The conclusion is the same as by observation, it takes a long time (7 hours) for the sample to completely lose water, even if this parameter is strongly dependent on the temperature and humidity of the room. But it is interesting to note that the DN gel can swell back in just 3 hours and fully regain its size and total weight (cf. Fig. 2-7 and Fig. 2-8).

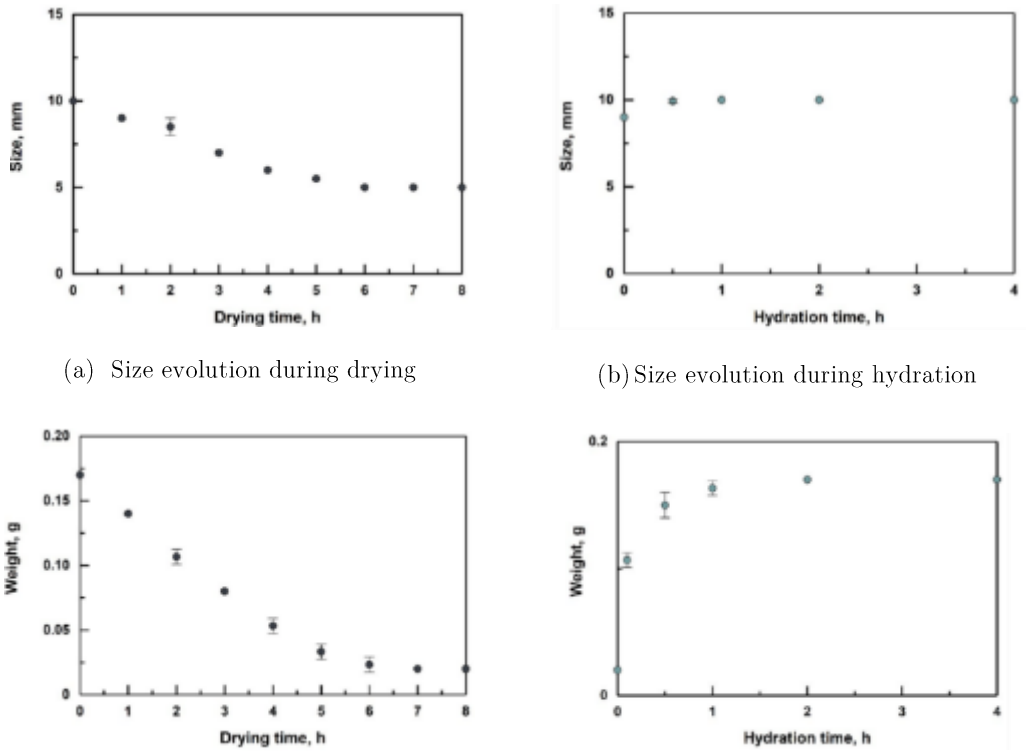

(a) Size evolution during drying

(b) Size evolution during hydration

(c) Weight evolution during drying

(d) Weight evolution during hydration

Fig. 2-8 – Size evolution of the DN gel along the time during (a) drying process and (b) hydration process. Weight evolution of the DN gel along the time during (c) drying process and (d) hydration process

2.2.2. Influence of hydration on mechanical properties

An interesting measure during these dehydration and rehydration processes is the change in mechanical properties. In this way, I understand the importance of water on them. After each time interval, adhesion force and reduced elastic modulus are measured in order to understand the function of water on the DN gel behavior.

In the Fig. 2-9 (a) and (b), the tendency of reduced elastic modulus is different from adhesion force trend in Fig. 2-9 (c) and (d). Indeed, the adhesion properties change immediately after a change of state (hydration or dehydration). After dehydration, the adhesion force immediately becomes less important while the reduced elastic modulus of the material does not change until a long period of dehydration (5 hours). By comparing the change in size and weight with the properties of the material, there is a relation with the reduced elastic modulus. Indeed, when the sample reaches its “total dry” state, its stiffness is higher,

suddenly. However, the adhesion force measured on the sample surface is high at the beginning and decrease rapidly because the water on the surface is the first to evaporate. Indeed, the adhesion force depends on the surface and not on the whole material.

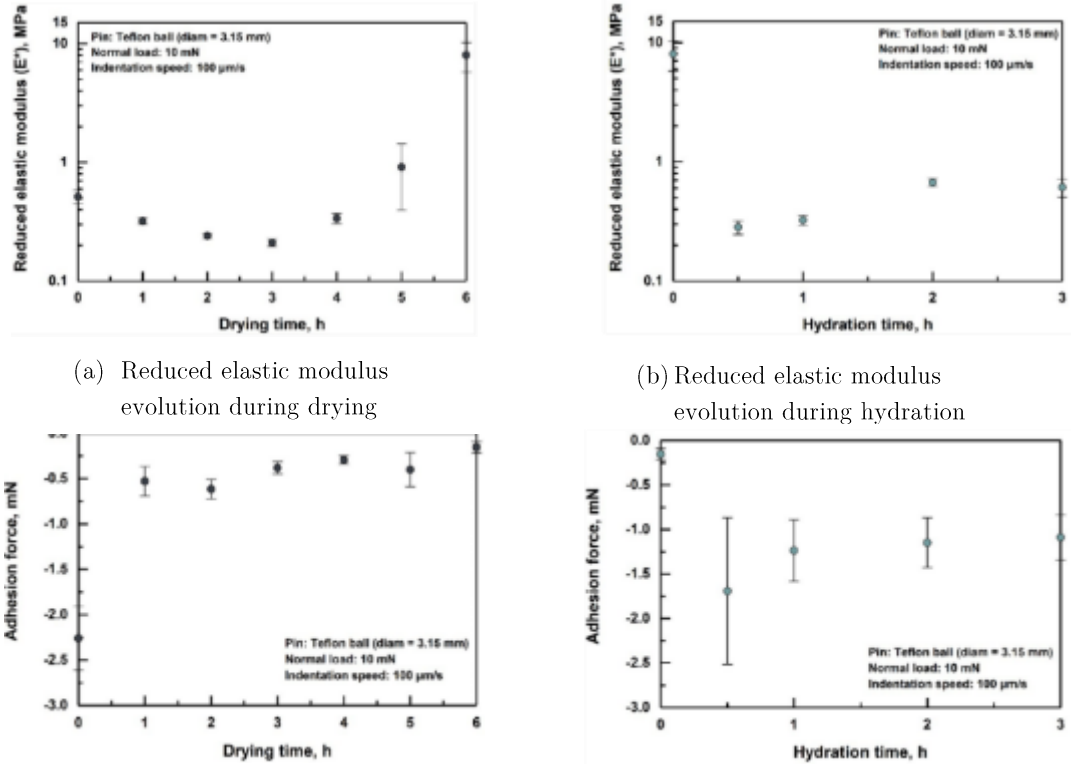

(a) Reduced elastic modulus evolution during drying

(b) Reduced elastic modulus evolution during hydration

(c) Adhesion force evolution during drying

(d) Adhesion force evolution during hydration

***Fig. 2-9** – Reduced elastic modulus evolution of the DN gel along the time during (a) drying process and (b) hydration process. Adhesion force evolution of the DN gel along the time during (c) drying process and (d) hydration process*

In the case of hydration, the adhesion force and reduce elastic modulus suddenly change after only 30 min of immersion in water and remain around their final state. On the other hand, the adhesion force never reaches back its initial value. This is a property that the DN gel loses during its dehydration and cannot regain.

The adhesion behavior of the DN gel is closely related to its water content. In less than an hour, the adhesion property of the material is completely reversed. However, it takes about 4 hours to notice a change in its elasticity.

In the following experiments, the friction tests are not performed beyond 1 hour 40 min. From this observation, and in order to maintain an environment favorable to the DN gel, the substrate will always be covered by water before tests (friction test) to prevent the water evaporation of the DN gel film and enable it to stay hydrated constantly. It is therefore estimated that elasticity and adhesion are stable during friction.

2.3. Experimental apparatus

2.3.1. Rotational tribometer

In order to study the performance of the gel in friction, a tribometer is used, it is a tribometer with rotational movement made in Japan presented on the schematic of Fig. 2-10. The disc is placed in the center of the rotor and the motor is controlled in speed and direction of rotation. Then, on the upper axis, on one side the ball is placed to touch the disc and on the opposite side a variable weight is loaded. The variable load is managed by the amount of water. The latter was predetermined by a previous experimental test with a load cell, establishing the conversion of amount of water into applied load.

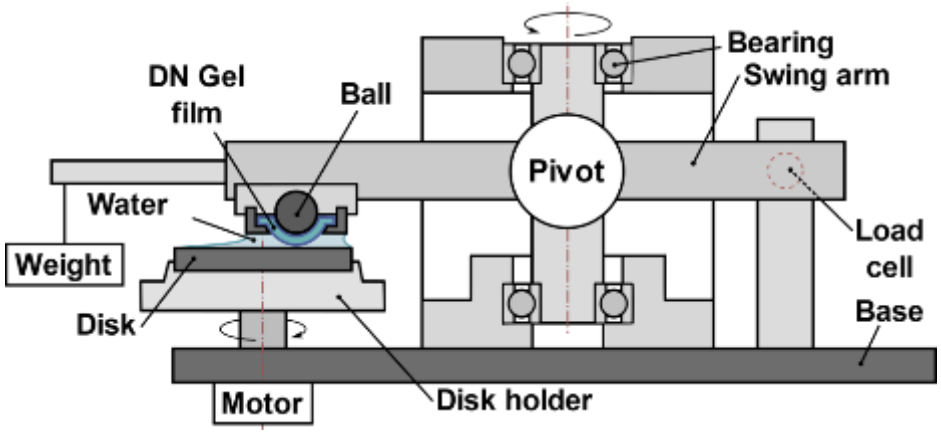

Fig. 2-10 - General view of the rotational tribometer

For this type of tribometer, the load is applied by weight. In addition, the accuracy of the system depends on the accuracy of the load sensor (model LMA-A-5N from Kyowa Electronic Instruments Co., Ltd.) and also on the bearings used in the pivot. Also, the same amount of water (1 mL) was dropped at the interface before making contact between the ball and the disc.

2.3.2. Experimental configuration

DN gel is manufactured as a flat sample initially and then cut into specimen of 10 mm diameter by means of laser cutter. Then, in order to apply our study in a realistic and applicable situation the configuration of DN gel as a ball on a ball-on-disc test was chose. In order to use the DN gel film as a ball, the 10 mm diameter film sample is placed into a specimen holder and is pinched with a SiC ball to give a spherical shape (cf. Fig. 2-11).

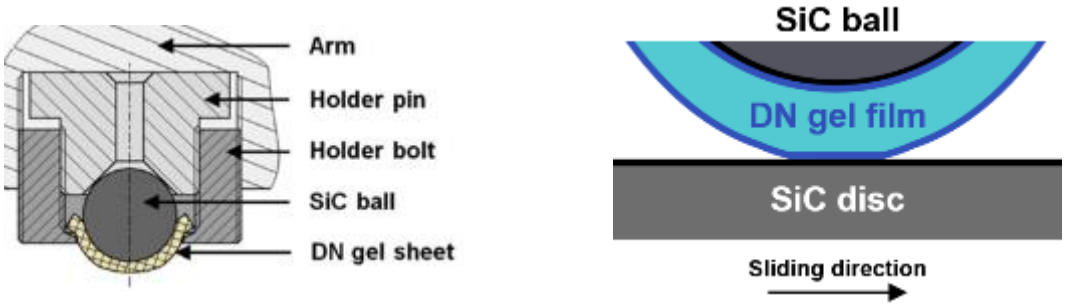

(a) Schematic of DN gel film pinch between SiC ball and specimen holder bolt

(b) Schematic of sliding pair set up

Fig. 2-11 - DN gel film assembly for friction test on rotating tribometer

By studying this configuration, it is consistent for future application. In fact, the thinner the DN gel is, the more it can be used. For instance, in a classic mechanical application, it can be compared with a rubber seal.

2.3.3. Experimental parameters

The load and the sliding speed were determined from previous tests on DN gel. The load cannot exceed 10 N because of the deformation of the DN gel film, otherwise the sample holder may touch the disc. Tests were therefore carried out for a load ranging from 0.5 N to 10 N and a sliding speed of 5 mm/s to 100 mm/s. Thus, the range of study is wide in order to understand behavior of the DN gel according to the lubrication regime which depends on the load and the speed of the friction test.

2.3.4. Method

The friction coefficient is, then, conventionally calculated from the Amonton-Coulomb friction law [7], from the non-variable and applied normal load (F_N) and the friction load (F_T) recorded by the sensor located at the back of the arm:

$$\mu = \frac{F_T}{F_N} \qquad (2\text{-}9)$$

Later, in history, definition and determination of friction coefficient were deepened, especially by Coulomb, including the static and dynamic concept of friction. Finally, later Bowden and Tabor studied the influence of deformation and adhesion on the definition of friction [8].

2.4. Friction pair influence

2.4.1. Choice of friction pair materials

The friction pair was defined from literature and previous experimental results. The material of interest for this study is DN gel, so the purpose is to reduce the external parameters influencing its behavior, in order to properly analyze and understand the behavior at its interface. Therefore, from previous studies, Silicon Carbide (SiC) was chosen as the counter material. Indeed, SiC is a ceramic of an extremely low roughness (Measured arithmetic mean height, Sa = 10.84 nm). Then, the hydrophobicity of this material is well known as its basic mechanical parameters. Besides, to choose a stiffer material as a counter surface will highlight the properties of the softer one. Several studies have also proven the promising

properties of SiC friction under water lubrication [9]–[11]. Moreover, ceramic material seems to be the best combination with hydrogel material. For instance, in this study [12] the ceramic-hydrogel combination showed the lowest friction coefficient. This is mainly due to the low roughness of ceramic, it does not attack the soft hydrogel, and can be coupled for long time with low friction.

The first idea concerned the replacement of cartilage. By biomimicry, the logical friction pair can be a DN gel on DN gel because the cartilage rubs against cartilage. However, the first drawback here is the quality of the DN gel surface. During the DN gel process, manufacturing alterations occur and it is difficult to have such a large area of DN gel without any default. The DN gel disc should have a size of 30 mm diameter (with the fixation margin) because the sliding is done 5 mm from the center. It is assumed that the contact diameter of the ball on the disc do not exceed 4 mm then, the contact area on the disc is a ring up to 40 $\pi =$ 125.6 mm². While the DN gel touching contact area on the ball is only 50.24 mm². Finally, the contact area on the disc is 2.5 greater than the contact area on the ball. Manufacturing errors of the DN gel can highly interfere by using the DN gel as a disc. Then, in the same way using SiC ball and DN gel disc a large area of DN gel is used and should be observed to understand the behavior at the interface. Finally, by using the SiC as the disc and the DN gel film as a ball, only about 50 mm² on DN gel is worn and should be studied.

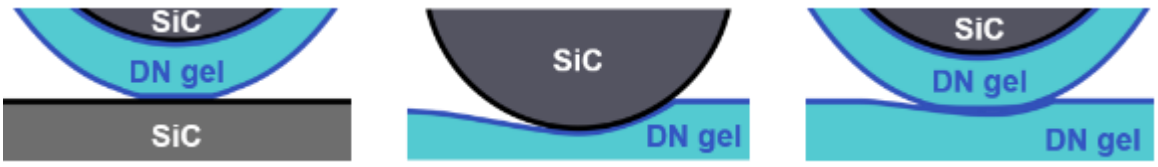

(a) Stationary contact (b) Migrating contact (c) Gemini contact

Fig. 2-12 - Test apparatus configuration

Moreover, the first assumption about the low friction of DN gel is a creation of interface by friction. In this last case, DN gel is worn faster and is always in constant contact with SiC. This small contact area is permanently in a closed interface. The purpose is to understand how the DN gel can blow up its best capacities, thus three configurations are tested. Moreover, in most of previous studies, hydrogel is always used as bulk material, in this study, the DN gel potential as a film covering hard material is explored. DN gel ball on SiC disc, SiC ball on DN gel disc and DN gel ball on DN gel disc presented in Fig. 2-12.

Similar sliding speed and load were chosen for each configuration. Then, for a 10 N load, each configuration was tested at 10 mm/s, 50 mm/s and 100 mm/s sliding speeds.

2.4.2. Results

After a controlled friction with determined parameters chosen as exposed before, the whole friction coefficient of the three different configurations was analyzed and summarized in 3 graphics representations in Fig. 2-13, separated according to the parameters applied, here the sliding velocity increases.

Thus, for each same conditions the friction coefficient curve shows a different behavior depending on the configuration. Indeed, the friction coefficient with DN gel like a disc does not show any run-in period. In other words, the friction coefficient measured over time does not show a significant difference between the start of friction and after 30 m of friction. Only DN gel as a ball with SiC as the disc configuration presents run-in behavior and super low friction especially. This drop of friction coefficient means a change occurs at the interface during the friction enabling a decrease of friction force. Therefore, the following study will focus on the understanding and the control of this run-in allowing to reach low friction coefficient. This unusual phenomenon appears at higher velocities and seems to be the key parameter to reach such a super low friction coefficient. Also, only the DN gel as a ball and SiC as disc enable a similar and continuous contact of the DN gel on SiC means a suitable interface is created during friction to obtain such results. It is suggested that wear or unknown reaction for the DN gel can enable extremely low friction.

Finally, for further investigation it has been decided to deeply study the friction occurring between the SiC as a disc and DN gel as a covering film on the ball. Especially the run-in period seems to be a key point to reach super low friction coefficient.

Therefore, it is necessary to understand and define the limits depending on load and sliding speed of the friction coefficient behavior of the DN gel on SiC.

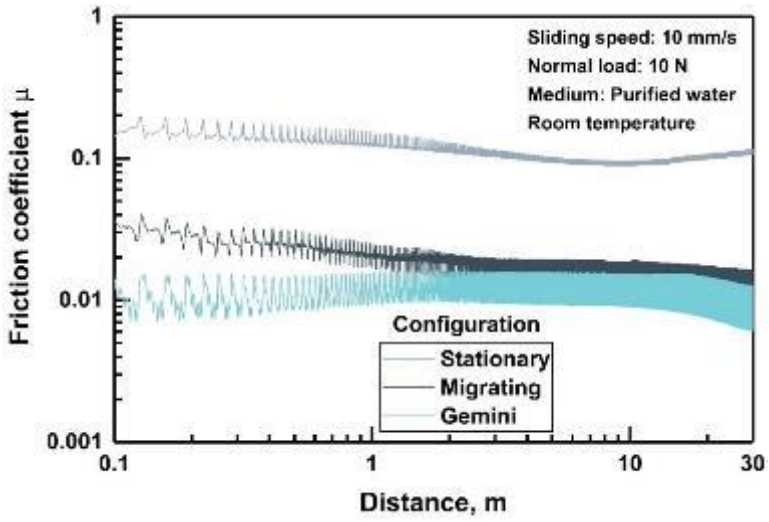

(a) 10 N – 10 mm/s

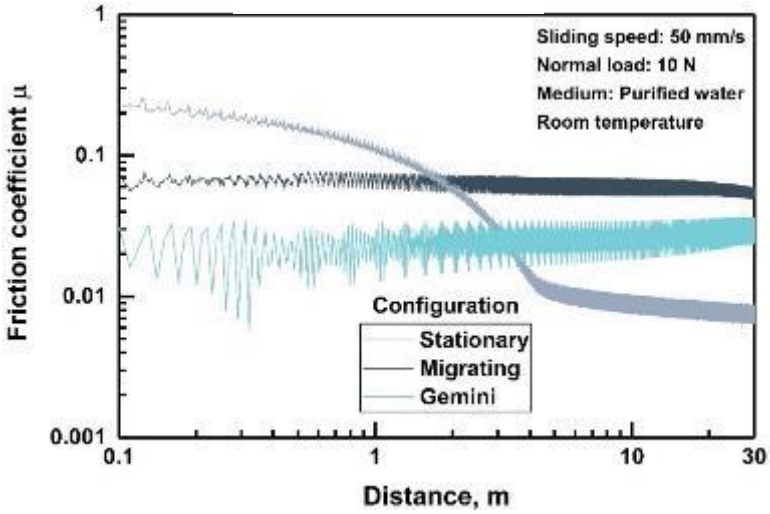

(b) 10 N – 50 mm/s

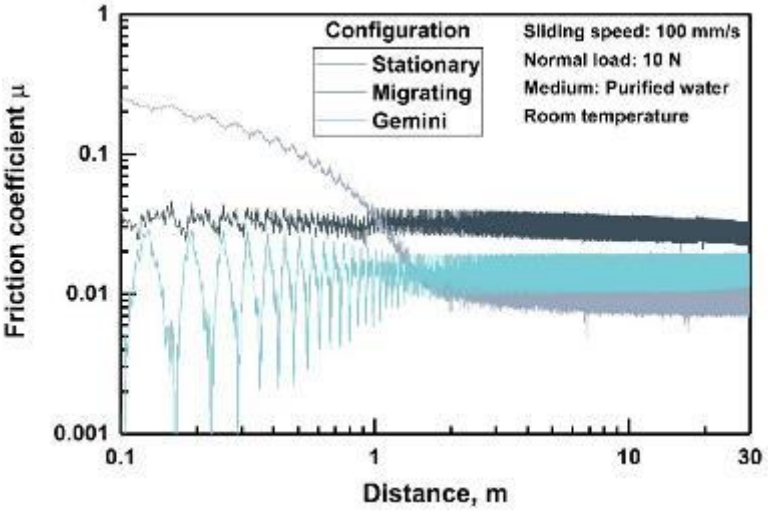

(c) 10 N – 100 mm/s

***Fig. 2-13** – Effect of configuration when sliding speed is (a) 10 mm/s, (b) 50 mm/s and (c) 100 mm/s*

2.5. Friction behavior of DN gel film on SiC, water lubrication

2.5.1. Introduction about friction and lubrication regime

2.5.1.1. Stribeck curve explanation

The coefficient of friction can show several types. Indeed, depending on the interface type and lubrication type the friction coefficient can be greatly different. In our study case water is the lubricant. First of all because SiC disc already proved great results about its friction capacity under water lubrication [10],[11]. Then, the DN gel is a material made of 80% of water. Therefore, if another liquid is used at the interface depending on its difference of density with water it probably can be swollen by the DN gel and completely change the interface.

This friction is then performed under constant lubrication, the water is added on the SiC surface before creation of the contact between both materials. Then, during friction the lubricant remain all along the test (30 m). Because of this lubrication, the system is governed by the Stribeck phenomenon. Indeed, the lubricant, depending on its viscosity, its thickness, the sliding speed and the applied pressure, greatly influences the friction coefficient. Based on the determination of the Hersey number:

$$H_S = \frac{\eta\omega}{p} \qquad (2\text{-}10)$$

With η the viscosity of the lubricant (Pa.s), ω the rotational speed (rps) and p the pressure applied (Pa) [13]. It is possible to plot the Stribeck curve.

There are three main lubrication regimes: the boundary, the mixed and the hydrodynamic. Non conformal contact can have an elasto-hydrodynamic lubrication regime (EHL). This late is different depending on the elasticity of the materials. Non conformal contact does not geometrically conform to each other and have small lubrication area. There are two types of EHL, in our case, the soft EHL occurs, it is also the case when rubber is used. Soft EHL implies a large elastic deformation even with low load at the contact. This is because the elastic modulus of the surface is really low and deforms when surfaces are in contact [13].

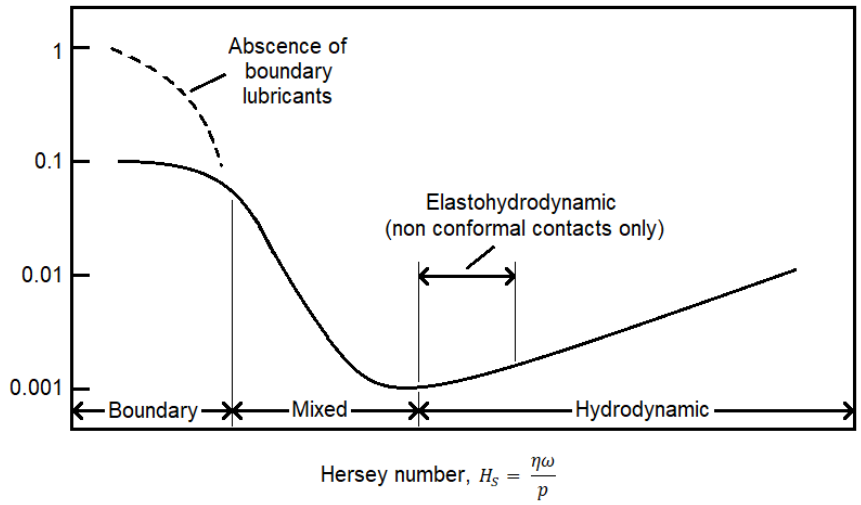

Fig. 2-14 - Typical Stribeck curve determined from the Hersey number [13]

The Stribeck curve is widely used to define a material. Indeed, this technic allows to have a quick overview on the material properties. This is greatly useful for this study and further studies on this material.

2.5.1.2. Friction coefficient

In order to obtain the Stribeck curve, the average value of the dynamical part of the recorded friction coefficient was calculated. In our case most of the friction coefficient have a long run-in period (cf. part. 2.5.2.). Thus, the range chosen for the average value of the friction coefficient is from 10 m to 30 m, in order to have a stable value. Each average of friction coefficient curve was calculated in order to plot the Stribeck curve.

2.5.2. Results about typical friction coefficient curve

By applying a range of load and speed previously defined (part. 2.3.3.), the existence of different friction coefficient behaviors is noticed.

A low friction seems to be reach at higher sliding speed and load. Also, the run-in period is particularly extended while the friction achieves low values (cf. Fig. 2-15). The main objective of any tribological system is to reach the lowest possible friction coefficient. This can be managed by controlling the pressure between surfaces (by material, load, speed, roughness), the nature of lubricant

(viscous or not), etc. The friction between two materials is governed by many parameters. For a first approach on the DN gel properties, the investigation of Stribeck curve is necessary. Consequently, by a variation of the load and sliding speed applied on the friction test it is possible to understand the interaction occurring.

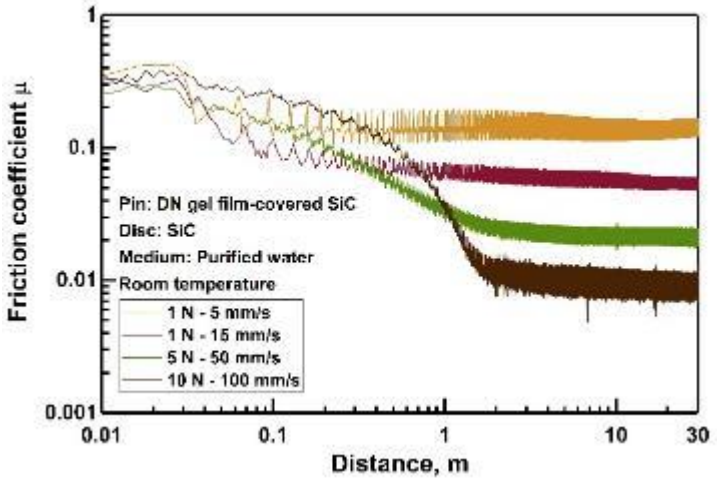

Fig. 2-15 - Friction coefficient curve tendency depending on the load and sliding speed

2.5.3. Determination of Stribeck curve of DN gel

The Stribeck curve of DN gel have been established thanks to a wide experimental test, about 50 conditions were experimented to obtain a complete curve.

The DN gel used as a covering film of SiC ball is able to achieve low friction. Indeed, below 0.01, the friction coefficient can be considered as low compared to the literature references on friction coefficient values [8],[14]. By observing the trend of this Stribeck curve different friction regime are determined by the lubrication regime as explain previously. Indeed, by increasing the sliding speed a hydrodynamic lubrication regime can be reached. The main hypothesis at this point is the creation of a thicker water film in the case of fastest speed.

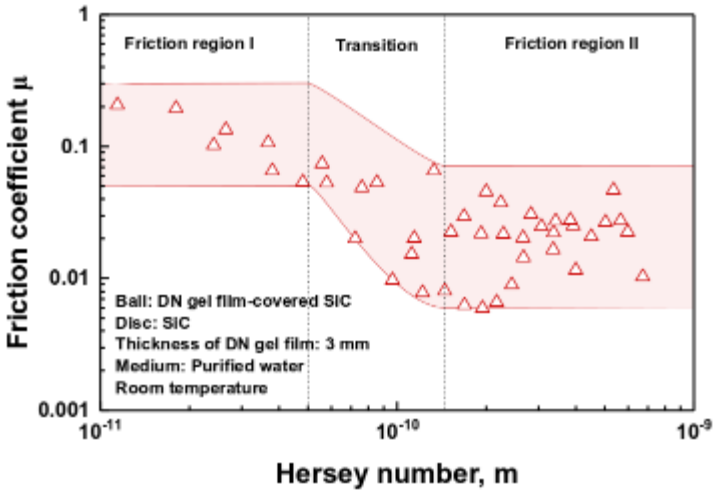

Fig. 2-16 - Stribeck Curve of DN gel film 3mm thick

In this particular case, with one type of DN gel film thickness it is possible to set up friction mode conditions. As noted on the Fig. 2-16, the friction region I, corresponds to a friction coefficient above 0.7. Considered as a high friction for this type of material, appears when the Hersey number is below $5{\cdot}10^{-11}$. Then, there is a transition period and the friction region II, translating a friction coefficient below 0.7, appears when Hersey number is above $1.5{\cdot}10^{-10}$.

- Friction region I: $H_s < 5{\cdot}10^{-11}$,
- Transition: $5{\cdot}10^{-11} < H_s < 1.5{\cdot}10^{-10}$,
- Friction region II: $1.5{\cdot}10^{-10} < H_s$.

Distribution of friction mode I and II is shown in Fig. 2-16. Local contact between SiC disc and DN gel sheet is main friction factor in friction mode I, thus higher friction coefficient ($\mu > 0.5$) is realized. On the other hand, in friction mode II, formation of water film between SiC disc and DN gel film is occurred relatively often than in friction mode I, thus lower friction coefficient is realized.

The purpose for future application is to extend the extremely low friction to slower speeds and higher loads. Most of application, especially bio application requires a low friction even in high load and low speed conditions. If I take as an example a knee's cartilage stress, in a static position the pressure applied is about 0.7 MPa, during walk is between 5 to 10 MPa and can reach 18 MPa in case of physical exercise [15]. In our case, the minimum surface contact is about 5 mm diameter for the maximum applied load, 10 N. Then, the maximal pressure at the contact do not exceed 0.6 MPa.

However mechanical applications could be interested into light loads and high-speed conditions. In our study the purpose is to understand how this super low friction is generated in order to be able to apply and reach it at any initial conditions.

2.5.4. Discussion on DN gel friction behavior

This typical friction behavior has already been observed for soft polymers. Indeed previous studies [16],[17] about friction of DN gels reported that soft polymers do not have same behavior as hard materials. The adhesive property of the hydrogel is essential in the friction. Moreover, as the lubricant in these cases is water the low viscosity of water has a role in the friction behavior. Based on Scaling relation by De Gennes [18] transposed to Schallamach model, the stretching velocity depends on the temperature, the elasticity of hydrogel and viscosity of the lubricant. The velocity-viscosity superposition principle can explain elastic friction of DN gel.

This phenomenon was called “elastic friction” because of the dependence to adhesion and deformation of the used polymer. In other words, there are two main cases of friction for soft materials: Attractive and repulsive. The attractive happens in lower sliding speed and the polymer chain adsorbs to the counter material. The repulsive depends on lubricant and sliding speed only, the polymer does not act in the interface presented on Fig. 2-17.

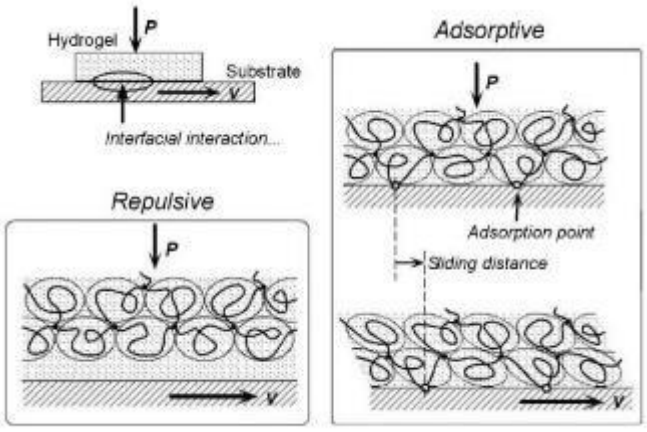

Fig. 2-17 - Polymer hydrogel interaction with a substrate, influence on friction behavior [16]

2.6. Friction behavior of DN gel on SiC compared to SiC pair

2.6.1. Background of SiC friction pair

In previous studies [19], [20] the SiC friction pair low friction under water lubrication was investigated. Especially its run-in capacity is found to be important key to realize super low friction. The rubbing of SiC material creates a favorable surface for sliding after a long sliding distance. Moreover, a SiC/SiC friction pair is known to show super low friction coefficient [9]–[11].

2.6.2. Used apparatus

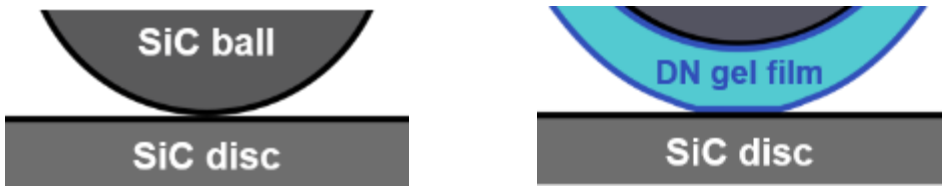

(a) SiC ball (b) DN gel film-covered SiC ball

Fig. 2-18 - Configuration for comparison between SiC and DN gel friction capacities

To compare the Stribeck curve of a conventional tribological pair, here SiC on SiC, with the DN gel results, the same rotational tribometer was used. The SiC recently proved high performances under water lubrication. This material shows extremely low friction whereas a high pressure was applied at the interface. Then, the exact same configuration (cf. Fig. 2-18) allows to compare both systems, using same load and speed conditions.

2.6.3. Results and comparison of Stribeck curve

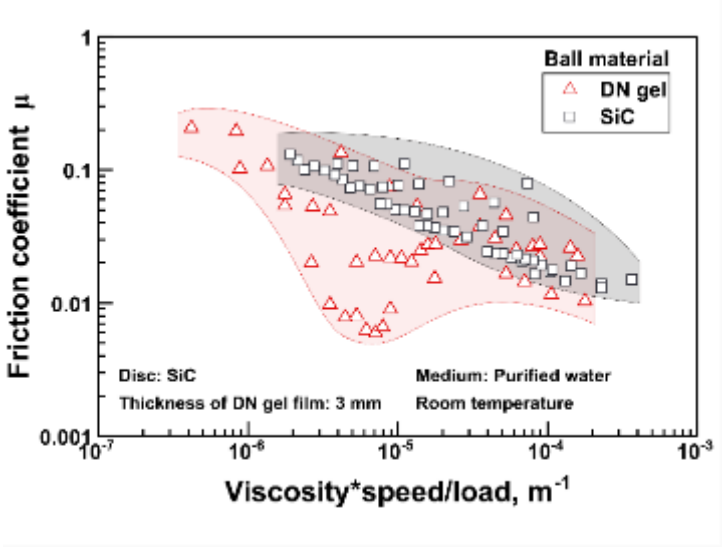

***Fig. 2-19** – Typical experimental result of SiC/SiC friction pair and SiC/DN gel friction pair*

SiC/SiC friction pair shows excellent results (cf. Fig. 2-19) under water lubrication. Then, by comparison between SiC/SiC and SiC/DN gel friction pair friction coefficient depending on the speed and load variation, I notice that lower friction coefficient can be reached by introduction of DN gel into friction system. In fact the friction trend is clearly different and it is not linear as SiC on SiC. This phenomenon is due to the soft property of DN gel also as explained previously the load and sliding speed used are extremely influent in the case of friction system using DN gel.

Moreover, as DN gel has a much higher deformation capacity, the pressure is reduced at the interface for a same load. Thus value of x-axis where minimum friction coffecient occurs shifts 1 digit lower and more by introduction of DN gel into frictional system.This is due to the stress relaxation realized by using DN gel

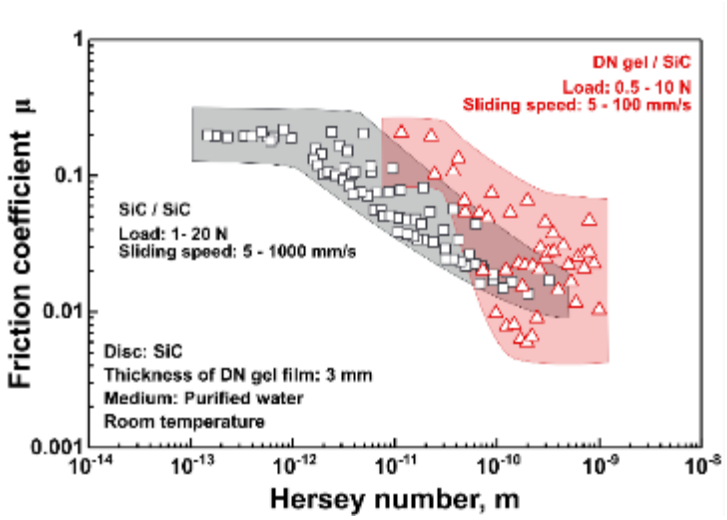

***Fig. 2-20** – Relationship between Hersey number and friction coefficient in case of SiC/SiC and SiC/DN gel friction pair*

Relationship between Hersey number and friction coefficient in case of SiC/SiC and SiC/DN friction pair is shown in Fig. 2-20. For high Hersey number, it is shown that SiC/DN gel friction pair can realize lower friction coefficient at similar Hersey number (at similar contact pressure). This indicates potential of further low friction of SiC/DN gel compared to SiC/SiC friction pair.

However, at lower Hersey number region, friction coefficient of SiC/DN gel friction pair shows higher friction coefficient than that of SiC/SiC friction pair. This drawback is expected to be solved by further investigation and surface treatment to give robustness to the system.

Finally, the wear has to be checked because of the difference of Young modulus the SiC material is less easily worn. The following of this study will investigate about the DN gel wear behavior.

2.7. Chapter conclusions

In this chapter the fundamentals properties of DN gel are exposed. By indentation and relaxation tests, we were able to establish data about the elasticity and viscosity of the DN gel. The water importance in the DN gel composition led to choose pure water as a lubricant to keep DN gel constantly hydrated.

Then, its promising character in terms of friction was highlighted and following statements have been proved:

First, the friction pair consisting of DN gel film covering SiC ball and SiC disc enable to reach lower friction compared to other combination using DN gel as a disc. A run-in period seems to be the key point to reach such a low value of friction.

Second, friction regime was determined on the typical Stribeck curve of DN gel film covering SiC ball against SiC disc friction, and was stated as follows:

- Friction region I: $H_s < 5{\cdot}10^{-11}$,
- Transition: $5{\cdot}10^{-11} < H_s < 1.5{\cdot}10^{-10}$,
- Friction region II: $1.5{\cdot}10^{-10} < H_s$.

Third, DN gel can relieve contact stress due to its deformability and can generate low friction under water lubrication. Also, from the viewpoint of application, DN gel realizes similar or even lower friction coefficient compared to SiC/SiC friction pair at similar Hersey number.

2.8. Bibliography

[1] C. Pailler-Mattei, S. Bec, and H. Zahouani, "In vivo measurements of the elastic mechanical properties of human skin by indentation tests," *Medical Engineering & Physics*, vol. 30, no. 5, pp. 599–606, Jun. 2008.

[2] C. Pailler-Mattéi and H. Zahouani, "Analysis of adhesive behaviour of human skin in vivo by an indentation test," *Tribology International*, vol. 39, no. 1, pp. 12–21, Jan. 2006.

[3] S. Tupin, "Caractérisation de l'effet de la microstructure collagénique sur le comportement mécanique global des peaux reconstruites," Ecully, Ecole centrale de Lyon, 2015.

[4] H. Zahouani, C. Pailler-Mattei, B. Sohm, R. Vargiolu, V. Cenizo, and R. Debret, "Characterization of the mechanical properties of a dermal equivalent compared with human skin in vivo by indentation and static friction tests," *Skin Research and Technology*, vol. 15, no. 1, pp. 68–76, 2009.

[5] T. Osswald and N. Rudolph, *Polymer Rheology*, vol. 37. München: Hanser Publications, Cincinnati, 2014.

[6] C. Pailler-Mattei *et al.*, "Rheological behaviour of reconstructed skin," *Journal of the Mechanical Behavior of Biomedical Materials*, vol. 37, pp. 251–263, 2014.

[7] Yannick Desplanques, "Amontons-Coulomb Friction Laws, A Review of the Original Manuscript," *SAE International Journal of Materials and Manufacturing*, vol. 8, no. SAE International, pp. 98–103, 2015.

[8] F. P. Bowden and D. Tabor, "Friction, lubrication and wear: A survey of work during the last decade," *British Journal of Applied Physics*, vol. 17, no. 12, pp. 1521–1544, 1966.

[9] X. Wang, K. Kato, K. Adachi, and K. Aizawa, "The effect of laser texturing of SiC surface on the critical load for the transition of water lubrication mode from hydrodynamic to mixed," *Tribology International*, vol. 34, no. 10, pp. 703–711, Oct. 2001.

[10] X. Wang, K. Kato, K. Adachi, and K. Aizawa, "Loads carrying capacity map for the surface texture design of SiC thrust bearing sliding in water," *Tribology International*, vol. 36, no. 3, pp. 189–197, Mar. 2003.

[11] M. Chen, K. Kato, and K. Adachi, "Friction and wear of self-mated SiC and Si3N4 sliding in water," *Wear*, vol. 250, no. 1–12, pp. 246–255, Oct. 2001.

[12] B. Stoimenov, V. Fridrici, P. Kapsa, H. Kosukegawa, and M. Ohta, "Bioengineering Materials and Conditions for Obtaining Low Friction with PVA Hydrogels," *Tribology Online*, vol. 8, no. 1, pp. 140–152, 2013.

[13] B. J. Hamrock, S. R. Schmid, and B. O. Jacobson, *Fundamentals of Fluid Film Lubrication*. CRC Press, 2004.

[14] N. P. Sun and M. Mosleh, "The Minimum Coefficient of Friction: What Is It?," *CIRP Annals - Manufacturing Technology*, vol. 43, no. 1, pp. 491–495, 1994.

[15] F. R. Elissar El Hayek, Caroline Chauvet, "Cartilage articulaire , stress mécanique et arthrose," pp. 12–16, 2013.

[16] J. P. Gong, "Friction and lubrication of hydrogels—its richness and complexity," *Soft Matter*, vol. 2, no. 7, pp. 544–552, 2006.

[17] S. Yashima, N. Takase, T. Kurokawa, and J. P. Gong, "Friction of hydrogels with controlled surface roughness on solid flat substrates," *Soft Matter*, vol. 10, no. 18, pp. 3192–3199, Mar. 2014.

[18] P. G. de Gennes, "Polymers at an interface; a simplified view," *Advances in Colloid and Interface Science*, vol. 27, no. 3–4, pp. 189–209, Jul. 1987.

[19] M. Chen, K. Kato, and K. Adachi, "The difference in running-in period and friction coefficient between self-mated Si3N4 and SiC under water lubrication," *Tribology Letters*, vol. 11, no. 1, pp. 23–28, 2001.

[20] S. Jahanmir, Y. Ozmen, and L. K. Ives, "Water Lubrication of Silicon Nitride in Sliding," *Tribology Letters*, vol. 17, no. 3, pp. 409–417, Oct. 2004.

Chapter 3 – Effect of thickness on friction properties

After the investigation about general properties of DN gel, the ideal configuration to use DN gel film in a tribological system was stated in the previous chapter. Also, the DN gel as a ball and SiC as a disc is the ideal material pair to emphasize the interesting run-in occurring at the beginning of the friction. However, to turn this configuration suitable for applications, the thickness of the DN gel used has a great importance. Therefore, in this chapter, the tests converge on three different thicknesses of DN gel. From the influence of the thickness on the contact area to the friction mode, the purpose is to understand the role of the thickness on the final friction coefficient and on the run-in period.

3.1. Effect of DN gel film thickness on contact pressure

3.1.1. Static contact measurement

3.1.1.1. Experimental apparatus

As the DN gel is a soft and transparent material, conventional technics cannot be applied in our case. Indeed, in the case of hard material the contact area is determined from the wear scare diameter, then the volume of removed material can also be determined from this data. In our case a lot of parameter are included. Its starts with the initial contact diameter far from a point. Indeed, the DN gel is soft enough to deform at the contact but hard enough to stay in place.

For a better understanding of the interface, the real contact area at the interface of friction was measured with a mesh sensor (cf. Fig. 3-1). This mesh allowed us to have the real time contact pressure value and distribution at the interface.

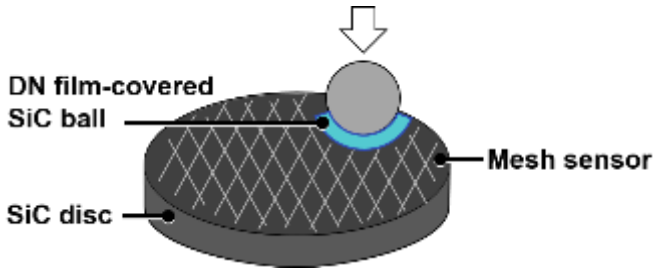

Fig. 3-1 - DN gel film covering SiC ball, pasted mesh sensor set-up for contact area measurement

With this apparatus, the contact radius and pressure while applying different loads at the contact are measured. The 256 steps scale of this mesh sensor enable us to determine the average and maximum contact pressure at the interface.

The load has been qualified as the first influent parameter on the resulted contact area, thus the applied pressure. Secondly, the thickness of the DN gel sheet showed a great importance. In that way, the influence of three thicknesses was tested. Basic DN gel sheet is 3 mm thick. 1.5 mm thick was made with the same manufacturing process (that could influence its intrinsic composition). Then, by stacking two 3 mm thick DN gel it was possible to create a 6 mm sheet. The following schematics in Fig. 3-2 expose the 3 configurations.

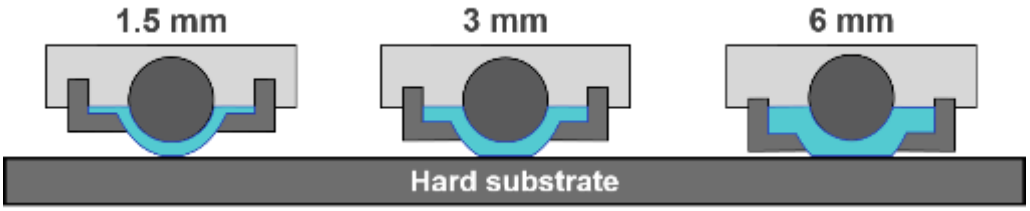

Fig. 3-2 - DN gel film covering SiC ball configuration, 1.5 mm thick configuration, 3 mm thick configuration, 6 mm thick configuration (2 times 3 mm)

The second point different from hard material is the time dependence. As the DN gel is visco-elastic material it has been necessary to calculate its contact area also depending on time.

3.1.1.2. Effect of DN gel film thickness on apparent contact pressure and area

Effect of DN gel film thickness on apparent contact pressure and contact area is shown in Fig. 3-3. Under 5 N it is difficult to measure the difference of contact area especially due to the mesh sensor resolution. However, the contact area shows significant difference for 5 and 10 N applied loads. For the 6 mm thick DN gel film a 10 N load could not be applied due to special interference of the specimen holder with the counter surface.

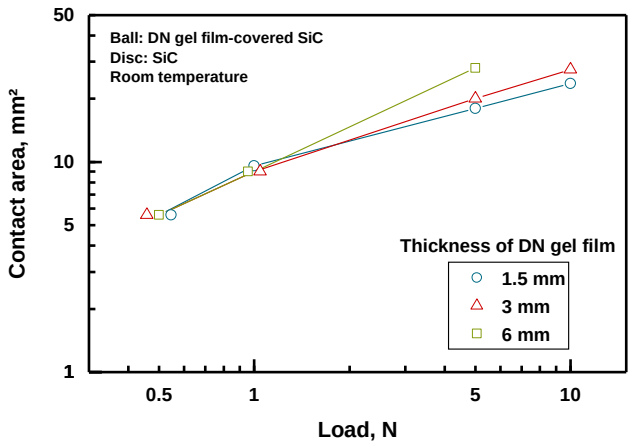

Fig. 3-3 - Contact area measured by mesh sensor depending on load and thickness

By measuring the contact area between the DN gel film covering the ball and the SiC as the disc, it highlights the thickness influence on the contact area. By increasing the thickness, the diameter area increases. Thus, the thickness has a role in the pressure distribution at the contact interface. Then, the distribution of the pressure was analyzed for a deeper understanding of phenomena happening at the interface by changing the DN gel film thickness.

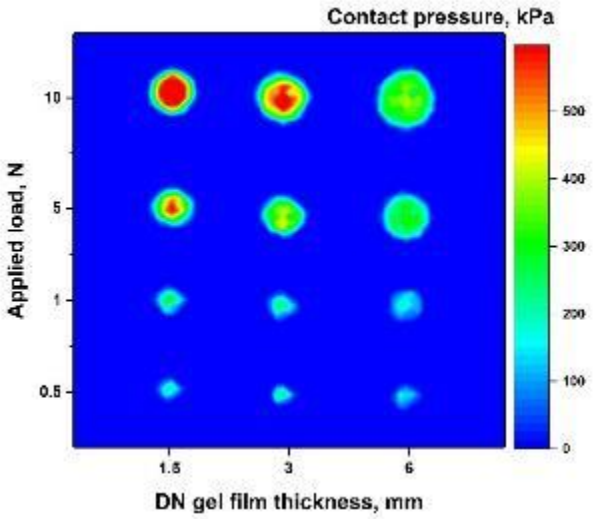

Fig. 3-4 - Contact pressure map depending on the load and on the DN gel film thickness

From these mesh sensor data exposed on Fig. 3-4, I could understand how the applied pressure is different depending on the DN gel film thickness used. Indeed, for a thin DN gel (1.5 mm thick) the applied pressure saturates, the local maximum pressure is up to 0.6 MPa. However, for a same load, and by using a thick DN gel (6 mm thick) the local maximum pressure does not exceed 0.45 MPa. Moreover, the distribution is also important, it does not shows pressure local peaks. This behavior has an impact from 5 N but not so much below or it is hardly measurable. For example, at 10 N, 1.5 mm thick DN gel present local peaks of contact pressure as well as 3 mm thick DN gel.

In any case, these measurements are statics. Of course, the DN gel is a soft matter, then when it is sliding the deformation is extremely important. A lot of studies work on this behavior. In this study [1] the role of finite deformation and adhesion on the soft material friction is discuss. Our study mostly focuses on the interface and running-in role in the friction, however a difference is clearly noticed between the “attack” side of the sliding and the “back” side. During friction, a part of the soft hydrogel undergoes to a tensile stress and the other a compressive stress as explain on the schematic Fig. 3-5.

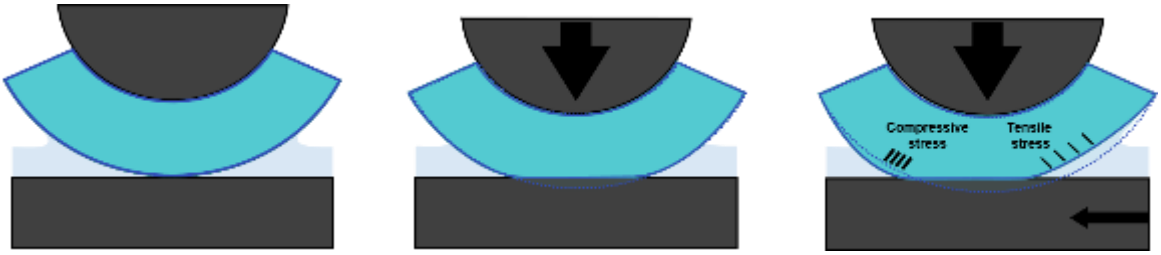

Fig. 3-5 - Schematic images of the dynamical deformation of the DN gel

3.1.2. Evolution along time

As mentioned before, the contact area, thus the pressure applied are closely linked with the time. In contrast to hard material, soft matters present a viscosity parameter that influences their behavior along the time. Hereafter, the variation graph of the contact area of the DN gel against the SiC disc depending on the thicknesses (1.5 mm, 3 mm and 6 mm) for a chosen load (5 N) is plotted. This Fig. 3-6 simply indicates that relaxation effect is influent in the contact area and then in the final pressure applied. The effect of relaxation is especially noticeable for the thicker DN gel film. Even for the more changing cases, after 10 min the contact area seems to stabilize. There is a change of relaxation time, then viscosity of the material depending on the thickness.

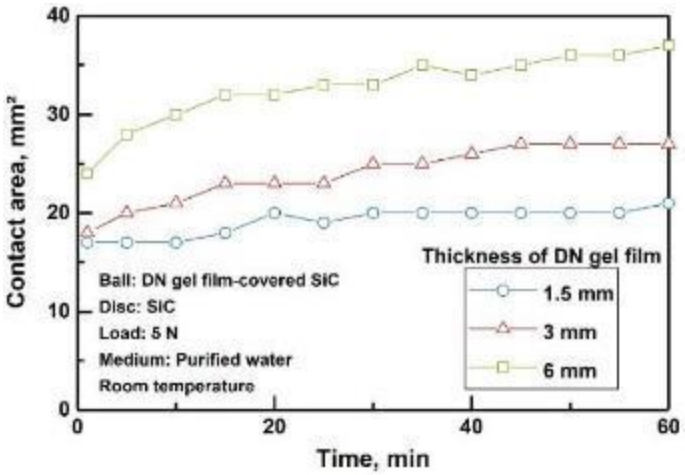

Fig. 3-6 - Influence of time on contact area dependent on thicknesses for 5 N load applied

In the case of 6 mm thick DN gel the relaxation effect is significant because the change of contact area is about 10 mm². However, this is a static measurement

and the change of pressure distribution due to dynamic friction is more important and takes over the effect of relaxation.

3.1.3. Results from indentation test

3.1.3.1. System contact stiffness

As estimated, the difference at the interface depending on the DN gel film thickness. Indentation tests was also performed (method presented in chapter 2), but here, during the indentation test the exact same configuration than for friction test is used (DN gel film covering SiC as a ball and SiC as a disc). Indentation curves are plotted depending on the thickness on Fig. 3-7. By this measurement I determined the stiffness at the contact interface: $K_Z = \frac{\partial F_N}{\partial \delta}$ with F_N the normal load applied and δ the depth displacement. Of course, in this case the counter ball of SiC is highly influent and finally these experiments give us an indication about how the thickness of DN gel film is influent on the whole system contact stiffness. Besides, by plotting the system stiffness depending on the DN gel thickness, Fig. 3-8, an important impact of DN gel film thickness on the general system contact stiffness is emphasized.

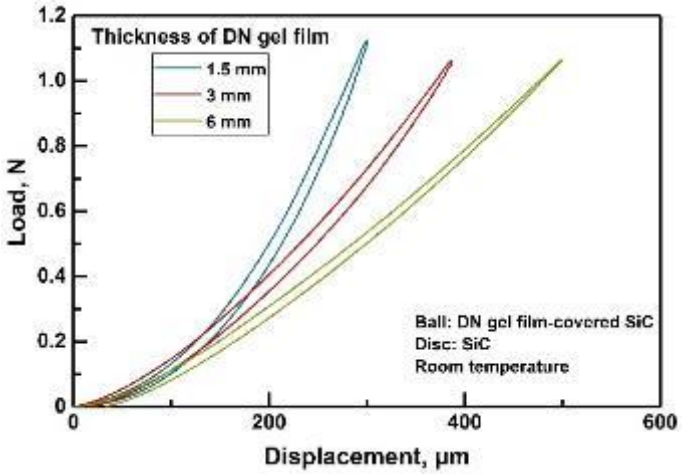

Fig. 3-7 - Indentation curves of DN gel film on SiC depending on thickness

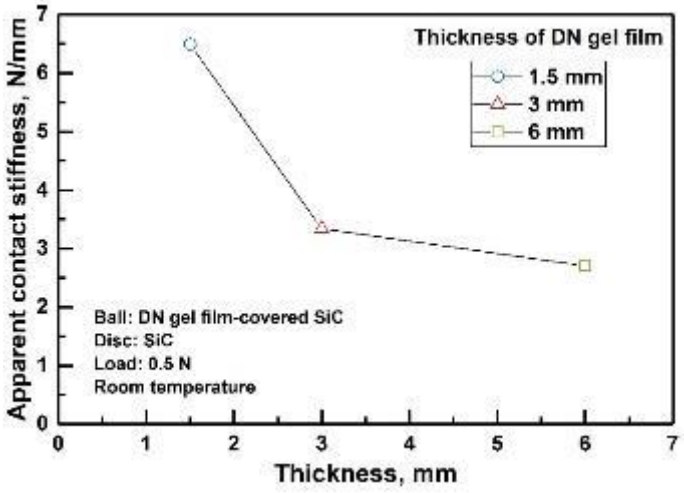

Fig. 3-8 - Apparent contact stiffness of the system using DN gel film depending on thickness

3.1.3.2. Adhesion force at the interface

Most of the studies implying hydrogel or other soft polymer materials, greatly focus on the adhesion force at the interface [2],[3]. Clearly, the adhesion between two sliding materials has a great role in the resulting friction coefficient.

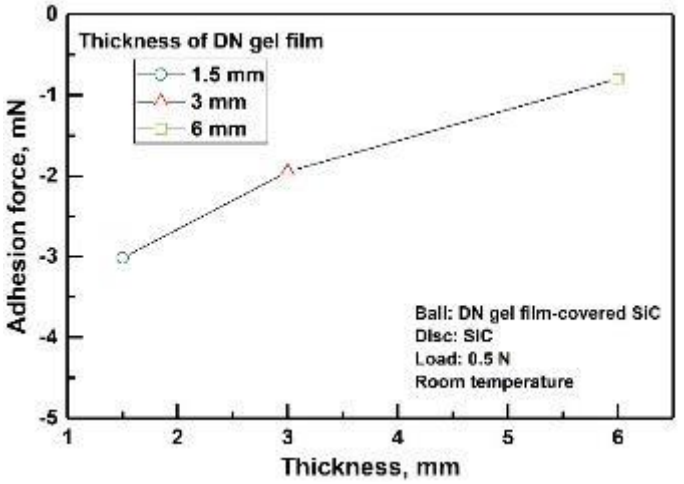

Fig. 3-9 - Adhesion force of the DN gel film on SiC depending on thickness

As the 1.5 mm thick was from a different fabrication process than 3 mm and 6 mm thick DN gel film, it was important to check out how the changing thickness does impact or not the adhesion properties. Then, adhesion force of three different

thicknesses was checked in order to understand their role on the friction properties. Fig. 3-9 presents adhesion forces measured using 1.5, 3 and 6 mm thick DN gel, the adhesion force seems linearly dependent to the thickness. However, the magnitude difference is not so important, 1 mN difference between each other. Besides, this is a static adhesion measurement, once again the dynamical behavior is expected to be greatly different.

3.2. Effect of DN gel film thickness on friction

3.2.1. Friction coefficient mode

Of course, the load and the thickness are main actors in the geometrical change at the interface. That means theses parameters are directly linked with the friction mode of the material. By performing friction tests using different DN gel film thickness three main behaviors of friction show up, called friction mode and defined as follows, on Fig. 3-10:

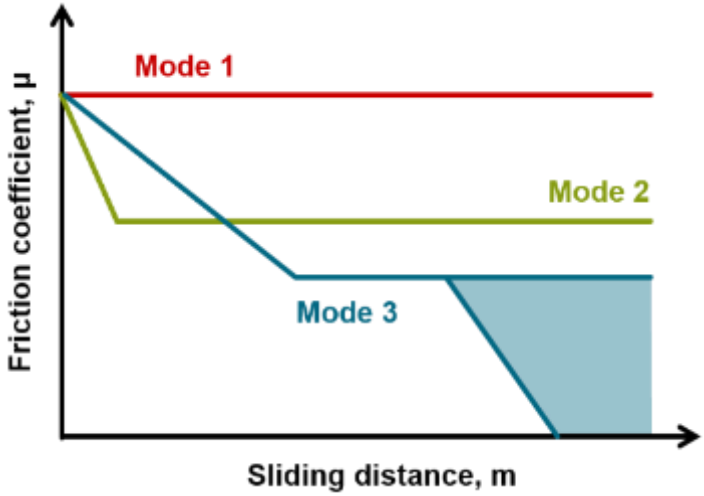

(a) Typical friction mode

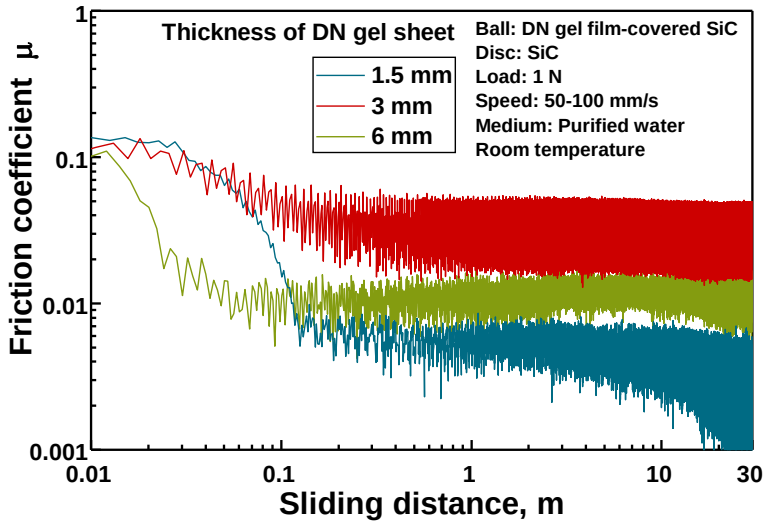

(c) Friction mode depending on DN gel film thickness

Fig. 3-10 - Definition of friction mode

- Friction mode 1: a stable friction coefficient
- Friction mode 2: a sudden decreasing friction coefficient
- Friction mode 3: a double decreasing friction coefficient with a longer first run-in period.

By sorting the friction coefficient mode this way it was possible to draw up the behavior map depending on load, speed and for the different DN gel film thicknesses.

There is a unique friction mode in the case of 1.5 mm thick DN gel. Indeed, the friction coefficient have a double run-in period. It can be split into three parts: A long first run-in period leading to a friction coefficient below 0.01, a stable transition and a second run-in period leading to a friction coefficient below 0.001.

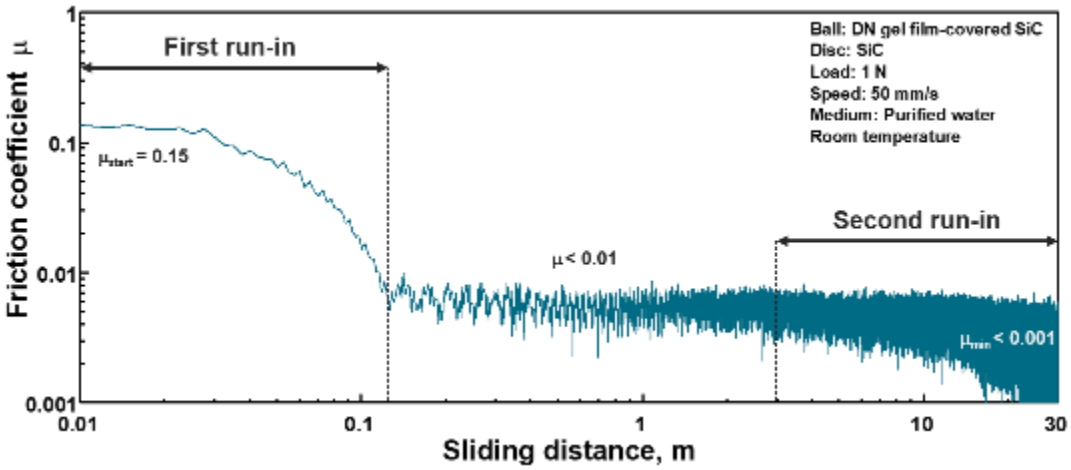

Fig. 3-11 – Typical friction coefficient mode 3, using 1.5 mm thick DN gel

As shown in Fig. 3-11, the friction coefficient corresponding to mode 3, shows a first run-in period during about 10 cm of sliding, leading to a friction coefficient lower than 0.01. Then, a second run-in period appears after 1 meter of sliding distance and enable to reach friction coefficient value below the detection limit of the sensor ($\mu < 0.001$). This friction coefficient behavior is quite unique and must be deeply investigated to be understood.

3.2.2. Thickness influence on friction mode

3.2.2.1. Map of friction mode

Then, by a classification of friction mode, a friction mode map was established depending on the DN gel film thickness used. Therefore, a dependence between the friction mode and the thickness of DN gel is quickly notice. Thus, the conclusion and further investigation focused about this difference depending on the thickness used. Besides, by a higher stiffness contact the thinner DN gel film does not present same phenomenon to reach lower friction as thicker DN gel film.

First, the 6 mm DN gel shows without surprise a spreading of the quickly obtained low friction, called mode 2 (cf. Fig. 3-12). It is quite expected because of the lower contact stiffness measured on the previous part. Indeed, by a soft contact the hydrodynamic lubrication regime can be easily reach. Moreover, this is combined with the increase of contact diameter, then a reduced applied pressure at the interface. A sudden low friction is obtained using a 6 mm thick DN gel, there is a majority of friction mode 2.

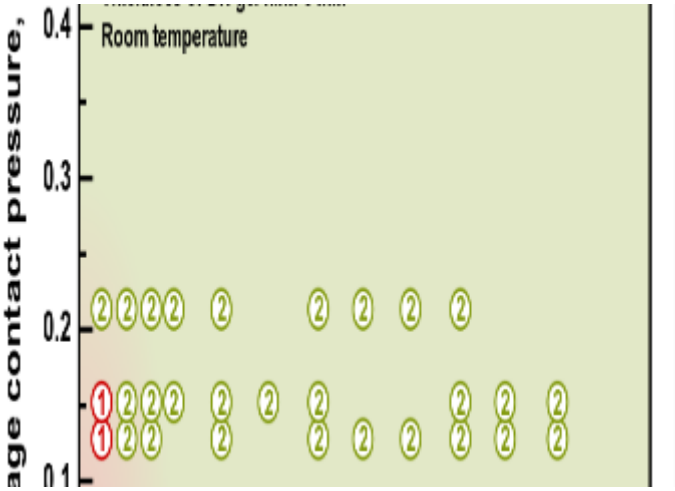

Fig. 3-12 - Friction mode map for DN gel film thickness = 6 mm

Then, the DN gel film of 3 mm thick map is quite heterogeneous. Nonetheless a high friction coefficient without decrease was observed in a wide range (cf. Fig. 3-13). It is assumed that by using 3 mm DN gel the load and sliding speed has a great influence in the lubrication regime.

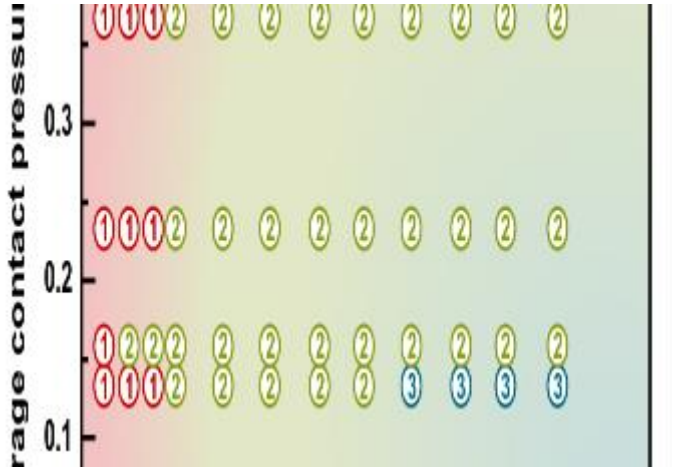

Fig. 3-13 - Friction mode map for DN gel film thickness = 3 mm

Surprisingly, and even if the number of sample test is reduced for 1.5 mm DN gel thick, due to fabrication process, the trend is clear and the friction mode 3 is spreading for sliding speed above 50 mm/s (cf. Fig. 3-14). Here the hydrodynamic lubrication regime is not reach, however an even lower friction coefficient is obtained. The mechanism of friction mode 3 has to be more deeply investigated. The 1.5 mm thick DN gel film can shows extremely low friction and can be promising for an application used.

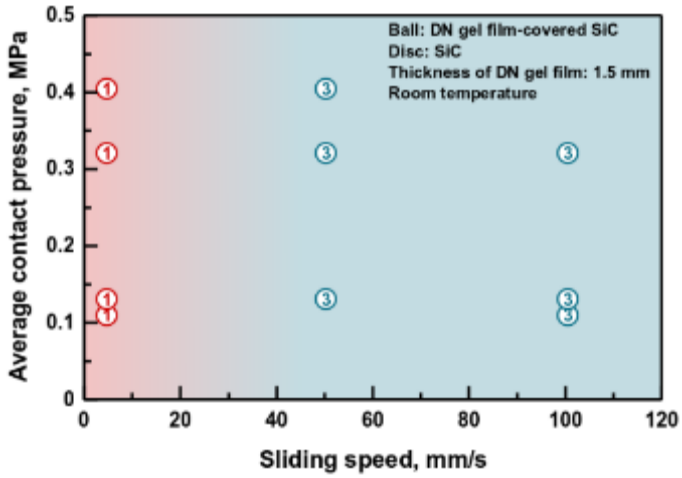

Fig. 3-14 - Friction mode map for DN gel film thickness = 1.5 mm

The tendency using 1.5 mm thick DN gel film or 6 mm thick enables to reach a super low friction at lower sliding speed and higher load than with the

conventional 3 mm thick DN gel film. However, there is a different phenomenon occurring at the interface depending on the DN gel thickness and then on the stiffness contact.

3.2.2.2. Stribeck curve

By using the Hersey number the different Stribeck curves depending on the DN gel film thickness were plotted in Fig. 3-15 for 1.5 mm thick, in Fig. 3-16 for 3 mm thick and in Fig. 3-17 for 6 mm thick. Then, complementary with the trend and the capacity of reaching super low friction for 1.5 mm and 6 mm thick DN gel film, these curves showed up the friction mode I, transitional mode and friction mode II at same Hersey number for each thickness. By using this information, it is clear that the thickness changes the frictional behavior but this is not due to the change of contact area, thus applied pressure.

Indeed, for the Hersey number calculation, the pressure applied is considered. Of course, depending on the thickness used, the pressure has been changed into the calculation: $H_{1.5} = \frac{\eta\omega}{p_{1.5}}$, $H_3 = \frac{\eta\omega}{p_3}$, $H_6 = \frac{\eta\omega}{p_6}$. Even if $p_{1.5} > p_3 > p_6$, the same combination is observed:

- Friction region I: $H_s < 5{\cdot}10^{-11}$,
- Transition: $5{\cdot}10^{-11} < H_s < 1.5{\cdot}10^{-10}$,
- Friction region II: $1.5{\cdot}10^{-10} < H_s$.

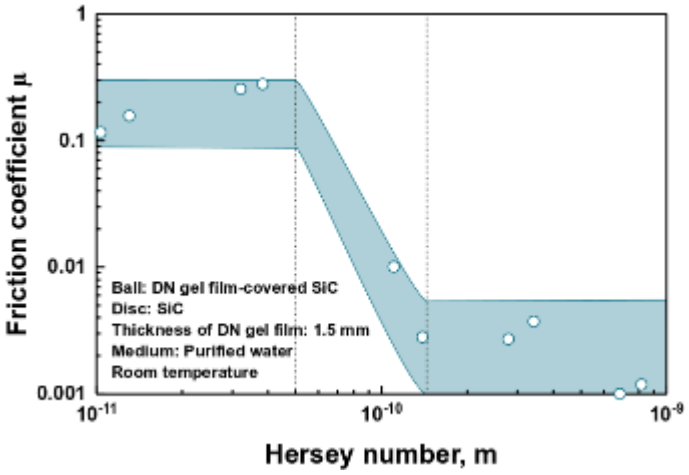

Fig. 3-15 - Stribeck curve and tendency for 1.5 mm thick DN gel film

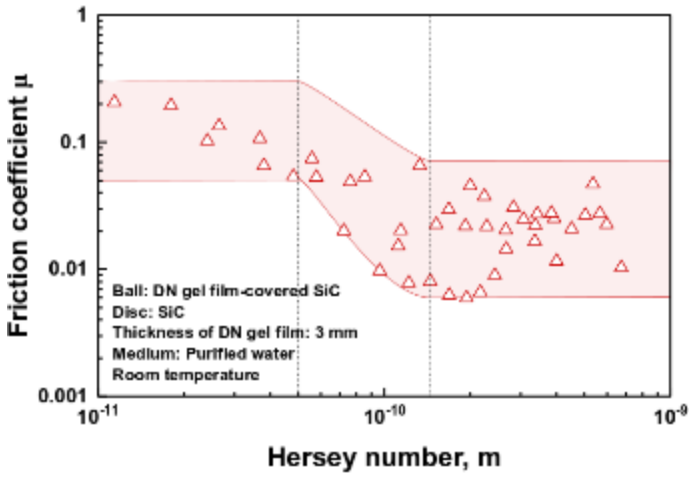

Fig. 3-16 - Stribeck curve and tendency for 3 mm thick DN gel film

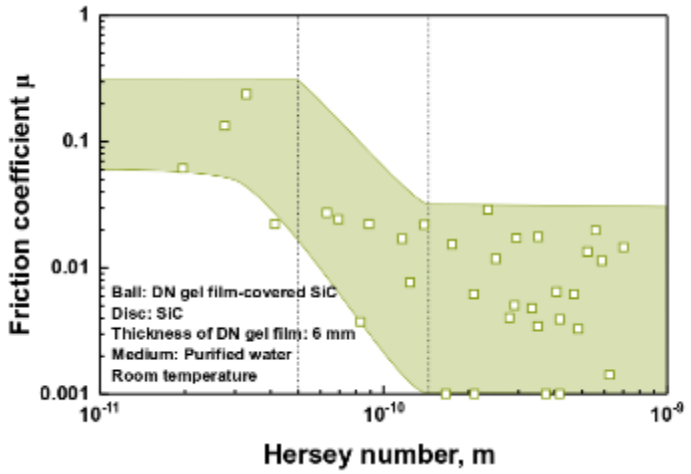

Fig. 3-17 - Stribeck curve and tendency for 6 mm thick DN gel film

Therefore, complementary investigation are performed in order to understand which parameter influences the friction mode. Indeed, the capacity of 1.5 mm thick DN gel to reach same properties as the thicker one is extremely interesting and promising for applications. However, it is necessary to understand how it occurs to obtain the best improvement of the system.

By plotting in the same graph (cf. Fig. 3-18), the different thickness behavior, it is clearer that for a same Hersey number the thickness of DN gel film plays a crucial role in the friction coefficient obtained *in fine*. However, as previously stated the final 20 m average friction coefficient value does not necessary describe the friction mode. Therefore, it is requiring understanding the mechanism by

which the final lower friction coefficient is obtained at a same Hersey number, for 1.5 mm thick DN gel film.

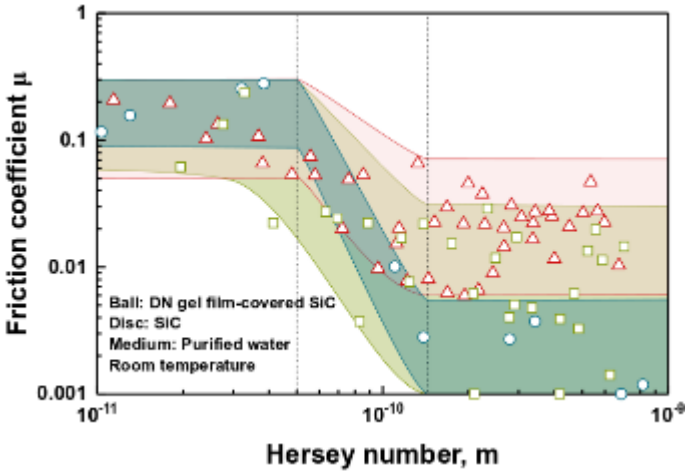

***Fig. 3-18** – Total stribeck curve and tendency depending on the DN gel film thickness*

3.3. Chapter conclusions

This chapter focused on the influence of DN gel film thickness on its friction properties. Moreover, the influence of the thickness on the contact area and the system contact stiffness was checked, in order to find out links between these multiple behaviors. Therefore, at this point, followings conclusions can be stated:

First, regardless of the DN gel film thickness, transition condition of friction regions can be expressed by Hersey number quantitatively as follows.

- Friction region I: $H_s < 5 \cdot 10^{-11}$,
- Transition: $5 \cdot 10^{-11} < H_s < 1.5 \cdot 10^{-10}$,
- Friction region II: $1.5 \cdot 10^{-10} < H_s$.

Second, 1.5 and 6 mm thick DN gel films have exhibit super-low friction ($\mu < 0.001$) under a wide range of friction conditions as friction mode II.

Finally, in the case of 1.5 mm thick DN gel film, a super low friction coefficient is obtained after a second run-in period.

3.4. Bibliography

[1] J. Lengiewicz *et al.*, "Finite deformations govern the anisotropic shear-induced area reduction of soft elastic contacts," *Journal of the Mechanics and Physics of Solids*, vol. 143, p. 104056, 2020.

[2] L. Lavielle, "Polymer-polymer friction: Relation to adhesion," *Wear*, vol. 151, no. 1, pp. 63–75, Nov. 1991.

[3] H. Kosukegawa, V. Fridrici, E. Laurenceau, P. Kapsa, and M. Ohta, "Friction of 316L stainless steel on soft-tissue-like poly(vinyl alcohol) hydrogel in physiological liquid," *Tribology International*, vol. 82, pp. 407–414, Feb. 2015.

Chapter 4 – Characterization of worn surface of DN gel

After sliding test, and analysis of friction coefficient depending on load, speed and DN gel film thickness, it was necessary to understand the interface. From previous statements, friction coefficient is dependent of the load, speed and DN gel film thickness. Load and speed dependence can be explained by lubricant regimes. Indeed, by increasing the speed and reducing the load a different dynamic is installed and creates a thicker lubricant film allowing to reach extremely low friction coefficient. However, the lubricant regime does not seem to be the only responsible for friction behavior. Besides, the final friction coefficient obtained by changing the DN gel film thickness cannot be explained by difference of system contact stiffness, difference of adhesion force at the contact, difference of contact area, then Hersey number. After this ascertainment, it was necessary to investigate about interface wear. Hypothesis could be the creation of a tribo-film, change of the surface organization, establishment of a damage layer on the DN gel surface for instance, as established for other material couples in these studies [1]–[4].

Mechanisms of surface modification during friction to reach super-low friction are multiple. These mechanisms determine the run-in period length. It exists several types, notable are: Physical adsorption (physisorption); chemical adsorption (chemisorption); chemical reaction not involving the substrate; chemical reaction involving the substrate [5]. This chapter aims to find the one occurring between SiC and DN gel.

4.1. Adhesion of DN gel on SiC disc

4.1.1. Apparatus and set-up

The substrate state has a great importance in the system friction then, the first observation was on the SiC disc friction track in order to better understand. After friction of DN gel film covering SiC ball against a polished SiC disc, the disc sample were prepared. Indeed, for SEM observation vacuum condition is required. Immediately after friction test, the "DN gel ball" was remove from the surface. The remaining water was absorbed by an absorbent paper without touching the friction interface. Then, by air blast the last water droplets were ejected. Finally, the SiC sample was ready for SEM observation.

It is estimated that many wear particles of DN gel left with the lubricant, however, by observing the surface after removing the lubricant, the observations are clear about the adhered DN gel on the SiC. The observation of substrate material gives us information about the surface state. As it is at the end of the friction it is not obvious at what point it is responsible of the run-in during friction.

With the SEM technology images of SiC are clear and can transcript much information. The friction track was easy to find because of a color difference between the disc area where the DN gel had slide and the other surface. Then focuses on the remains particles located on the friction track area were done.

4.1.2. SiC friction track images

4.1.2.1. Identification of friction track

To identify the phenomenon occurring at the interface extreme sliding condition was used to amplify the interaction. Thus, a non-lubricate sliding test was performed between SiC disc and DN gel film. During this sliding test without water a high DN gel adhesion is expecting. Indeed, as proved in the chapter 2, the water content in the DN gel material is highly influent on its properties, especially its adhesion capacity. Then, by removing the water lubrication the adhesive phenomenon is amplify and enable to understand the transition occurring on the SiC disc.

The friction coefficient curve is clearly dependent on the lubrication, then on the adhesion of DN gel on the surface (cf. Fig. 4-1). By not adding lubricant at the interface the friction coefficient behave exactly as there were water however,

after 6 – 7 m sliding distance, the water contained in the DN gel is not sufficient to lubricate the surface. Then, the friction curve is similar to the dried and not lubricated surface. Since the water provided by the DN gel itself is not enough to lubricate the surface, the strong adhesion occurs at the interface between DN gel and SiC disc. Observation of SiC surface after friction in the case of no lubrication and previously dried surface is in Fig. 4-2.

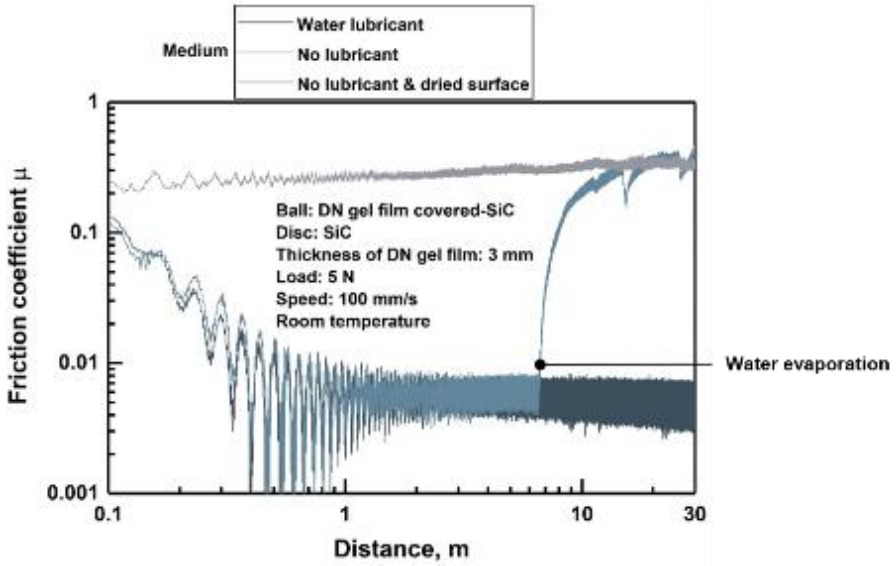

Fig. 4-1 - Friction curve of DN gel against SiC depending on the lubrication

In the SEM images of SiC the DN gel adhesion can be clearly stated. The whole contact surface has a different color, disc shape. Also, the image focusing on the DN gel track on SiC shows a typical soft polymer track shape. This is another clue orientating to the hypothesis of DN gel adhesion. Finally, this phenomenon was quite expected and the adhesion of DN gel on the SiC surface is clear. However, the future application system will probably not be under these kinds of extreme condition. Then, the change of the friction track on SiC disc depending on the friction behavior in classical running condition, with water lubricant, is analyzed.

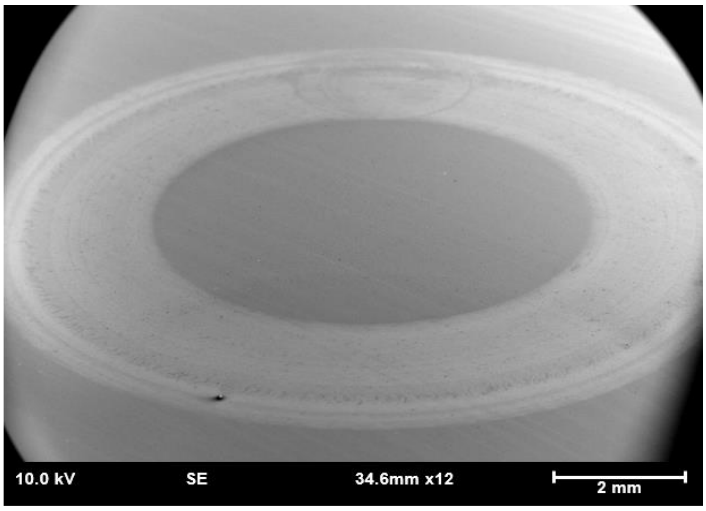

(a) General view

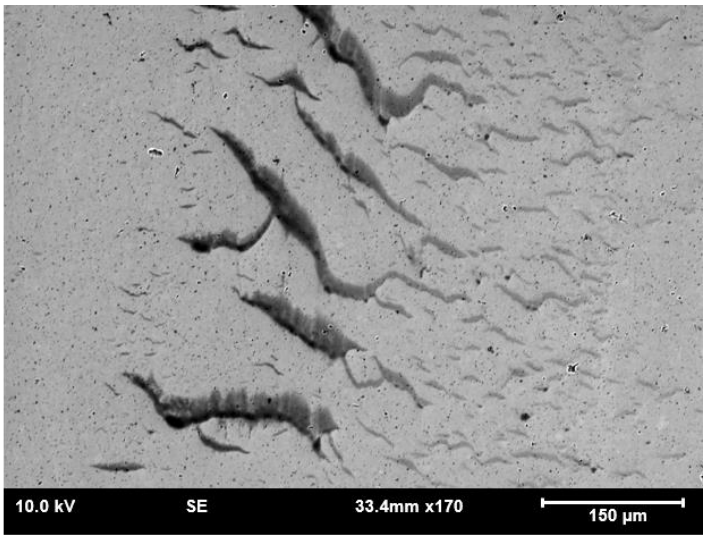

(b) Focus on the friction track

Fig. 4-2 - SEM images of SiC surface after friction with DN gel film as a ball in extreme condition (a) general view and (b) focus on adhesion track

4.1.2.2. DN gel adhesion type depending on friction mode

In order to understand the influence of observed SiC surface on the friction mode, the friction coefficient curve and images of friction track on SiC are exposed in the following Fig. 4-3, Fig. 4-4, Fig. 4-5:

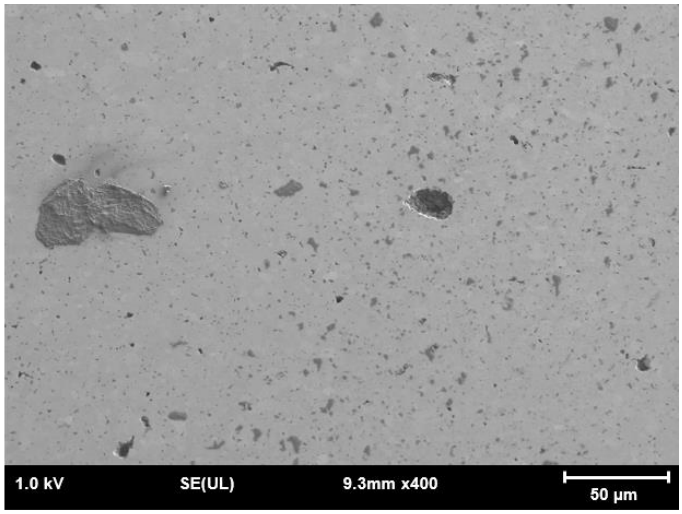

(a) Friction track

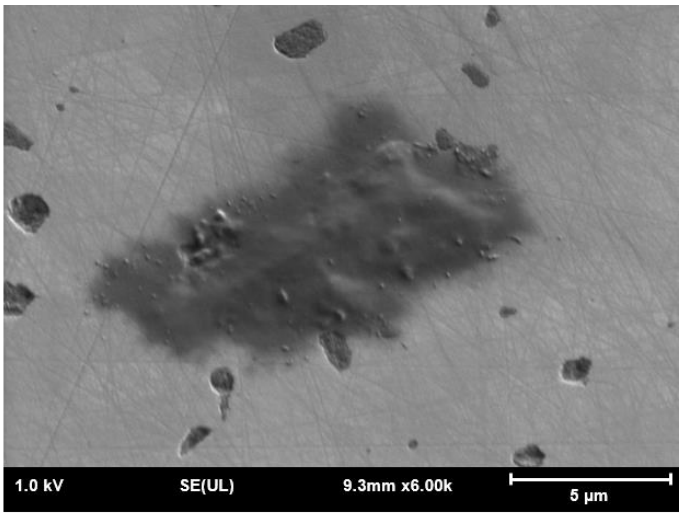

(b) Focus on DN gel particle

Fig. 4-3 – SiC surface after a friction mode 1 (10 N – 10 mm/s), (a) Friction track and (b) focus on a DN gel particle on the friction track

It shows an interesting phenomenon, indeed, for a stable friction coefficient along the 30 m sliding distance (friction mode 1), the friction track is clearly delimited. Out the friction track DN gel particle of about 50 µm can be found. Probably carried out by the lubricant out of the contact. Besides, the on-friction track remaining particles are much smaller. The size magnitude of the DN gel particle on the friction track is about 5 µm. A high particle stick to the surface, indeed thanks to the shadow I can see the edge part of the speck being quite

adhere, and the center part of the mot is higher than the edges, it seems more consistent.

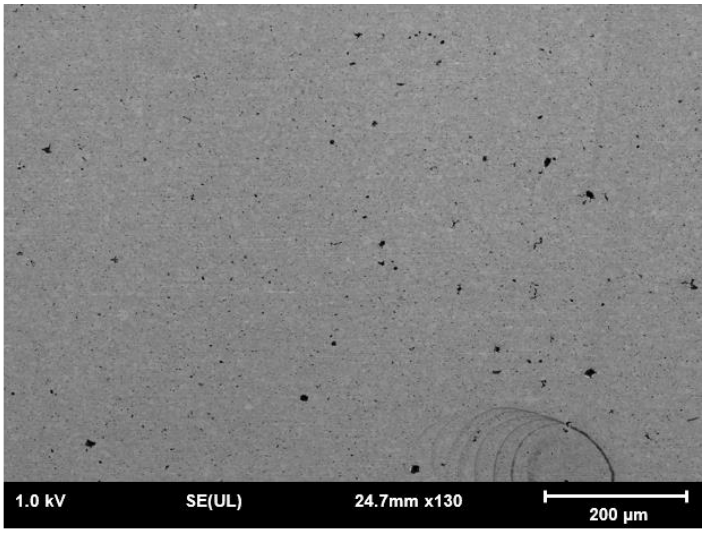

(a) Friction track

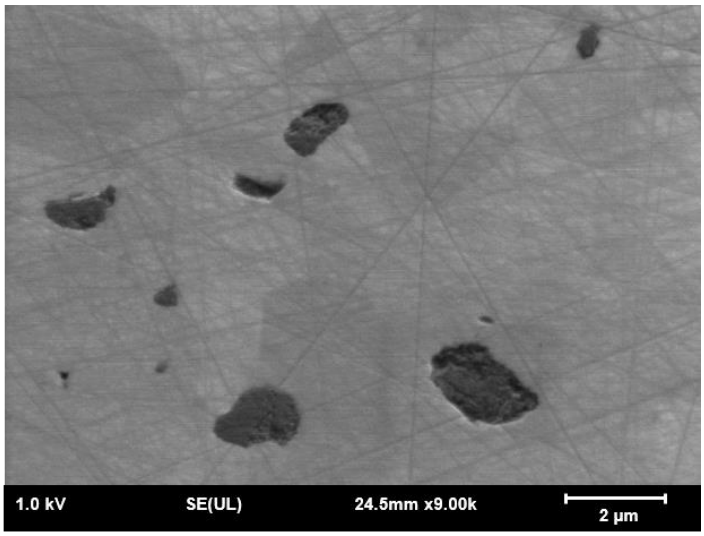

(b) Focus on DN gel particle

Fig. 4-4 – SiC surface after a friction mode 2 (1 N – 100 mm/s), (a) Friction track and (b) focus on a DN gel particle on the friction track

For a simple decreasing friction coefficient, called friction mode 2, the SiC surface is different. No particles can be found, indeed, the gray nuances noticed on the surface are from the SiC phases and spots are SiC pores. It seems clear that for this relatively short run-in case the phenomenon occurring is mainly based

on the lubrication regime. In this case, if the hydrodynamic lubrication regime is occurring the surfaces are less in contact and the lubricant is the shearing material allowing a low friction. It can explain why the SiC surface does not show any DN gel spot or adhered particles.

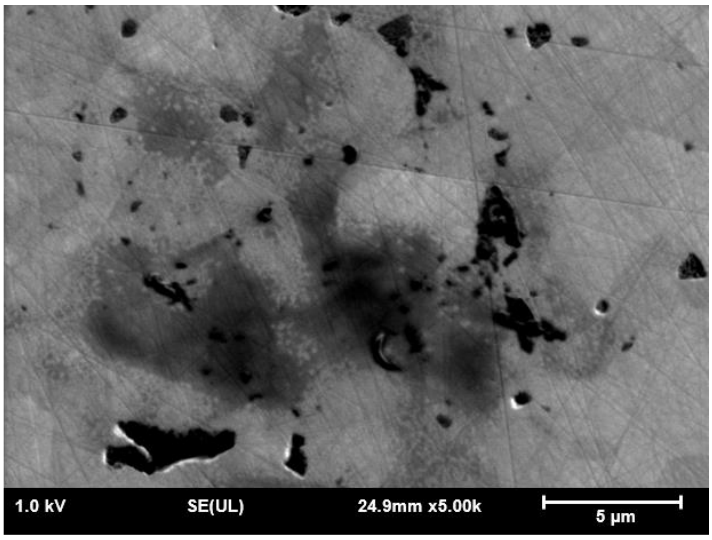

(a) Focus on DN gel particle

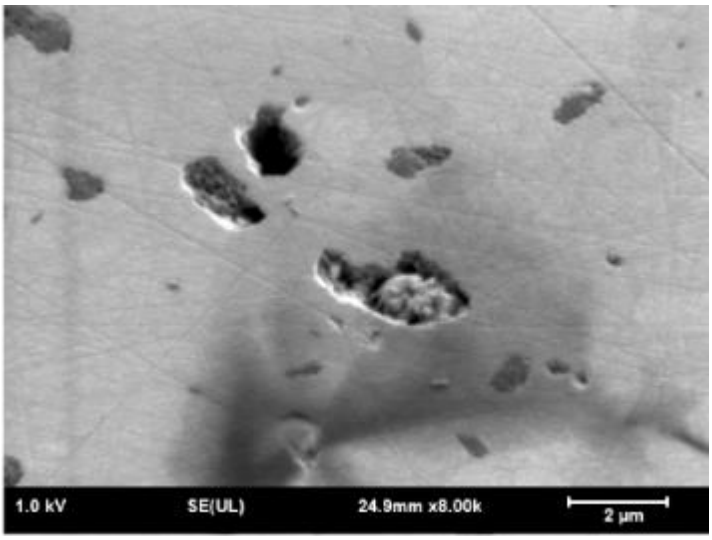

(b) Focus on DN gel particle

Fig. 4-5 – SiC surface after a friction mode 3 (0.5 N – 90 mm/s), (a) and (b) focus on a DN gel particle on the friction track

Finally, for the double decreasing and super low friction coefficient (friction mode 3), the SiC surface has a different appearance after friction. Friction track

is more difficult to find with a low magnification. However, some DN gel particle on the estimated friction track are found. Conversely of particles from the mode 1, here specks are almost fade, seems like encrusted into the SiC surface. These images proved a real adhesion of the particles on the SiC. This can be the creation of a hydrophilic surface, because it is made of DN gel, that improve the sliding of the thick water film during hydrodynamic friction and reduce to an out range value the friction coefficient.

4.2. DN gel wear observation after friction by optical microscopy

4.2.1. Protocol before observations

In the DN gel wear the roughness of the counter material has an extreme importance as explained on this study [6], the sliding speed will graduate the influence of roughness on the soft material sliding. As describe in this study [7], damage type on polymers are multiple and it is a complex process. Several systems implies a friction between a soft and a hard material. As, for example, the tires on the road, the joints in waterproof mechanical systems or other bio applications. Most of the studies concerning soft material on metals expose three different mains and typical wears [8]:

- Abrasive wear (depending on the roughness of the hard material the soft polymer is often affected by the metallic friction)
- Fatigue wear (from a repetitive stress applied on the soft material some cracks can be created)
- Adhesive wear (the soft material often adhere on the metallic side)

Exact interaction occurrence between two solid materials is difficult to fully understand. Then, if I replace a solid material by a soft one, it becomes even more complex. Indeed, chemical interaction and nonlinear following soft material comes in the interaction. The understanding of the interaction becomes difficult to elucidate. In our case, the resulting wear on the DN gel film side was investigated. Finally, after the friction test, the DN gel film sample was removed from the sample holder. Its shape, then, goes back to initial position, meaning it is flat. The wear scar's shape will be changed by the sample's shape changing. However, as every sample were observed the same way, the information given by this observation can bring a better understanding on the interface action.

4.2.2. Results of wear on DN gel

First, the optical microscope was used to take images of the wear scar on the DN gel film, after removing it from the sample holder.

4.2.2.1. Full wear

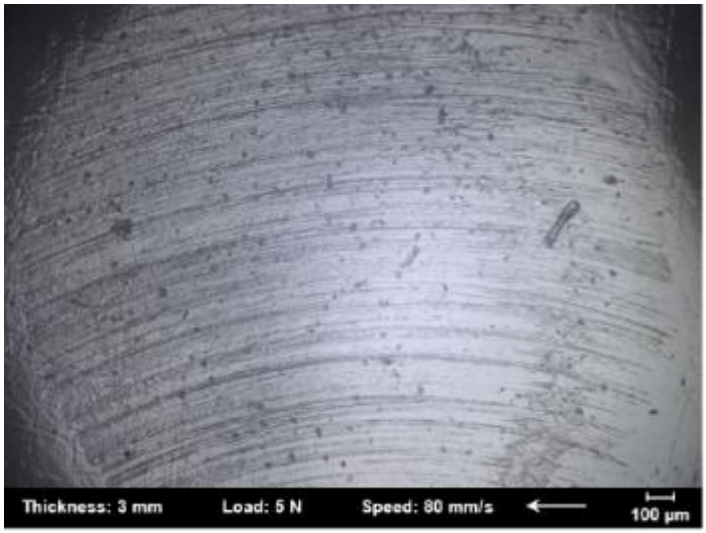

(a) After a friction of 5 N – 80 mm/s on a 3 mm thick DN

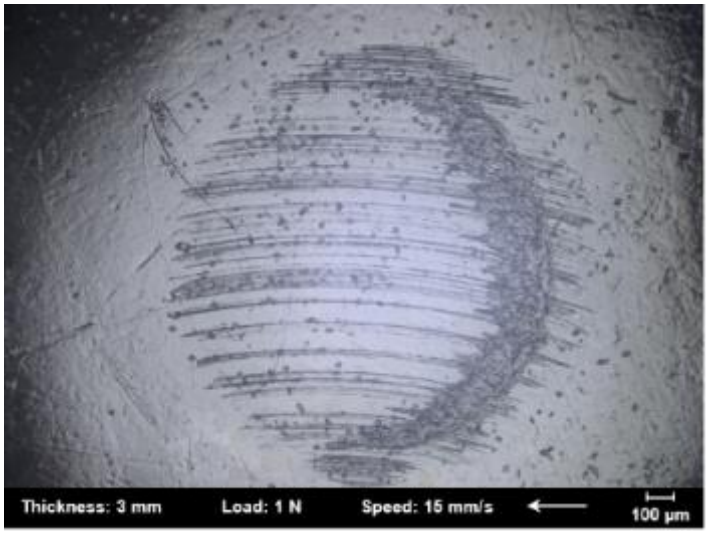

(b) After a friction of 1 N – 15 mm/s on a 3 mm thick DN gel

Fig. 4-6 – DN gel wear scar observed by optical microscopy in case of full worn surface after a friction of (a) 5 N and 80 mm/s and (b) 1 N and 15 mm/s

Fig. 4-6 regroups two images in the case of full worn surface, the friction direction of the counter surface is indicated by the white arrow, sliding parameters are notify at the bottom of the image. For most of 3 mm thick cases, the observed wear scar appears to be all along the friction contact. Indeed, the diameter of the worn surface is similar to the contact diameter measured during indentation on the mesh sensor, depending on the applied load.

In these images I notice repeatable linear scratches following the friction direction. Also, I can see the typical polymer wear, a Schallamach wave like pattern, on the “attack” side of friction. On this side of the contact area a tensile stress is applied instead of the other side. The surprising thing is the Schallamach wave like pattern is slightly deported from the edge of the contact.

4.2.2.2. Partial wear

Fig. 4-7 represents two pictures of typical called partial worn surface of DN gel. This type of wear is noticed on both thicknesses. It is even more representative of the tensile stress occurring at the "attack" side of the friction.

(a) After a friction of 1 N – 5 mm/s on a 6 mm thick DN gel

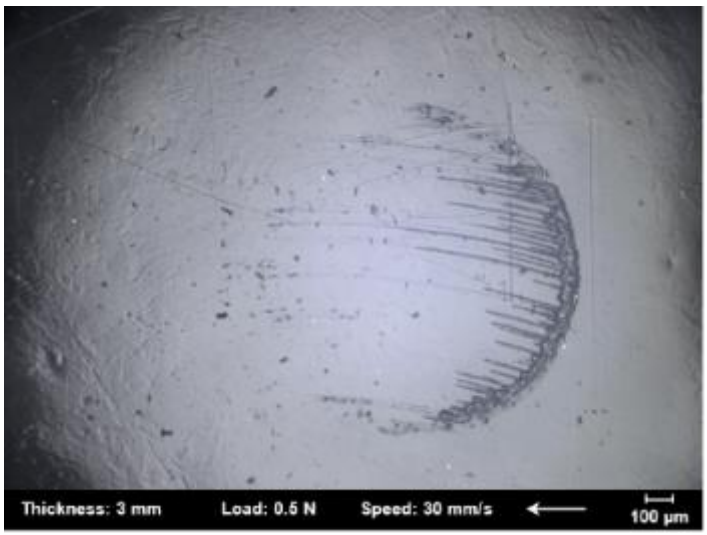

(b) After a friction of 0.5 N – 30 mm/s on a 3 mm thick DN gel

Fig. 4-7 - DN gel wear scar observed by optical microscopy in case of partial worn surface after a friction of (a) 1 N and 5 mm/s and (b) 0.5 N and 30 mm/s

4.2.2.3. No visible wear by optical microscope

(a) After a friction of 0.5 N – 30 mm/s on a 6 mm thick DN gel

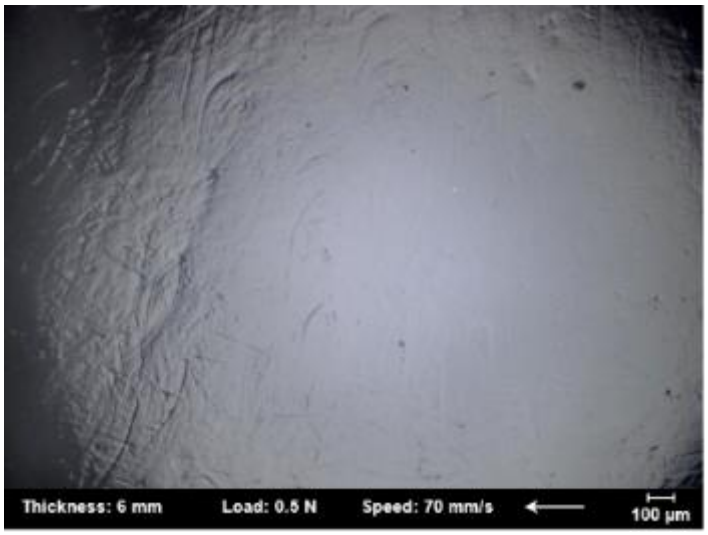

(b) After a friction of 0.5 N – 70 mm/s on a 6 mm thick DN gel

Fig. 4-8 - DN gel wear scar observed by optical microscopy in case of not worn surface after a friction of (a) 0.5 N and 30 mm/s and (b) 0.5 N and 70 mm/s

Some DN gel samples observed did not shows visible marks of wear. This behavior is unexpected but even under several types of observation no scar can be noticed on some surface samples. This is particularly noticed on thicker DN gel (6 mm). Also, it seems to be link with a super low friction behavior. Certainly, the wear type and the friction mode of the friction coefficient are closely link but it is not linear.

4.2.3. Wear shape

The wear can be categorized as previously presented (full, partial, not visible by optical microscope). Besides, the wear scar itself, independently from the surface proportion, also has different appearances.

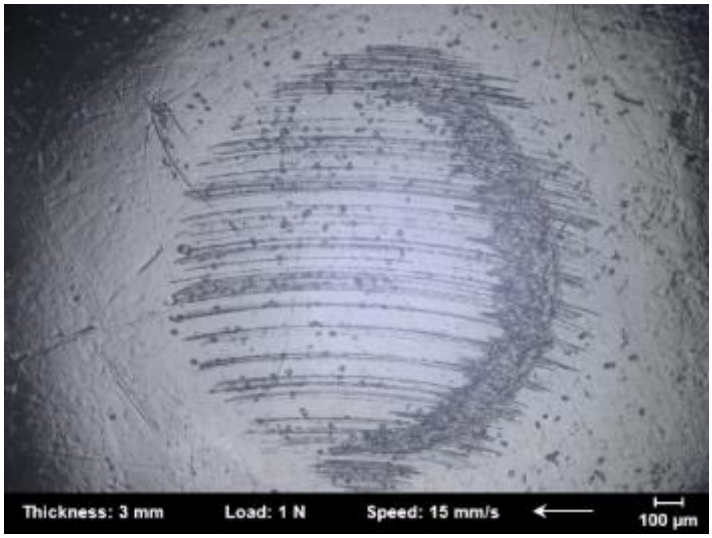

Fig. 4-9 - SEM image of the DN gel film after friction, adhesion and abrasive wear after a friction of 1 N and 15 mm/s

This image shows the abrasive character of the wear because of the marks all along the wear interface. It is also a proof of the adhesion of DN gel against SiC. These marks are caused a fatigue stress, due to adhesion of the DN gel. It is tensed and compressed alternatively because of the not continuous adhesion. This hypothesis has been proved by a video. Then, by filming the friction interface using a glass plat instead of SiC, it was clear that the adhesion create this kind of pattern. In this case the glass plate and the DN gel film have a stronger adhesion than SiC and DN gel film. Then, the adhesion process was much clearer. An alternative adhesion forced the DN gel to tense and release repetitively. Fig. 4-10 shows the adhesion process at different moment of the friction; the arrows indicated the sliding direction of the counter surface. The different times (T1, T2 and T3) are taken at 0.05 m, 0.15 m and 0.5 m distance respectively. This process led to the particular damage I can observe at the surface of most of the samples. That means even by using a lubricant at the interface the adhesion probably occurs and can be fatal for the friction coefficient.

However, even by trying to link the friction coefficient final value or behavior with the appearance of the adhesive mark it was not possible to find a clear relationship. Thus, there is no relation between the adhesion and the friction values. Finally, a link between the friction mode and value with the first definition of wear types (full, partial and not visible) is established. This relationship is exposed thereafter.

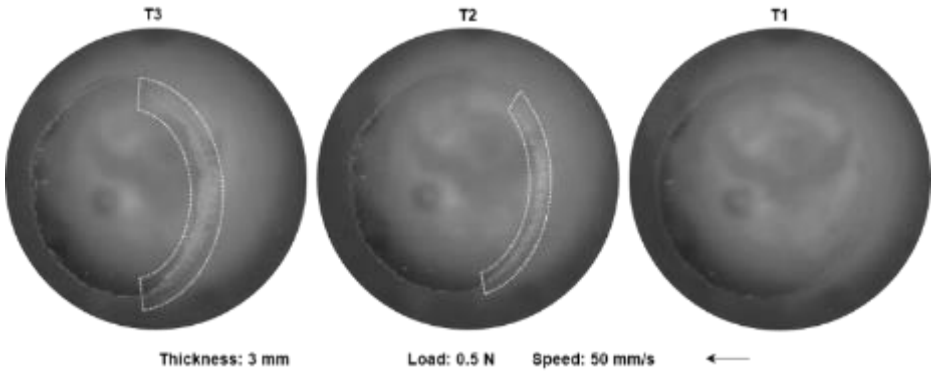

Fig. 4-10 - Interface of DN gel film on a glass plate during friction at 0.5 N and 50 mm/s

4.3. Relationship between wear type and friction mode

4.3.1. Hypothesis

Then, by a first hypothesis the DN gel film is expected to not show any abrasive wear on its surface if the friction mode correspond to an extremely low, then hydrodynamic regime. However, this result is not always observed. There is some incertitude link with the sample itself. The other hypothesis is to understand why thinner and thicker DN gel are capable to reach low friction. In our opinion, two phenomena are occurring at the same time. The hydrodynamic regime, especially for the thicker DN gel is occurring. Indeed, the 6 mm DN gel has the lower contact stiffness, also, its wear is sometimes not observable by optical microscope. However, the 1.5 mm thick DN gel shows different properties, the super low friction coefficient can be reached but the contact stiffness is much higher in this case. Then, hypothesis could be a sparse layer is forming at the interface in the case of thinner DN gel because exact good condition are gathered. Then, the association of sparse layer and hydrodynamic regime can allow thinner DN gel to reach low friction.

4.3.2. Type of wear scar probable repartition depending on DN gel thickness

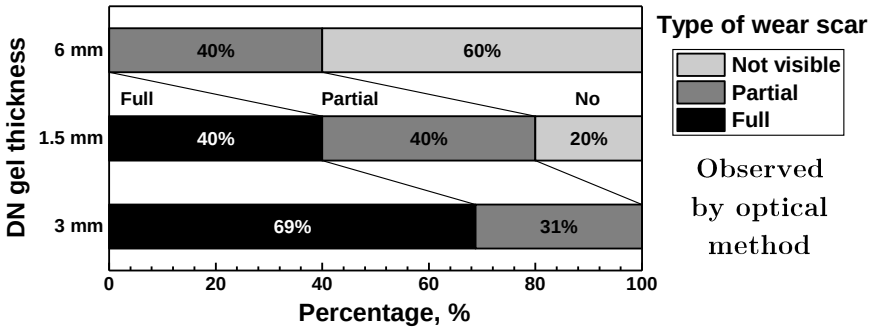

Fig. 4-11 –Percentage of different wear types depending on the DN gel thickness

From Fig. 4-11, the proportion of three wear types are different and linearly changing depending on the thickness used. It is clear that 3 mm thick DN gel, a full wear scar is observed mainly. By using a 6 mm thick DN gel the wear cannot be observed by optical method. Finally, the 1.5 mm thick DN gel shows full or partial almost equally, also 20% are not observable.

The phenomenon occurring using 1.5 mm thick DN gel still needs to be understood by means of detailed observation or in-situ test apparatus. Then, for future application, to understand the DN gel material, it is necessary to take care of its damage level. The wear of hydrogel is the main drawbacks and important factor to consider friction mechanism.

4.3.3. Relationship between friction property and wear property

In order to find out this relation and also understand why a thinner DN gel film can reach same friction coefficient as a thicker one. By plotting the relation between friction mode and wear type observe on the DN gel film side, it is possible to find out what is occurring at the interface.

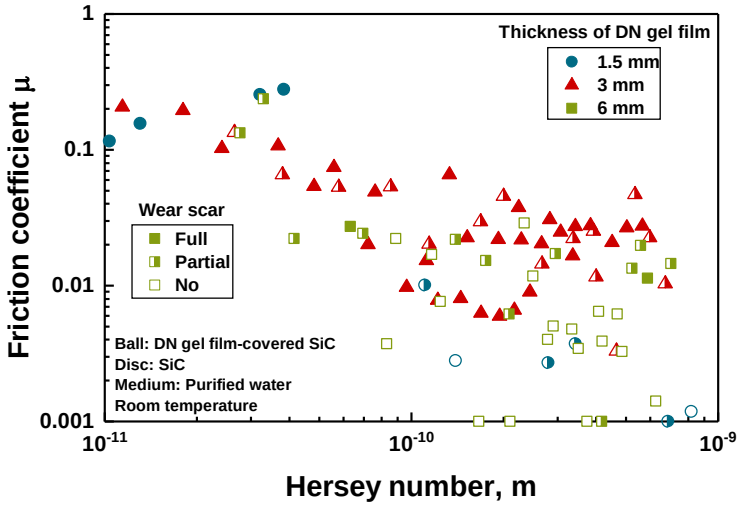

Fig. 4-12 - Relationship between friction property ad wear property

The average of the friction coefficient depends on Hersey number and the comparison with the wear type observed, clearly indicates the dependence between the wear type and the final average friction coefficient and reciprocally (cf. Fig. 4-12). One observation is for friction mode 1 there is a majority of full wear, for friction mode 2, there is mainly no visible wear and for friction mode 3 partial or no visible wear are noticed. Finally, as exposed previously, the wear is probably not the only influent parameter but also damage, which includes the inner surface change. At this stage, the optical microscope technic is probably limited to understand the phenomenon occurring on the DN gel surface during friction mode 3, with the double run-in period and understand the different mechanisms of friction mode 2 and 3.

4.4. DN gel wear observation after friction by Scanning Electron Microscopy (SEM)

4.4.1. Sample preparation

. The DN gel is a particular material, first of all it is a hydrogel. Then, its water content is its main composition. Then, this material is fully transparent.

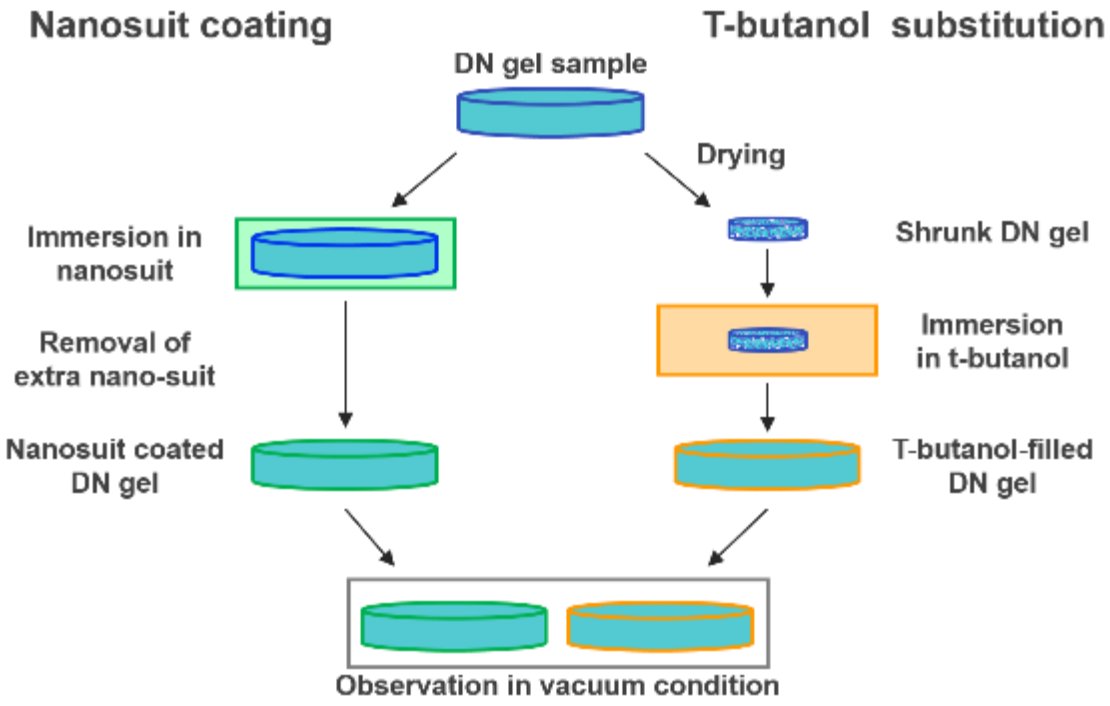

Fig. 4-13 - Sample preparation technics before SEM observation

The Scanning Electron Microscopy (SEM) observation was a suitable apparatus to understand what is happening at the interface. Indeed, the method allows to reach extremely small scales. However, this apparatus needs to run under vacuum condition. Then the water content in the DN gel sample can highly evaporate. In order to avoid and significantly reduce this phenomenon, two technics were used: the first one is by using a nano-suit covering thin polymer [9] and the second one is by using T-butanol solution, both solutions are exposed in Fig. 4-13.

The first solution is based on a technic used by researchers to observe living insects [9]. They used a thin polymer film to cover insects and prevent from water

evaporation. By using the same technic it is possible to observe DN gel by SEM [10].

However, as a thin film is deposed on the surface it is difficult to determine the thickness of this film and how it is covering the worn surface. Then, the T-butanol technic was also used. First the DN gel sample was dry to remove all its water content. Then, it was immersed into a T-butanol solution. Then, it was possible to observe the sample swollen by this solution but the roughness is not covered by it.

4.4.2. Observation using nano-suit covering

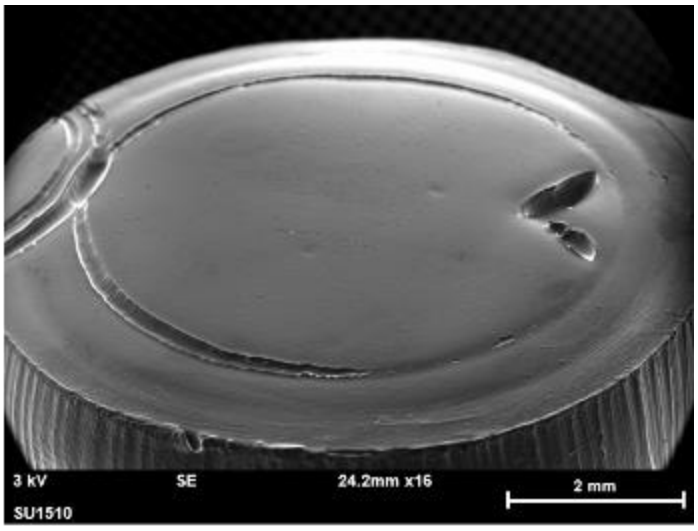

(a) General view of the sample after friction

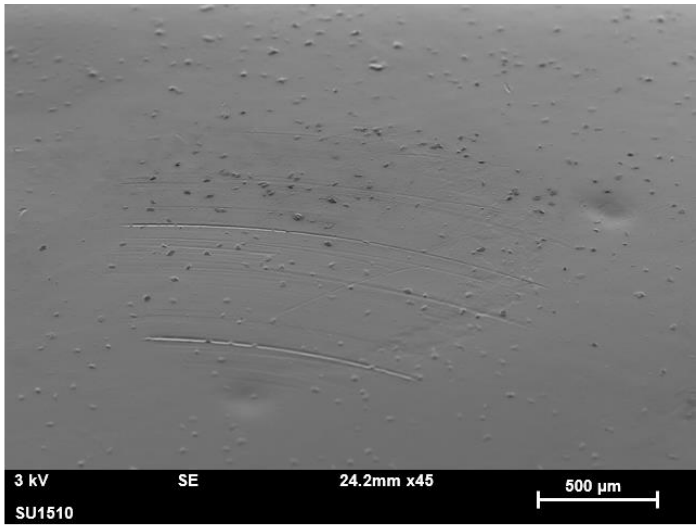

(b) Focus on the wear mark after friction

Fig. 4-14 – Wear on 3 mm DN gel after friction of 1 N and 60 mm/s with nano-suit covering

The nano-suit covering is suitable to avoid the evaporation of water during DN gel observation. The sample does not shrink due to the lack of water. The Fig. 4-14 is an image of the DN gel sample after friction. A mark all around the sample is noticeable because of the sample holder. Also, an arrow was drawn in order to recognize the direction of friction during observation. On the following, mark after friction is clearly observable after friction. The worn area is a circle of about 1.5 mm diameter. Of course, the worn diameter cannot be exact because the DN gel have been folded to take place into the specimen holder, the DN gel have a curved shape during friction. However, for the observation under SEM the DN gel sample was remove from its holder and it recovered to a flat position.

Even through the DN gel does not shrink and the water is kept thanks to the nano-suit covering, the scratches are hardly distinguished. It is assumed that the nano-suit cover a part of information about what is occurring at the interface during the double decreasing friction mode.

4.4.3. Observation using T-butanol solution

By using T-butanol the wear after friction shows a different aspect depending on the friction mode. Indeed, this observation technic does not cover micrometrical information. From the Fig. 4-15 each image is an observation of the DN gel sample after a mode of friction, compared to initial surface. First, after a friction mode 1 (high and stable friction coefficient), the most severe and scale-like wear scar was noticed. Second, after a friction mode 2, sudden decrease of friction coefficient, the wear is much less important than before. Only fussy scratches along the sliding direction. Finally, after a friction mode 3, linear wear scar of a much smaller geometry are observed.

In this last case, the creation of a typical wear during the first step of friction coefficient probably led to the second decrease and enable to reach a super low friction coefficient. The observable wear is not the only changing parameter. It is assumed that the wear induced on the DN gel surface probably involves internal destruction of the material. This hypothesis is then exploited in the next chapter.

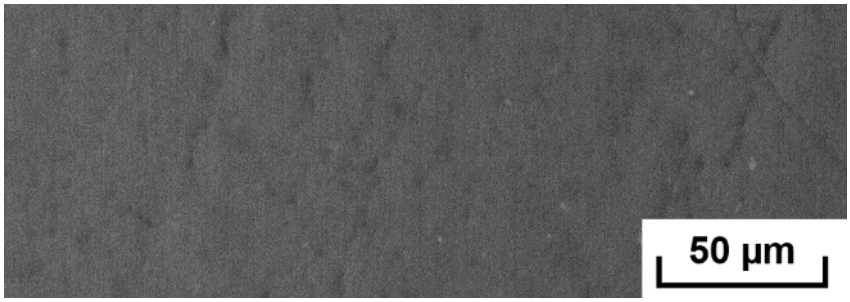

(a) Initial surface

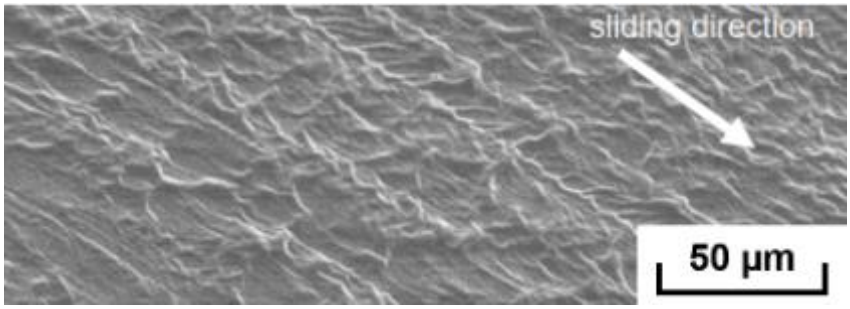

(b) Wear after friction mode 1

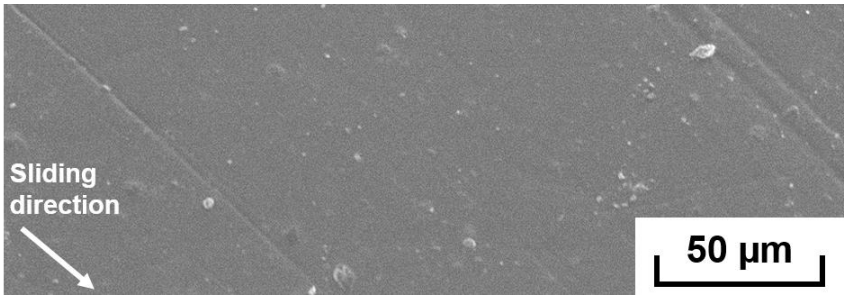

(c) Wear after friction mode 2

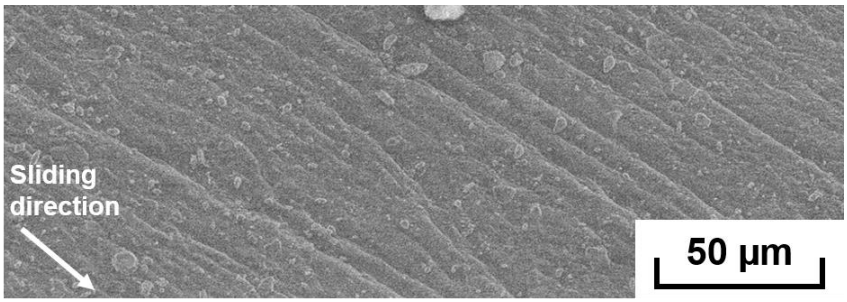

(d) Wear after friction mode 3

Fig. 4-15 – DN gel friction wear after (a) friction mode 1, (b) friction mode 2 and (c) friction mode 3, under SEM using T-butanol technic

4.5. Chapter conclusions

First of all, by analyzing the interaction and focusing on the SiC side, it was highlighted that DN gel particles adhere on the SiC disc. For this observation, the level of adhesion was classified depending on the friction mode. Then, a first conclusion is for the friction mode 1 (stable), the adhesion is strong ~ 10 µm length particles can be found. For the friction mode 2 (simple and sudden decrease) there are almost no adhesion of DN gel on SiC. Finally, for the friction mode 3 (double decreasing and super low friction), adhesion of DN gel can be hardly find, the shape of the adhered particles are different from the friction mode 1. In the super low friction case, DN gel particle are almost incrusted into the SiC surface.

Then by optical microscopy observation the typical adhesion of polymers impact on wear was observed. The adhesion create a scale like wear. Moreover, three main type of wear were defined: a full wear (all along the contact area), a partial wear (on the tensile zone of the contact) and no visible wear (not observable with this apparatus).

That led us to use SEM observation. In order to do so and to avoid the water evaporation due to the vacuum condition, two sample preparation were used: nano-suit covering and T-butanol. The nano-suit covering enable an observation keeping the sample out of shrinkage, however, the nano-suit cover also micrometrical wear. Finally, by using the T-butanol substitution, three different wear can be defined depending on the friction mode:

- Friction mode 1 results in a scale-like severe wear scar
- Friction mode 2 results in a few linear wear scar
- Friction mode 3 results in a micrometrics linear scratch.

4.6. Bibliography

[1] Y. Wang, J. Xu, Y. Ootani, N. Ozawa, K. Adachi, and M. Kubo, "Proposal of a new formation mechanism for hydrogenated diamond-like carbon transfer films: Hydrocarbon-emission-induced transfer," *Carbon*, vol. 154, pp. 7–12, 2019.

[2] M. O. F. Boundary and W. Zinc, "Mechanism of Boundary Lubrication with Zinc Dithiophosphate," *Wear*, vol. 53, 1979.

[3] K. Kato and K. Adachi, "Wear of advanced ceramics," *Wear*, vol. 253, no. 11–12, pp. 1097–1104, 2002.

[4] K. Adachi and K. Kato, "Formation of smooth wear surfaces on alumina ceramics by embedding and tribo-sintering of fine wear particles," vol. 245, pp. 84–91, 2000.

[5] B. J. Hamrock, S. R. Schmid, and B. O. Jacobson, *Fundamentals of Fluid Film Lubrication*. CRC Press, 2004.

[6] B. N. J. Persson and E. Tosatti, "Qualitative theory of rubber friction and wear," *Journal of Chemical Physics*, vol. 112, no. 4, pp. 2021–2029, 2000.

[7] B. Briscoe, "Wear of polymers: an essay on fundamental aspects," *Tribology International*, vol. 14, no. 4, pp. 231–243, 1981.

[8] J. K. Lancaster, "Abrasive wear of polymers," *Wear*, vol. 14, no. 4, pp. 223–239, 1969.

[9] Y. Takaku *et al.*, "A thin polymer membrane, nano-suit, enhancing survival across the continuum between air and high vacuum," *Proceedings of the National Academy of Sciences*, vol. 110, no. 19, pp. 7631–7635, 2013.

[10] J. I. Goldstein, D. E. Newbury, J. R. Michael, N. W. M. Ritchie, J. H. J. Scott, and D. C. Joy, *Scanning Electron Microscopy and X-Ray Microanalysis*. New York, NY: Springer New York, 2018.

Chapter 5 – Super low friction mechanism of tribological system

From the previous chapters, the friction properties and wear properties of DN gel have been widely investigated. From three last chapters the link between DN gel film thickness and capacity to reach super low friction with the resulting wear, is establish. By grouping these information, the mechanisms occurring during friction can be understood, these are exposed in this chapter.

5.1. Super low friction

5.1.1. Friction coefficient trend

As a reminder, the friction coefficient obtained in the friction region II are found out to be different depending on the friction mechanism occurring. The rubbing process is dependent on the DN gel film thickness used.

Indeed, the 1.5 mm or 6 mm thick DN gel can reach super low friction coefficient, $\mu \leq 0.01$. Their run-in period do not have the same tendency. The 1.5 mm thick DN gel have a double decreasing friction coefficient, called mode 3 in the following.

Usually, friction curve of 1.5 mm thick DN gel in the friction region II conditions, follows the friction mode 3, whereas 6 mm thick DN gel follows the friction mode 2, as presented in the chapter 3. Fig. 5-1, puts in parallel the real friction curves and the model of the friction modes previously established.

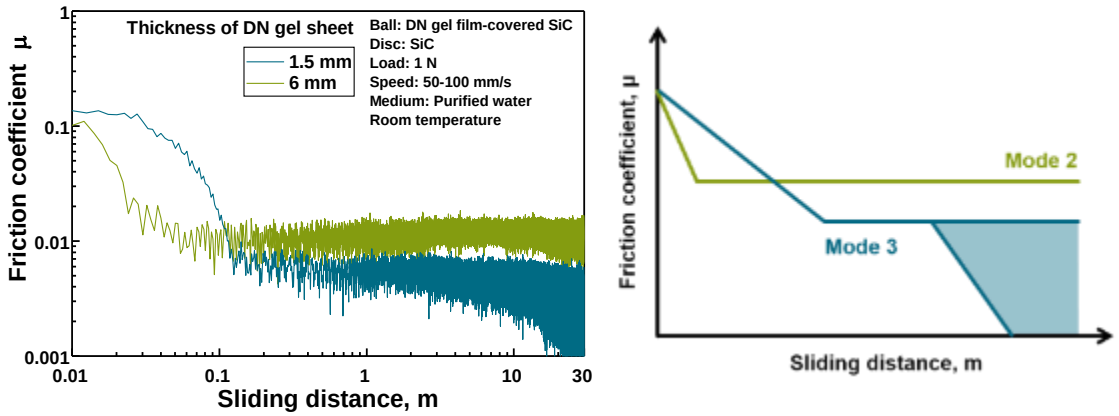

(b) Typical friction coefficient curve using 1.5 and 6 mm thick DN gel

(c) Schematic of typical friction mode 2 and mode 3

Fig. 5-1 – (a) Typical friction coefficient curve using 1.5 and 6 mm DN film and (b) Typical friction mode 2 and 3

5.1.2. After low friction worn surface

Then, in the chapter 4 the wear on the DN gel was underlined. Based on the SEM observation using T-butanol technic it was possible to see a clear difference of the damaged surface of the DN gel depending on the friction mode.

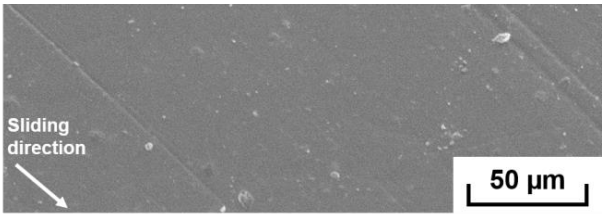

(a) DN gel worn surface after friction mode 2

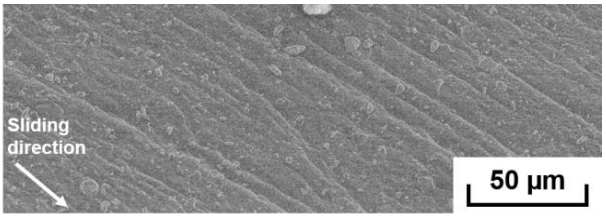

(b) DN gel worn surface after friction mode 3

Fig. 5-2 – SEM observation of wear scar after (a) friction mode 2 and (b) friction mode 3

After a friction mode 2, which is a sudden decrease of the friction coefficient, the DN gel worn surface shows dispersed scratches with a flat surface in between. After friction mode 3, the wear scar for DN gel is much more damaged, however, the scale of the damage does not exceed micrometer.

This discovered damage surface seems to be the key for the double decrease friction coefficient mode 3 understanding.

5.2. DN gel under mechanical stress change

5.2.1. Definition of sacrificial bonds

In these more recent studies [1]–[5], the phenomenon of sacrificial bond is described by other researchers. It was initially qualified as really advantageous for the mechanical resistance of the material. The sacrificial bond is a general principle, it consists of long chains which bear several bonds, coming from its name. These bonds, called sacrificial bonds, have a peculiarity: they can be broken without breaking the chain. Then, the network gains a "hidden length". This is how the PAAm network acts as a shield because it can absorb deformations without breaking.

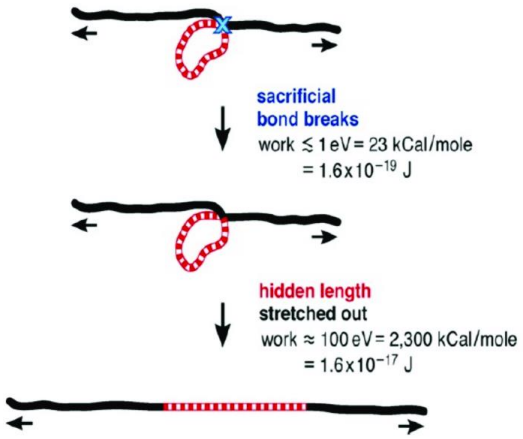

Fig. 5-3** – **Schematic of the sacrificial bonds principle [6]

It is now interesting for other properties. In this recent study [4], the unbinding of the sacrificial bonds is understood to bring a high toughness to the DN gel similarly to the bones. Then, properties can be used differently than only for

strengthening the material. Therefore, this property may be the cause of a positive modification for the tribological properties of the DN gel.

5.2.2. Internal damaged layer caused by tensile stress

From several studies about double networks hydrogels (DN gel) their high resistance is demonstrated. In fact, the creation of these new hydrogels principle relies on a different role for each of the polymer network. As one entity cannot meet all the requirements for an ideal material, the combination of two inhibits a better hydrogel; this is why the DN gel was created. Even though the components among DN gels vary, the idea is the same. In our case, the polymers used are PAMPS and PDMAAm. The parallel can easily be drawn with the PAMPS and PAAm DN gel. Indeed, the latter has been extensively studied, especially about the role of each network. The first network is the same (PAMPS) and the second is also coming from the acrylamide family (PAAm and PDMAAm). For example, in this study by Prof. Gong [7], the DN gel is analyzed in terms of mechanical resistance. The conclusion is that both networks play an important role in the strength of the material. One is brittle and the other is flexible.

Fig. 5-4 (a) shows the behavior of the DN gel (here PAMPS / PAAm) during a tensile stress. This diagram clearly shows the role of each network. PAMPS is the brittle network resisting sudden stresses while PAAm is the flexible stress absorbing network. This study, from 2010, does not yet name this behavior of elongation which do not break the PAAm network. Later, in 2012 and after, this behavior is called sacrificial bonds, in several research works [1]–[5]. Then, by the sacrificial bond principle the PAMPS chain can break without breaking the PAAm chain, thus a new type of surface called sparse layer appears, its creation is clearly shown in Fig. 5-4 (b).

The PAAm chain is elongated by the sacrificial bond principle. The resulting appearance of DN gel is changed. This is due to an internal damage of the structure. This sparse layer is less dense than the inner structure of DN gel, the water can easily come into the top layer, allowing it to become more hydrophilic [8].

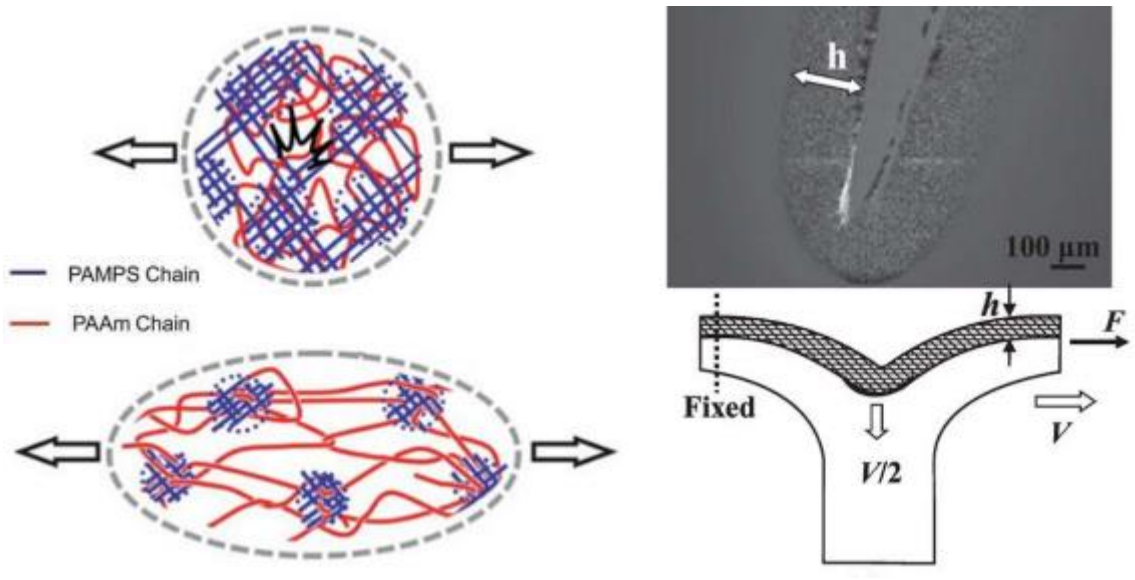

(a) Schematic of damaged DN gel by tensile stress

(b) Image and schematic of the creation of an internal damaged layer by tensile

***Fig. 5-4** – (a) Schematic of a damaged DN gel by tensile stress and (b) image and schematic of the creation of a sparse internal damaged layer by tensile stress* [7]

5.3. Realization of double running in by formation of sparse layer

From the comparison of different volume of polymer in the DN gel, it has been clarified that a low polymer density keep water more easily than high condensed polymer [8]. I estimate that the internal damaged layer, previously presented, presents a lower fraction density. Therefore, the mode 3 could be the process creation of a damage layer enabling more water at the interface and a thicker water film creation. Then, this hypothesis was investigated using an in-situ apparatus.

5.3.1. Apparatus for in-situ observation

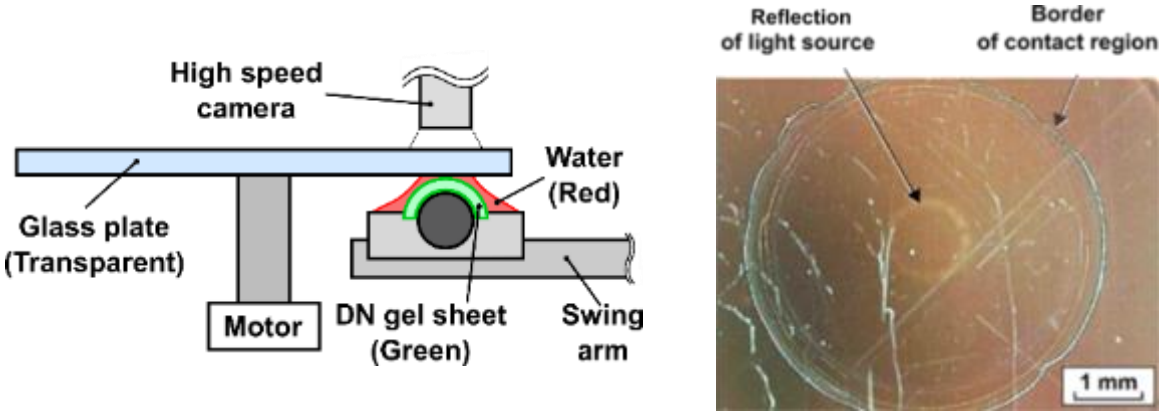

(a) Schematic of in-situ friction apparatus

(b) Image of the contact between DN gel and glass plate

***Fig. 5-5** – (a) Schematic of in-situ friction apparatus and (b) initial image of DN gel in contact*

A glass plate tribometer (cf. Fig. 5-5 (a)) is used to observe the direct contact of friction. By this tribometer equipped with a camera (VW-9000, Keyence and lens (VH-Z20T, Keyence), the interface can be seen through the glass plate, as shown in the Fig. 5-5 (b). This in-situ apparatus allows to understand the phenomenon at the interface. The water was colored in red and DN gel sample in green, to improve the observation quality.

The Fig. 5-5 (b) is the initial image of the loaded DN gel through the transparent glass plate. White circular lines indicate the border of contact between the deformed DN gel and the glass plate. White linear scars were initially presenting on the opposite side of the glass plate, they are not involved in the friction process against the DN gel. Also, the reflection of light source is seen as a circumferential white region at center of the contact.

5.3.2. Results during friction

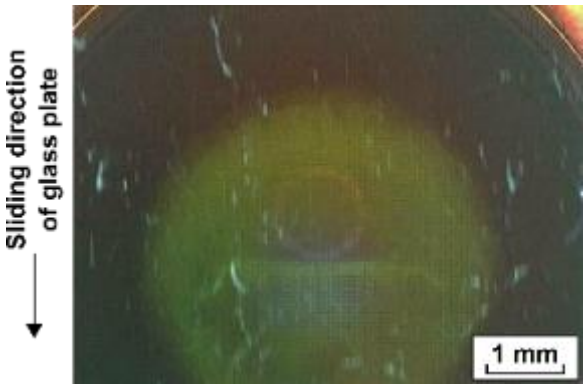

(a) Observation during friction mode

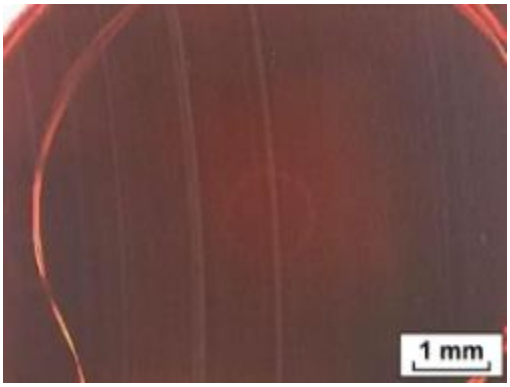

(b) Observation during friction mode 2

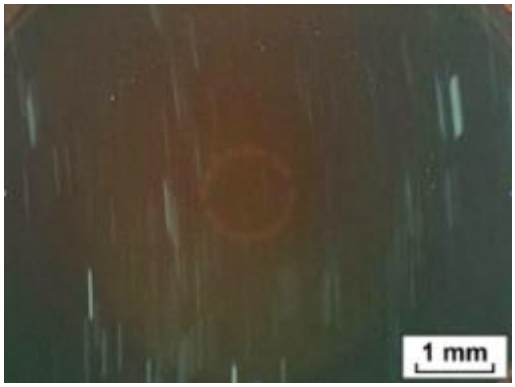

(c) Observation during friction mode 3

Fig. 5-6 – In-situ typical image of sliding interface at a saturated state during (a) friction mode 1, (b) friction mode 2, and (c) friction mode 3

These *in situ* images of corresponding friction mode 1, 2 and 3 highlighted about the lubrication regime occurring during friction. Indeed, in the case of

friction 1 it was determined as a direct contact between DN gel and glass plate due to the boundary lubrication regime occurring the green color of the DN gel can be clearly seen in Fig. 5-6 (a). In the friction mode 2, the hydrodynamic lubrication regime is found out due to the consistence presence of water red color, in Fig. 5-6 (b). Finally, the complementarity of red a green color show a dark color in the case on friction mode 3, Fig. 5-6 (c), meaning a mixture of red water into green DN gel.

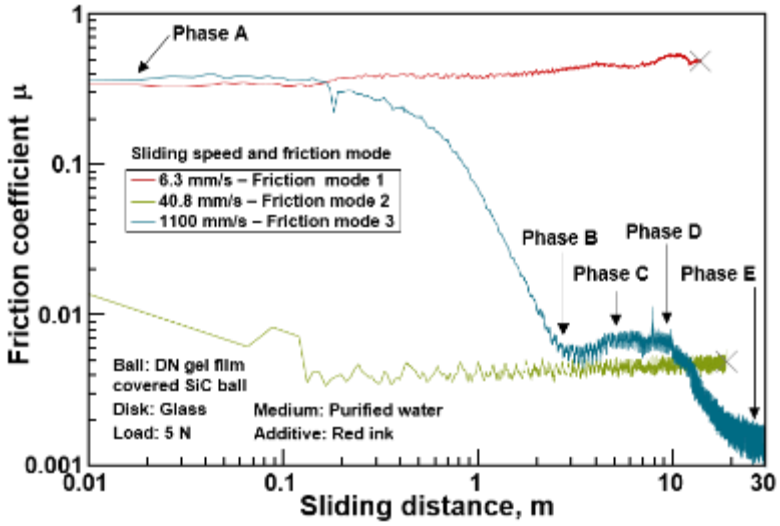

***Fig. 5-7** – Friction coefficient obtained using glass apparatus for the friction mode 1, 2 and 3*

Typical friction behavior achieved by the *in-situ* apparatus are shown in Fig. 5-7. The friction mode 3 was cut into 5 phases:

Phase A: Friction begins, decrease of friction coefficient.

Phase B: Friction coefficient saturates after the first decrease.

Phase C: Friction coefficient shows stable value.

Phase D: Friction coefficient starts to show a second decrease.

Phase E: Friction coefficient saturates after the second decrease.

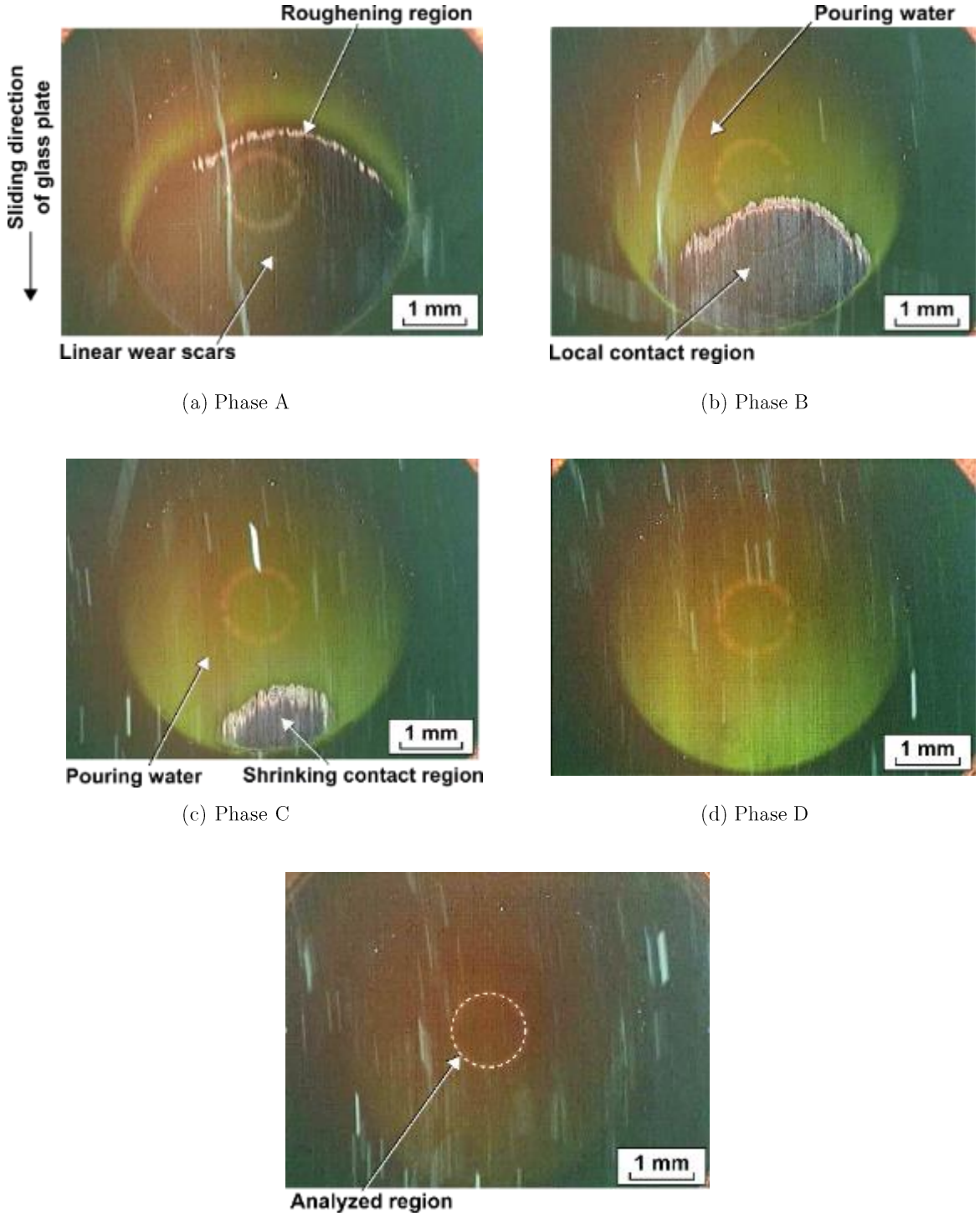

(a) Phase A

(b) Phase B

(c) Phase C

(d) Phase D

(e) Phase E

***Fig. 5-8** – In-situ observation of DN gel at (a) phase A, (b) phase B, (c) phase C, (d) phase D, and (e) phase E during friction mode 3*

A series of DN gel surface images at phases A, B, C, D, and E are shown in Fig. 5-8. At phase A, a roughening region is seen as a curved white belt on the top of the DN gel contact region. In addition, linear wear scars are formed below the white belt region along the sliding direction of sliding glass plate. A green region, where the red external water disappeared between the glass plate and the DN gel surface, is seen above the white belt region. As the phase shifts from A to B, the curved white belt region moves lower along the sliding direction of the counter surface. At phase B, the contact region is shrunk at the bottom of the initial contact region from phase A and more apparent linear wear scars are seen in the localized contact region. In addition, red water flows between the DN gel and the glass plate from above. From phase B to C, the localized contact region still moves lower and shrinks. Moreover, the red water continues to flow between the DN gel and its sliding counterpart. At phase D, the localized contact region disappears and the DN gel starts to have uniform contact with its sliding counterpart. From phases D to E, the whole region gets darker.

Based on the DN gel images and friction properties, the first decrease of the friction coefficient in mode 3 is estimated as follows: the local contact region between the DN gel and its sliding counterpart dominates the friction process due to adhesion and the friction coefficient decreases as contact area causes. Finally, applied tensile stress by sliding counterpart forms internal damaged layer automatically beneath the DN gel surface.

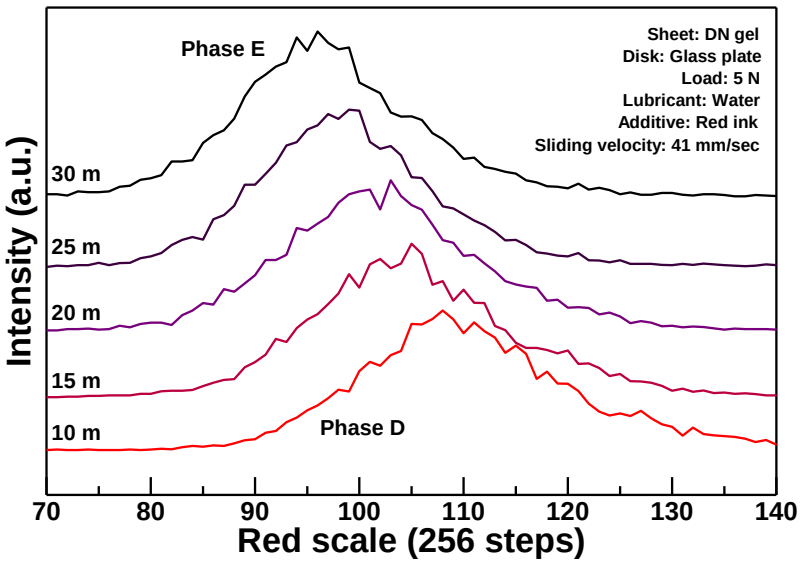

Fig. 5-9 – Transition of red scale at the contact region of the DN gel

From phase D to phase E, the friction coefficient shows a second decrease, the red scale at the center of the contact region on the DN gel was analyzed every 5 m of sliding distance. The transition of the red scale is shown in Fig. 5-9. The red scale has a broad distribution and shows a peak value at approximately 110 steps at phase D in mode 3. Then the peak value of the red scale shifts lower as the sliding distance increases from phase D to E. Finally, a peak position is observed at 95 steps approximately, when the sliding distance is 30 m (at phase E). Since the mixture of the red and green ink shows a black color, the darkening of the DN gel images from phase D to E indicate that water including red ink penetrates more and more into the internal damaged layer formed beneath DN gel surface. It is not only a creation of water film between the surfaces but it is a change of the DN gel top surface that led to this color change.

Finally, from this observation, the generation mechanism of mode 3 is estimated as follows: The internal damaged layer is formed beneath the DN gel surface when this surface is roughening from phase A to phase D due to shear stress. Furthermore, the water between the DN gel surface and its sliding counterpart penetrates the internal damaged layer and the water concentration at this region becomes higher than initial state. As explained by previous research [8], water-rich region in hydrogel enables to keep water interface than water-depleted surface, thus internal damaged layer is believed to form water interface automatically through generation process of mode 3.

After phase D, the internal damaged layer enable the creation of a thicker water layer. It suppresses the direct contact between the DN gel networks and sliding counterparts; thus, a second decrease of the friction coefficient occurs due to an increase of water concentration in the internal damaged layer.

However, as the friction mode 2 does not shows a double decrease friction coefficient, this interface is a thick water film as shown in Fig. 5-6 (b). Finally, the formation of an internal damaged layer is a necessary but is not sufficient condition to enable a double decrease of the friction coefficient. Since mode 3 occurs under relatively smaller load conditions compared to mode 2, a larger contact load can disable the role of the internal damaged layer to attract a water layer. Higher mechanical toughness of the DN gel prevents the wear of internal damaged layer and the remaining internal damaged layer continue to form a thin water layer.

5.3.3. Discussion of mechanisms depending on friction modes

5.3.3.1. Friction mode 2, without second run-in, mainly occurs using 6 mm DN gel

As previously stated, the super low friction coefficient reached with a thick DN gel film (6 mm) is due to the hydrodynamic lubricant regime occurring from the beginning (cf. Fig. 5-10). Indeed, the system contact stiffness is much softer than for other cases. Also, it was shown in the chapter 4, only a few wear scratches can be observed. This induce a thick water layer separates both surfaces during friction.

(a) System with 6 mm thick DN gel film

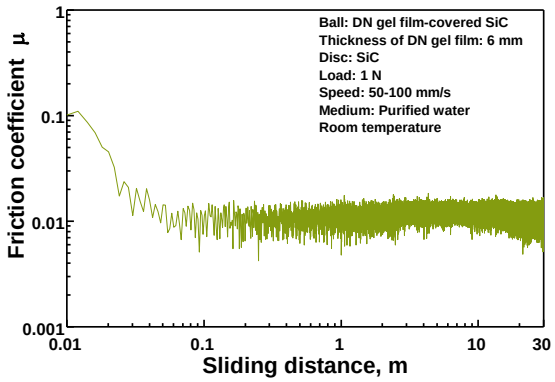

(b) Friction coefficient using 6 mm thick DN gel film

(c) Mode 2 friction interface

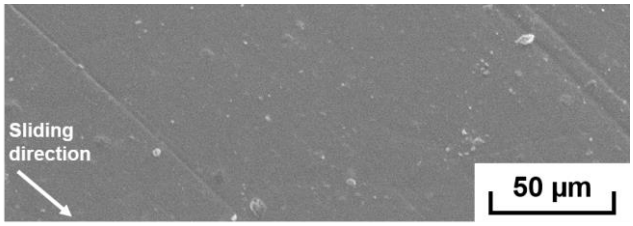

(d) Wear on DN gel after friction mode 2

***Fig. 5-10** – Data obtained previously for the (a) 1.5 mm thick DN gel film system, (b) its friction coefficient, (c) its friction interface and (d) the wear on the DN gel surface*

5.3.3.2. Friction mode 3, with second run-in, mainly occurs using 1.5 mm DN gel

Friction tests also revealed a super low friction by using 1.5 mm thick DN gel film, however, the friction coefficient tendency was different with a double run-in

period (cf. Fig. 5-11). Thus, mechanisms are different. The stiffer contact of the system leads to the formation of a damage layer during the first run-in period due to the tensile stress. Then, the sparse layer enable the attraction of water, inducing a thin layer formation during the second run-in period. Finally, another lubrication regime is reached by the thinner film creation at the interface. The run-in period is crucial to achieve such a low friction due to the creation of a sparse layer by high stiffness contact, enabling a water layer. Therefore, the creation of a sparse layer, suitable for low friction.

(a) System with 1.5 mm thick DN gel film

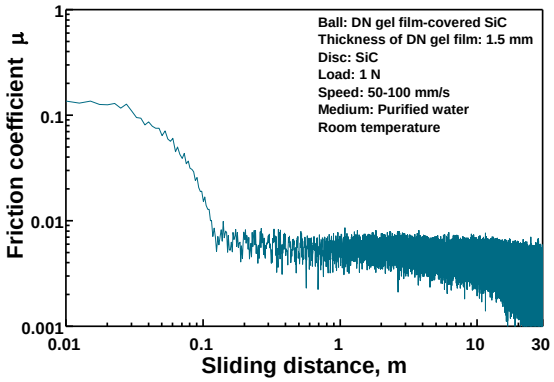

(b) Friction coefficient using 1.5 mm thick DN gel film

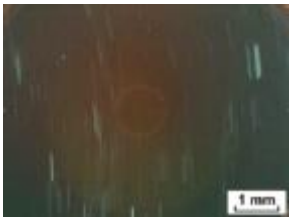

(c) Mode 3 friction interface

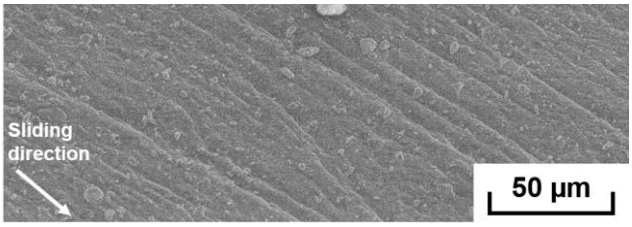

(d) Wear on DN gel after friction mode 3

***Fig. 5-11** – Data obtained previously for the (a) 1.5 mm thick DN gel film system, (b) its friction coefficient, (c) its friction interface and (d) the wear on the DN gel surface*

As widely introduced, the cartilage, this excellent natural tribological material also has a structure changing with its depth, chondrocytes and collagen fibers are parallel to the surface on the top layer to improve the friction whereas they are oriented perpendicularly to ensure the strength in the depth. Also the sliding surface has a concentration of water higher than the deeper one [9]. Finally, it is what is happening with the DN gel by the damage layer creation. This mechanism enable a water concentration more important on the sliding surface.

5.3.3.3. Mechanisms of friction

By grouping the information from previous chapter and this chapter, the aim is to understand the phenomena occurring during friction mode II, especially for 1.5 mm thick and 6 mm thick DN gel film. Because each thickness mainly highlight the friction mode 2 and 3, respectively. The friction region 2 presents complex situation, depending on the thickness of the DN gel film and on the system contact stiffness different phenomena occurs. The difference between friction mode 2, without second run-in and friction mode 3 with a second run-in is represented in the Fig. 5-12.

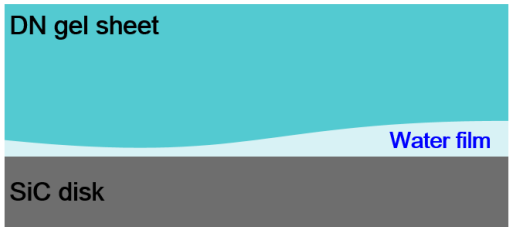

(a) Without second run-in

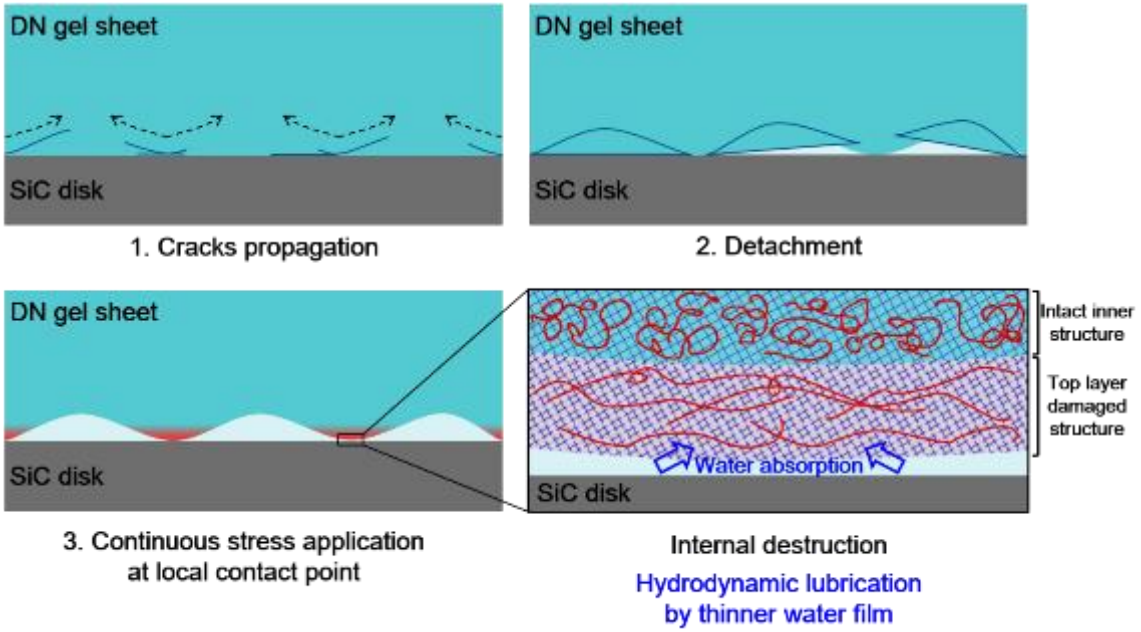

(b) With second run-in

Fig. 5-12 – Schematic of friction mechanisms occurring in case of friction mode 2 (a) without run-in and in case of friction mode 3 (b) with second run-in

5.4. Chapter conclusions

In this chapter, mechanisms processes involved in the friction on the DN gel are understood. Friction of DN gel has 2 mains regions: Friction region I which is driven by the adhesion of DN gel on SiC. The friction mode in this region is friction mode 1. Then, in the friction region II, which is driven by the water interface, two main types of friction mode can be found: Friction mode 2 mainly found using 6 mm thick DN gel film and friction mode 3 mainly found using 1.5 mm thick DN gel film. These two lasts were deeply investigated in this chapter. Thus, from the correspondence to the friction mode, the DN gel film thickness and the observed wear, the mechanisms occurring can be explained as follows:

1. By using 6 mm thick DN gel, the contact stiffness of the system is softer. Then, a thick water film can be formed at the interface easily and hydrodynamic lubrication is realized due to relaxed contact stress.
2. By using 1.5 mm thick DN gel, a stiffer contact interface is obtained. Then, shear-induced tensile stress causes damaged region on the DN gel surface, allowing thin water film to be formed since damaged region attracts water. Finally, the super low friction coefficient is obtained by the creation of thinner water film absorbing external water in the interface.

Preparation of low friction interface for DN gel before its usage is expected to apply DN gel for various types of sliding part in actual machine design.

5.5. Bibliography

[1] Q. Chen, H. Chen, L. Zhu, and J. Zheng, "Fundamentals of double network hydrogels," *Journal of Materials Chemistry B*, vol. 3, no. 18, pp. 3654–3676, 2015.

[2] J.-Y. Sun *et al.*, "Highly stretchable and tough hydrogels," *Nature*, vol. 489, no. 7414, pp. 133–136, Sep. 2012.

[3] M. A. Haque, T. Kurokawa, G. Kamita, and J. P. Gong, "Lamellar bilayers as reversible sacrificial bonds to toughen hydrogel: Hysteresis, self-recovery, fatigue resistance, and crack blunting," *Macromolecules*, vol. 44, no. 22, pp. 8916–8924, 2011.

[4] T. Nonoyama, "Robust hydrogel–bioceramics composite and its osteoconductive properties," *Polymer Journal*, vol. 52, no. 7, pp. 709–716, 2020.

[5] M. A. Haque, T. Kurokawa, and J. P. Gong, "Super tough double network hydrogels and their application as biomaterials," *Polymer*, vol. 53, no. 9, pp. 1805–1822, 2012.

[6] G. E. Fantner *et al.*, "Sacrificial bonds and hidden length: Unraveling molecular mesostructures in tough materials," *Biophysical Journal*, vol. 90, no. 4, pp. 1411–1418, 2006.

[7] J. P. Gong, "Why are double network hydrogels so tough?," *Soft Matter*, vol. 6, no. 12, pp. 2583–2590, 2010.

[8] Y. Gombert, R. Simič, F. Roncoroni, M. Dübner, T. Geue, and N. D. Spencer, "Structuring Hydrogel Surfaces for Tribology," *Advanced Materials Interfaces*, vol. 6, no. 22, p. 1901320, Nov. 2019.

[9] A. J. Sophia Fox, A. Bedi, and S. A. Rodeo, "The Basic Science of Articular Cartilage: Structure, Composition, and Function," *Sports Health: A Multidisciplinary Approach*, vol. 1, no. 6, pp. 461–468, Nov. 2009.

Chapter 6 – Application of DN gel as tribological and biomedical material

This final chapter is split in two parts: tribological material application and biomedical material application. In the first part and based on previous chapters, the role of a damaged layer creation in the resulting friction coefficient was understood. The purpose here, is to induce the damaged layer before friction test. The second part is based on biomimicry. Indeed, the DN gel appears to be an ideal material for cartilage replacement from literature. Based on this background, the DN gel properties (elasticity, viscosity) and its resemblance to cartilage are controlled. An improvement of the DN gel to suitable cartilage regeneration substrate (elasticity and surface texture influence) is envisaged.

6.1. Tribological application

In this first part the aim is to use facts previously founded to improve the DN gel in friction. The mechanism was understood and the method to obtain it must be clarified. Then, voluntary damage layer will be produced on the DN gel surface.

6.1.1. Texture effect on friction, state of the art

6.1.1.1. Hard material texture influence

1.1. In the tribology field, research topics more and more concentrate about the texture and the roughness of the contact materials. Indeed, several studies focused, for example, on texture application on SiC. This texture change of the SiC surface can provide a better load capacity and results in a lower friction coefficient. This is due to the change of hydrodynamic pressure [1]–[3]. The applied texture can also have a positive effect during the boundary lubrication regime. That is to say,

the texture will improve the friction in the case of low sliding speed and/or high load applied conditions. In this following study [4], the size and shape of the texture have also been investigated. The texture have a great influence on the boundary lubrication and can drastically reduce the friction coefficient due to the creation of small reservoirs of lubricant. This observation cannot be true when there is no lubricant at the interface. Other studies focused on the texture to change the wettability of the surface in order to create, depending on the lubrication regime, a thicker lubricant film at the interface [5].

6.1.1.2. Soft material texture influence

Other studies also focused on a texture applied on the hydrogel side [6], clamming the importance of a well-chosen texture shape and size. Indeed, I easily imagine the texture on hydrogel creating small reservoirs of lubricant (most of the case water for hydrogel), then helping to drastically reduce the friction coefficient. However, the right equilibrium must be found. The texture on hydrogel can also be reservoirs of air, in this case, it can increase the adhesion if there is a lack of lubricant. Then, a lot of parameters must be considered to efficiently use the texture on either hard counter surface side or hydrogel side. The texture induced on hydrogel can also be initiation of wear than can easily degrade after friction.

In our case, the purpose of the addition of texture is to manage the sparse layer before using the DN gel. The creation of a damage layer by friction led to a double run-in behavior friction coefficient.

6.1.2. Application of texture on DN gel

6.1.2.1. Process of application

First, from the previously presented hypothesis of 1.5 mm thick DN gel having a stiffer contact can create a favorable texture for low friction. By using a thin grain (2000) abrasive paper at the interface between SiC disc and DN gel film a defined texture was applied.

The same apparatus than for friction test was used (cf. Fig. 6-1), with a similar load (1 N) and a low sliding speed (5 mm/s) for every sample for the texture process. Then, motor rotates 1 cycle to the left and 1 cycle to the right to avoid a texture direction influence.

Also, the texture was applied without water at the interface. However, after the application of the texture the sample was firstly rinsed under pure water and then soak into pure water for several hours before using it for friction test. This step allows to remove any extra particles coming from the abrasive paper that could increase the wear on the DN gel surface during friction test.

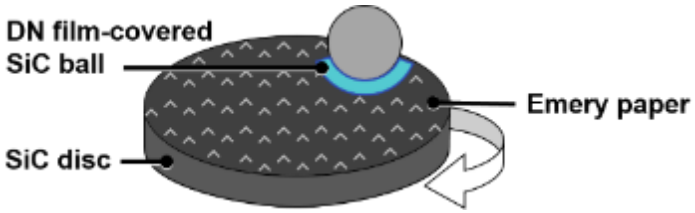

Fig. 6-1 - Schematic representation of the application of a texture on DN gel surface

The following image Fig. 6-2 is the abrasive paper observed in SEM. The abrasive particles are bright in the gray scale and the binder is dark. The abrasive particles are about 10 µm scale.

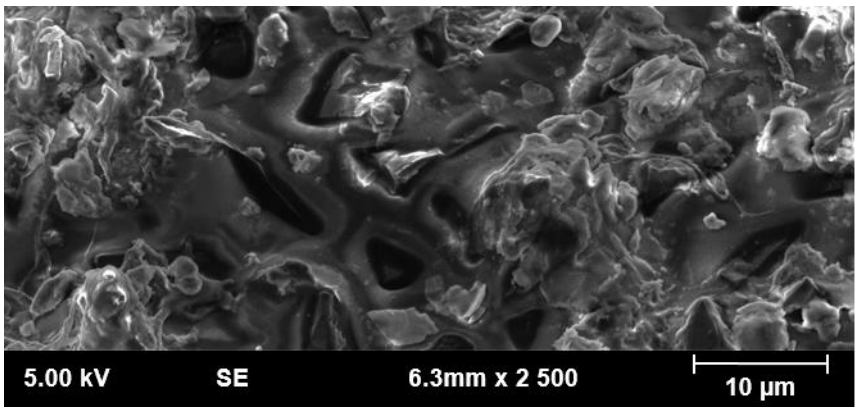

Fig. 6-2 - Emery paper of 2000 observed in SEM

6.1.2.2. Observation of the applied texture

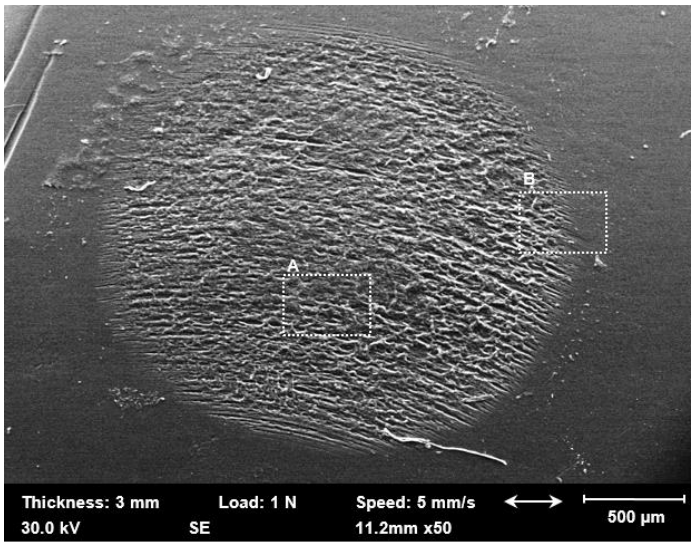

Fig. 6-3 - SEM observation of the textured DN gel by abrasive paper

After application of the texture, the DN gel sample was checked by SEM apparatus. The size and shape of the applied texture was observed to have an estimation of the texture magnitude.

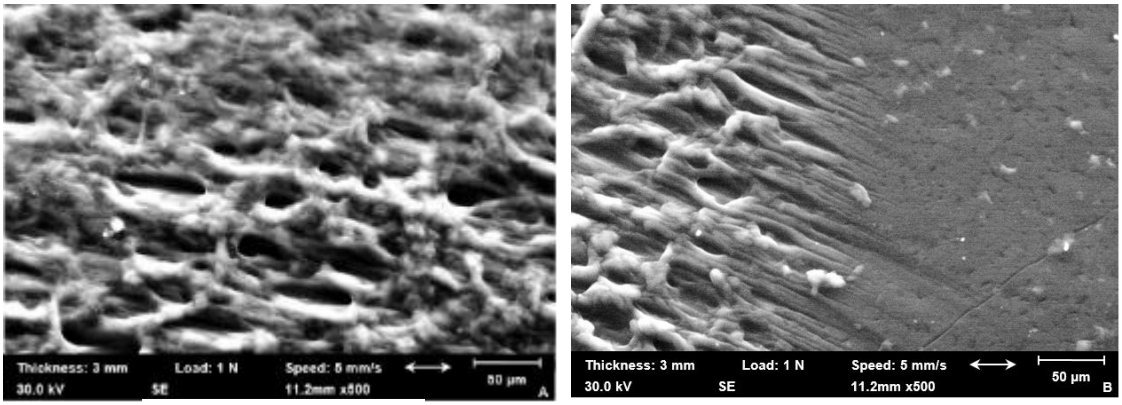

(a) Focus on zone A (b) Focus on zone B

Fig. 6-4 – (a) focus A and (b) focus B of the previous image Fig. 6-3 on the texture and on the limit between the initial and the textured surface

Through these images it is clear that the textured surface lets the inner network of polymer appears. On the Fig. 6-4 (a) the network with pore of 10 to 50 µm length are exposed and not protected by the initial surface. By applying the texture on the DN gel, inner networks is show outside. Also, the direction of the network is oriented on the abrasive paper friction direction. Then, the holes between the connections are slightly oblique due to the movement direction.

6.1.3. Effect of texture on DN gel properties

6.1.3.1. Effect of texture on stiffness and adhesion force

6.1.3.1.1. Apparatus used

For this evaluation of texture influence on DN gel properties, the indentation tests was used. In this case the indentation depth was set up as fixed. In order to understand the effect of the texture on the top surface was indented. For this test, the textured DN gel results were also compared with the different thicknesses. Moreover, this indentation test was performed by a Teflon ball of about 3 mm diameter into the DN gel surface for 500 µm depth. These results are benefic to understand how the texture on the DN gel change the behavior of the top layer, then how it change the interface.

6.1.3.1.2. Stiffness and adhesion force change by texture

Then, after the analysis of the indentation curves for different parameters, the stiffness and adhesion force can be plotted depending on the thickness and on the surface state (pristine or textured).

Fig. 6-5 shows a difference between thicknesses as already understood on the chapter 3. However, it is also noticeable the difference for a same thickness and different surface state. Then, a 3 mm thick DN gel will have a contact stiffness and closer to 6 mm thickness. By introducing a texture, the DN gel film has different surface properties, whereas in Fig. 6-6 it shows an unchanged adhesion force. Then, the friction properties will probably be impacted.

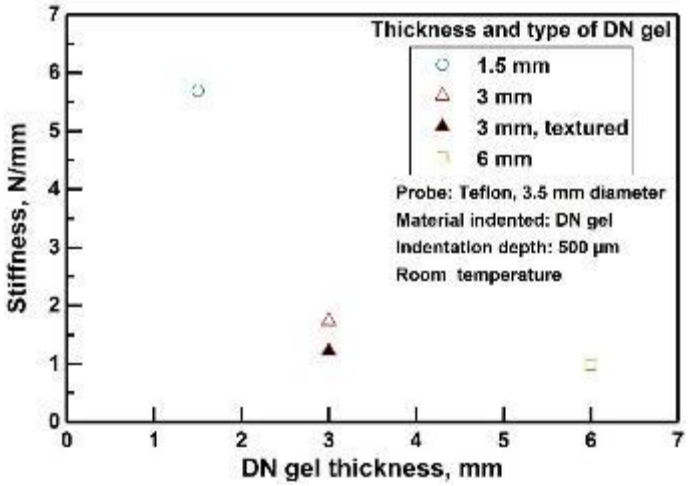

Fig. 6-5 - Stiffness measured by indentation on pristine and textured DN gel

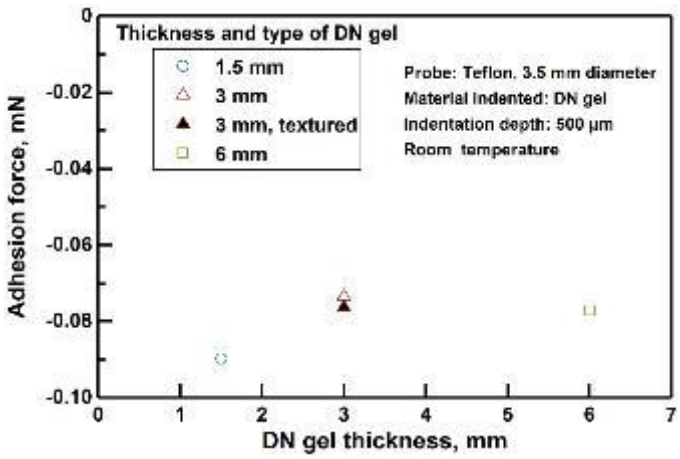

Fig. 6-6 - Adhesion force measured by indentation on pristine and textured DN gel

6.1.3.2. Effect of texture on friction force

6.1.3.2.1. Apparatus used

As for results presented on the chapter 2 and 3, the friction experiments are performed with the same apparatus. By using the rotational tribometer on a range of load and sliding speed similar enough measurements were obtained to draw a conclusion about the influence of the texture on DN gel film. Also, for these experiments and to avoid additional influencing parameters. Experimental tests were performed using a single thickness. The 3 mm standard thickness of DN gel film was used.

6.1.3.2.2. Results of texture influence on friction

6.1.3.2.2.1. Friction coefficient of initial versus textured DN gel

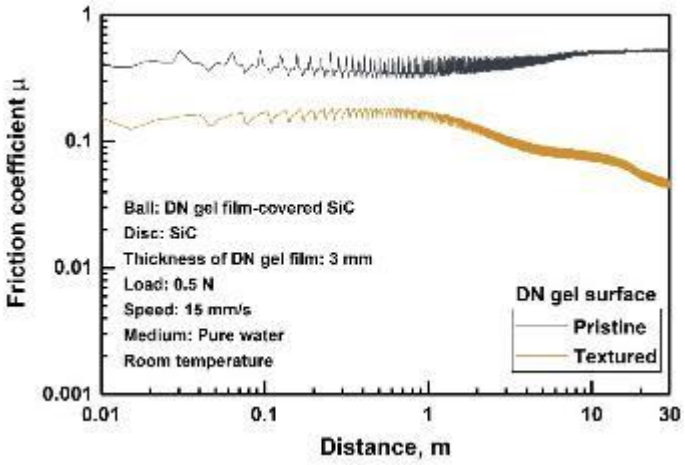

Fig. 6-7 - Friction coefficient of DN pristine and textured DN gel, friction mode 1

The additional texture to the DN gel changes the initially friction mode 1, which means, stable, into friction mode 2. Indeed, the textured sample shows a decreasing friction coefficient after 1 m sliding. Then for a low sliding speed, a friction mode 1 is expected but a decreasing behavior for the exact same conditions is noticed in the case of textured DN gel (cf. Fig. 6-7).

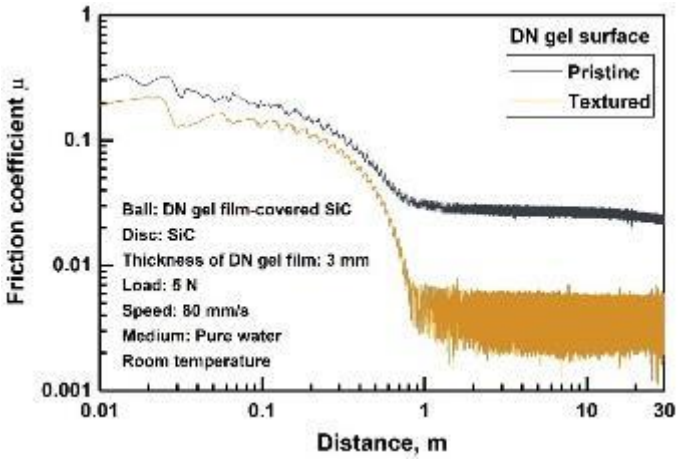

Fig. 6-8 - Friction coefficient of DN pristine and textured DN gel, friction mode 2

A positive influence is also noticed for the friction mode 2, decreasing friction coefficient. The textured DN gel sample shows a similar decreasing trend but in most of the cases it reaches a lower friction coefficient value if compared to the final average friction coefficient of both cases (cf. Fig. 6-8). Finally, by adding a texture to the DN gel surface. It was possible to change the friction mode 2 into a friction mode 3, with an anticipated run-in period. It seems that the initially applied textured reduce the first run-in period (cf. Fig. 6-9). To generalize about the results of textured DN gel friction, it clearly allow the same thickness, then contact area and applied pressure, to reach a lower friction coefficient. By adding a texture on the surface, a favorable interface to obtain super low friction coefficient is introduced. For an exact same condition, a lower friction coefficient is obtained by prior addition of a suitable texture on the sample.

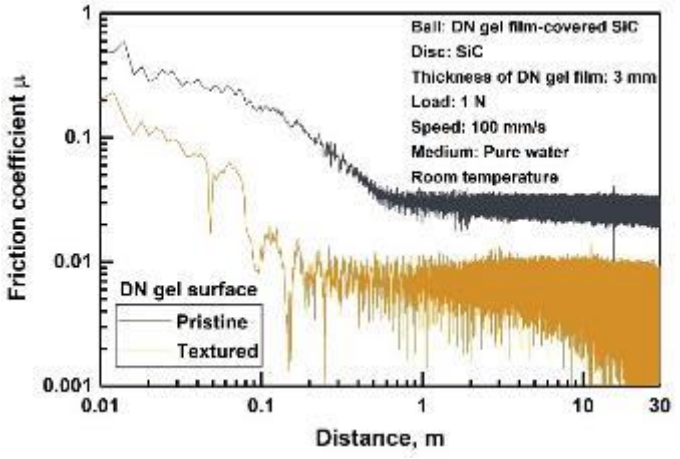

Fig. 6-9 - Friction coefficient of DN pristine and textured DN gel, friction mode 3

6.1.3.2.2.2. Stribeck curve of initial versus textured DN gel

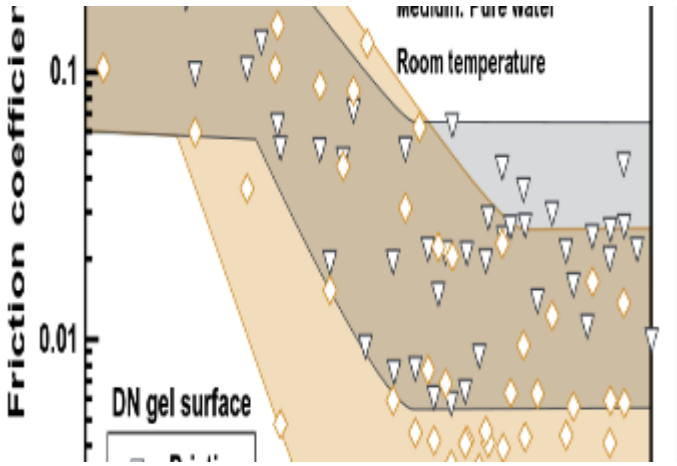

Fig. 6-10 - Stribeck curve of DN gel film pristine vs. textured

Then, as for the thickness comparison, final average values of friction coefficient are plotted depending on the Hersey number. By doing so, it is possible to compare for a same Hersey number, the friction coefficient obtained. Then, the effect of sliding speed and load cannot be responsible of the friction coefficient change but only the texture change. As previously noticed, the friction coefficient can be reduced by the introduction of the texture. Also, the transition occurs previously compared to initial DN gel and the general trend of the Stribeck curve using a texture DN gel is drop to lower friction coefficient. In Fig. 6-10 there is a slight translation of the Hersey condition for friction region I, transition and friction region II to lower values.

6.1.4. Appearance after friction

For this observation, another technic is used. Indeed, in this case the sample was dried before observation in that case the water does not evaporate and the nano-suit do not cover the DN gel sample. Then, the after-friction SEM images of not texture and texture hydrogels shows a difference in term of wear.

Clearly in the case where no texture is applied on the DN gel, the wear is similar as what I already know; that is to say, clear scratches can be noticed and especially at the tensile stress location (Fig. 6-11).

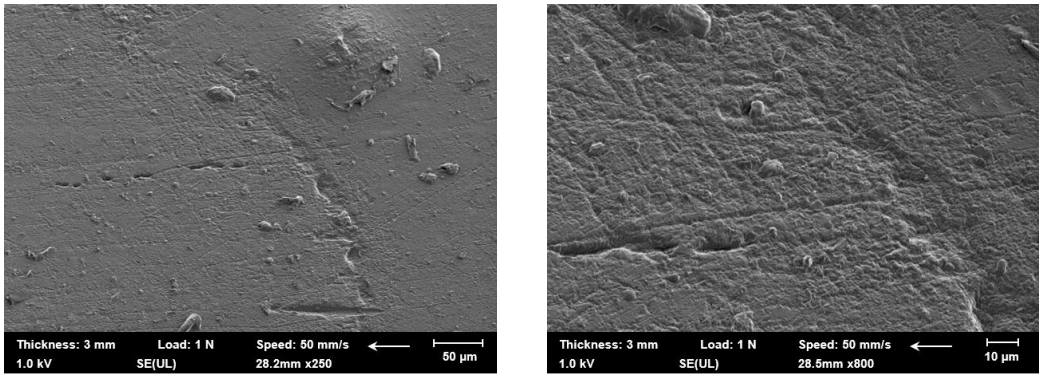

(a) General view (b) Focus view

Fig. 6-11 - Images of DN gel with the initial surface after friction (a) general view, (b) focused view

Fig. 6-12 shows the wear after the exact same friction conditions but this time with a texture applied. From these images, the main conclusion is there is a homogeneity of the surface with the texture. The appearance is slightly different from the initial image presented in section 6.1.2.2. , this is because of the different observation process. However, by comparing the after friction of initial surface and after friction of textured surface, the wear is almost no noticeable on this last case. Then, a texture applied by abrasive paper can reduce the friction coefficient and can drastically reduce the wear. No material removing is observed.

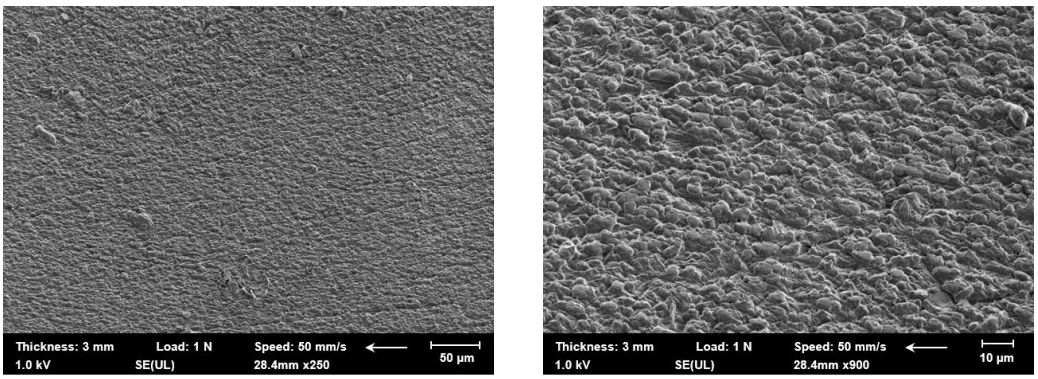

(a) General view (b) Focus view

Fig. 6-12 - Images of DN gel with the textured surface after friction (a) general view, (b) focused view

6.2. Bio-application

Many studies used DN gel as a support to help the regrowth of the cartilage [7]–[10]. The resemblance with this natural cartilage will be checked in term of elasticity and viscosity. Then, the chondrocyte regrowth on DN gel will be explained and our purpose is to improve the quality of these cells. A lot of studies already implies the positive influence of the texture on the cell culture [11]. Then, the texture DN gel will be used to create a better support for the chondrocytes regeneration and improve the usage of DN gel as a direct support for cartilage regeneration.

6.2.1. Comparison with cartilage

6.2.1.1. DN gel mechanical properties

By using indentation and relaxation methods, presented in chapter 2, the mechanical properties of DN gel were measured. In order to entrench the elasticity of this new material in the literature, its values are compared with other material's Young modulus mainly used for biomechanical applications, especially for cartilage substitute. Then, as shown in Table 6-1 the elastic modulus of DN gel and cartilage are almost similar.

Table 6-1 - DN gel elastic modulus comparison with other materials

DN gel	**UHMWPE**	**Substitute of cartilage**	**Chromium Cobalt Molybdenum**	**Natural cartilage**	**PVA/HA composite hydrogel**
0.5 – 2 MPa	1000 – 1258 MPa [12][13]	6 – 10 MPa	210 000 MPa [13]	0.8 – 1.3 MPa [14]	1.07 MPa [13]

It is crucial to have a range of elastic modulus value of this new material because this mechanical parameter is extremely important and play a role in its friction and wear behavior. In the case of biomechanical application, the DN gel is the most promising for mimicking the natural cartilage.

From previous studies viscosity parameters have been determined from cartilage and simple hydrogel. Here these parameters of DN gel are much closer from the cartilage than simple hydrogel. However, the relaxation time is faster in the case of DN gel. That means, the DN gel can recover its shape 10 times faster than cartilage (cf. Table 6-2).

Table 6-2 - Table of viscosity parameters of DN gel, simple hydrogel and cartilage

Cartilage [15]			**DN gel (2mm thickness)**			**Simple hydrogel (PAAm)** [16]		
E_{inst} (kPa)	E_{inf} (kPa)	**T** (s)	E_{inst} (kPa)	E_{inf} (kPa)	**T** (s)	E_{inst} (kPa)	E_{inf} (kPa)	**T** (s)
258 kPa	233 kPa	10.6 s	**388 kPa**	**365 kPa**	**1.95 s**	42 kPa	34 kPa	1. 5 s

6.2.1.2. DN gel aspect and wear

The cartilage aspect has been investigated by several studies. One of the study observed the cartilage before and after friction of sheep joint articulation [17]. This study used a 10-nm layer of gold and carbon for SEM observation of the cartilage. In our case, the DN gel was covered by a thin polymer nano-suit layer to avoid water evaporation and allowed the SEM observation. This methods have been already used for insect observation, in order to keep their water and avoid their immediate death [18].

In some cases, studies about cartilage do not respect a constant hydration state of the cartilage (for example kept in saline solution or other). Therefore, the cartilage can show perturbed surface state. As shown in the study on sheep articulation observation previously cited. This aspect of DN gel can be found also in some DN gel samples under SEM observation. Indeed, since the DN gel loose too much water a different aspect appears and strangely looks like the dehydrated cartilage, with a wave pattern (cf. Fig. 6-13).

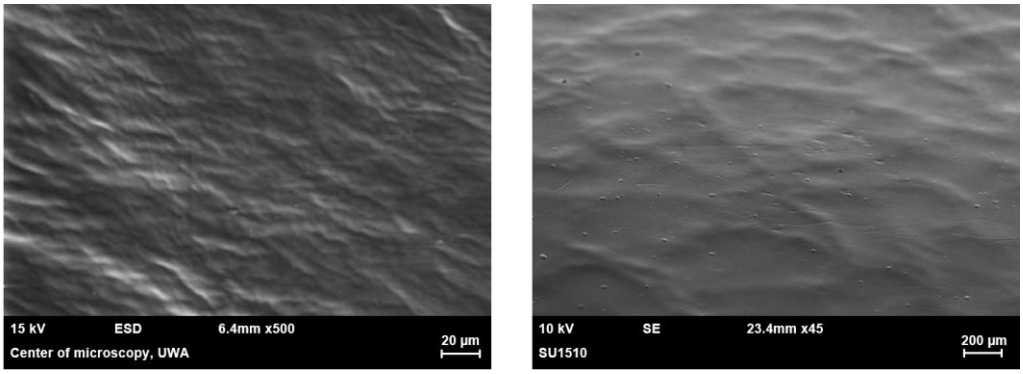

(a) Dehydrated cartilage (b) Dehydrated DN gel

Fig. 6-13 - SEM images of dehydrated (a) cartilage [17]***, (b) DN gel***

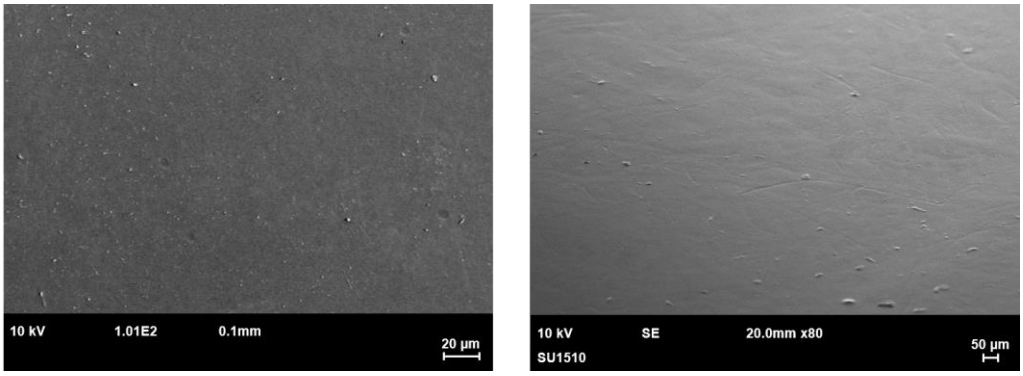

(a) Unworn cartilage (b) Unworn DN gel

Fig. 6-14 - SEM images of unworn (a) cartilage [17]***, (b) DN gel***

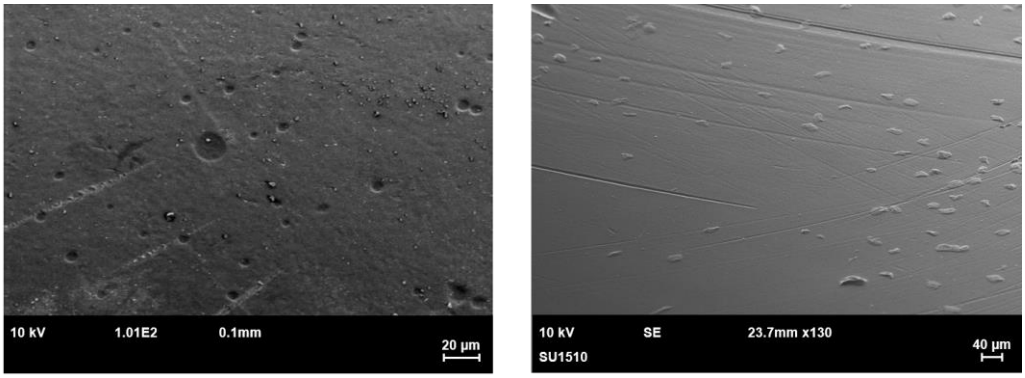

(a) Worn cartilage (b) Worn DN gel

Fig. 6-15 – SEM images of worn (a) cartilage [17]***, (b) DN gel***

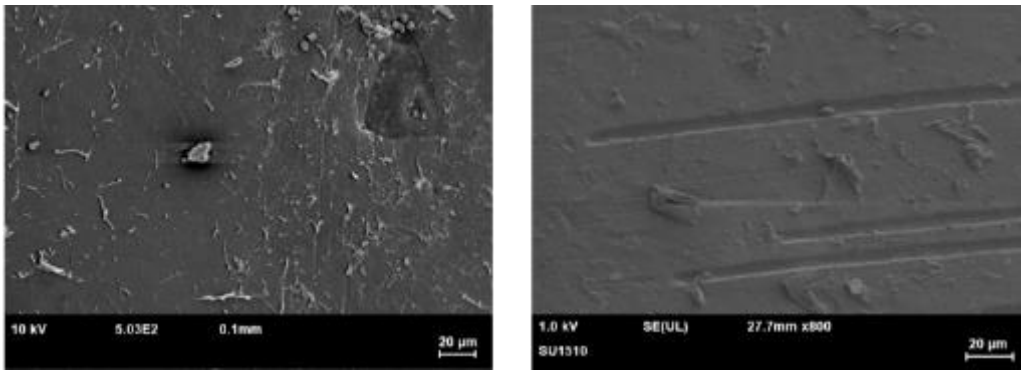

(a) Highly worn cartilage (b) Highly worn DN gel

Fig. 6-16 – SEM images of highly worn (a) cartilage [17]***, (b) DN gel***

By observation of the surface structure of DN gel and comparison with cartilage. There is a strong similarity, the unworn surface is extremely smooth and only presents spotted defects (cf. Fig. 6-14). In our case the scale is slightly different, but the magnitude is close. Then, most surprisingly, the wear on the cartilage is strongly looking like the one on the DN gel. This is then an interesting point. Both images of slightly and highly worn surface presents coherences with the DN gel. About the slightly worn, a linear scare, scratches can be observed. The depth cannot be measured but it is comparable both are similar. Also, a lot of particle aside can be noticed on Fig. 6-15. The DN gel presents the same particularity. Finally, the highly worn surface shows filaments wear particles. The main difference is the scale of these filaments wear particle, larger in the case of DN gel as observed on Fig. 6-16.

Utilization of DN gel

As DN gel have a strong similarity with cartilage, the possibility of using DN gel as a cartilage or for cartilage regeneration support is promising. Then, for a complete study on the capacity of the DN gel, the investigation should also be on its behavior in a biological environment, in other words its comportment with cells. Indeed, its main advantage is its biocompatibility. Then, the way it is integrated by cells should also be checked. As introduced in the first chapter there is a lot of drawbacks about prosthesis material and uses. However, cartilage diseases are generally small or medium. Thus, more and more researchers investigate the possibility of self-regeneration. Unfortunately, cartilage hardly regenerate itself. That is why solutions to help this phenomenon are being developed. DN gel could be one solution. If it is reliable, this natural process: to

induce cartilage spontaneous regrowth; is much safer than removing a whole articulation to replace it by artificial material. Moreover, the post operation is also safer by using biocompatible and non-metallic material.

6.2.2. Introduction about cartilage repair

6.2.2.1. Autologous cartilage implantation

A solution for small to medium cartilage defaults is the autologous implantation. Firstly tested on human in 1994 [19], this method consists in taking few cartilage cells from others articulations origin such as hips to replace a deficiency in the knee for example. Then, these cells are used to profiler and duplicate, thus in a laboratory, *in vitro*, cells are immersed in a culture medium to develop and multiply cells. Finally, these cells are implanted on the defected cartilage directly or on a bio-membrane in order to helps the regeneration of a new cartilage. Unfortunately, the extraction and collection of chondrocyte cells is complex. Even if the results are generally good, in a post operation study, it has been noticed a first layer of fibrocartilage initially filled the hole in the case of direct chondrocytes transplantation. The preferable case should be direct hyaline production [20] on an implanted material. Finally, in this study [21] the addition of chondrocytes on the gel did not change the final cartilage quality, by using chitosan-hyaluronic acid dialdehyde hydrogels either alone or seeded by chondrocytes. Hydrogel cannot be used as sponges but as a support for the cartilage regrowth.

6.2.2.2. Chondrocytes culture

As it is complex to extract chondrocytes cells, actual solution is oriented to human Mesenchymental Stem Cells (hMSC). Actually, it is easy to collect from various part of the body. Then, a popular idea consists in collecting these hMSCs and cultivate onto predefined culture environment and support, the stem cells will differentiate into chondrocytes: main cells consisting of the cartilage. The solution of cartilage creation by cells is seducing, however it still presents drawbacks. In order to create cartilage, chondrocytes need to conserve their phenotypes. The proliferation of chondrocytes on classical Petri plastic surface is active and quick. However, it is highly unstable, then, due to several parameter a dedifferentiation occurs and the chondrocytes change their phenotypes [22],[23]. This is due to:

- A shape changes of the cells from circular to fibroblastic
- A progressive decrease of collagen and aggrecan synthesis.

It has been highlighted that the shape but also the organization of the cells are responsible for this change [24]. Then, more and more culture in a three dimensional arrangement are investigated for the chondrocyte culture success [25]. In other words, for a stability of the cells, to avoid the change of phenotype.

6.2.2.3. Cell culture on hydrogels

A wide range of studies are investigating about hydrogels as a support for culture cells. Indeed, the hydrogel is a highly biocompatible material. The PVA (Polyvinyl alcohol) hydrogel have been especially investigated for this function. Indeed, after a first trial on rabbits knees [26], this method also shows positive results when implanted in human knees. The implant allows a reduction of the severe pain and an improve of knee function [27].

The DN gel is also attractive for this function. Indeed, a first study worked about the biocompatibility of this material [10],[28]. Then, the function as a support for cartilage regeneration was verified by an implantation in rabbits articulation [8],[9]. The most advanced study is performed on sheep knee's articulation [7],[29]. With a positive results further investigation are led to consider the DN gel as a support for chondrocytes growth.

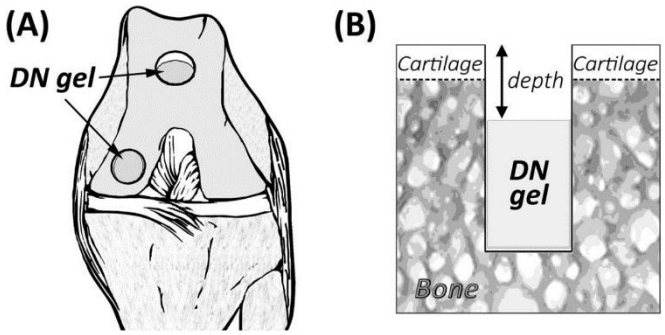

Fig. 6-17 – Surgical implantation of PAMPS/PDMAAm DN gel plug in a cylindrical osteochondral defect [7]

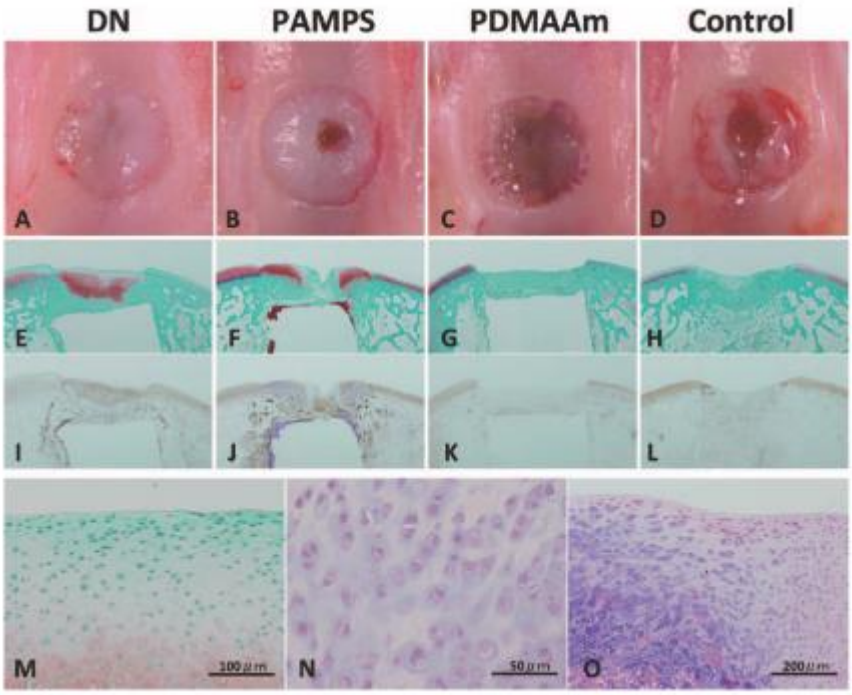

***Fig. 6-18** – Histologic and immunohistochemically observations at 4 weeks of cartilage defect filled by (a)(e)(i)(m)(n) PAMPS/PDMAAm DN gel, (b)(f)(j)(o) PAMPS SN gel, (c) PDMAAm SN gel, (d) untreated control* [30]

Moreover, after approving the DN gel as a good substrate for cartilage regeneration, it has been found that the conditions during cartilage growth are also important. In the case of a PAMPS/PDMAAm DN gel implantation into a cartilage defect, the final cartilage had a better quality if the articulation was not immobilized during healing. Indeed, this study [31] showed a better cartilage quality in the case of a mobile joint. Thus, tribological properties of DN gel also need to be investigated.

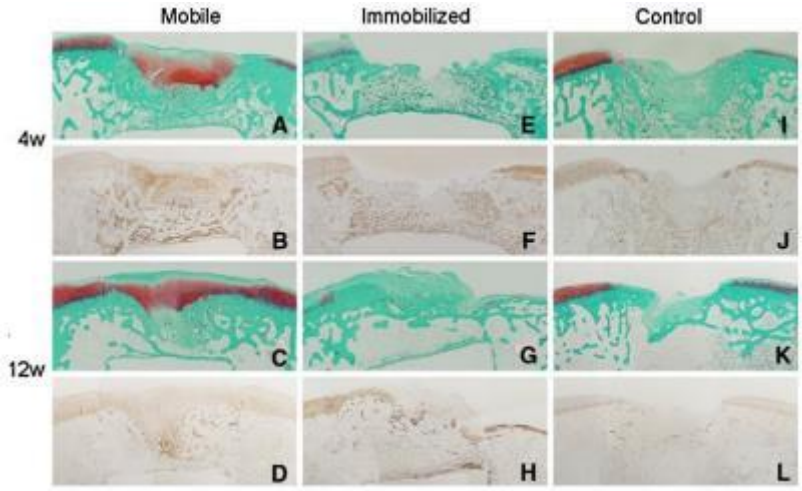

Fig. 6-19 – Comparison of histological observations. Mobile knee filled with enriched tissue substitution after 4 weeks observation (a),(b), and 12 weeks (c),(d) / Immobile knee after 4 weeks, (e)(f), and 12 weeks (g),(h) / Control knee (i-l) [31]

6.2.3. Initial parameters for culture

6.2.3.1. Changed DN gel properties after sterilization

First of all, the DN gel has to be sterilized for a cell seeding. Then it was necessary to investigate the influence of the sterilization process on the DN gel properties. Therefore, indentation test has been performed on the DN gel before and after sterilization; from this test, several parameters have been defined. Then, adhesion force on the surface of the material, contact surface on the material and reduced elastic modulus have been determined.

Fig. 6-20 and Fig. 6-21 summarize results obtained by indentation test on DN gel before and after sterilization. Normal force used was 10 mN in order to avoid the influence of the environment. Sterilization process slightly influences the adhesion force measured on the DN gel surface. After sterilization, the DN gel surface is slightly less adhesive. However, this difference is not significant. Then, the elastic modulus calculated by JKR method for a same load is different. A sterilized DN gel has a significantly reduced elastic modulus from about 0.46 MPa to about 0.14 MPa. This study informed about the influence on mechanical properties after sterilization process. However, parameters of DN gel before and after sterilization does not change as much compared to the support. Indeed, plastic Petri dishes are much stiffer than DN gel, either before or after sterilization. In comparison, depending on the material used, a Petri plastic dish has a Young's modulus around 3 MPa.

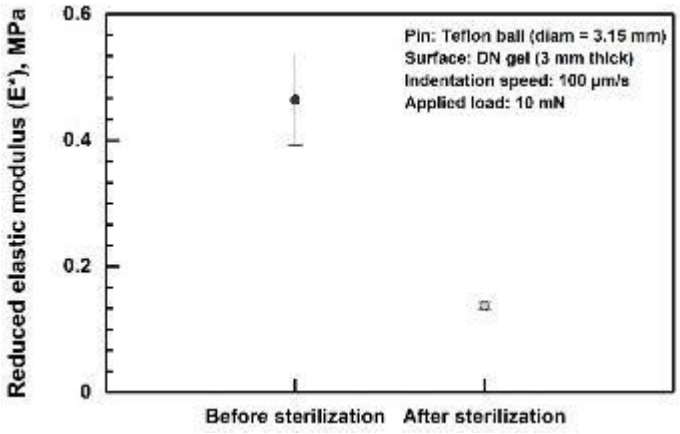

Fig. 6-20 – Error bar of reduced elastic modulus, defined by indentation test of DN gel before and after sterilization

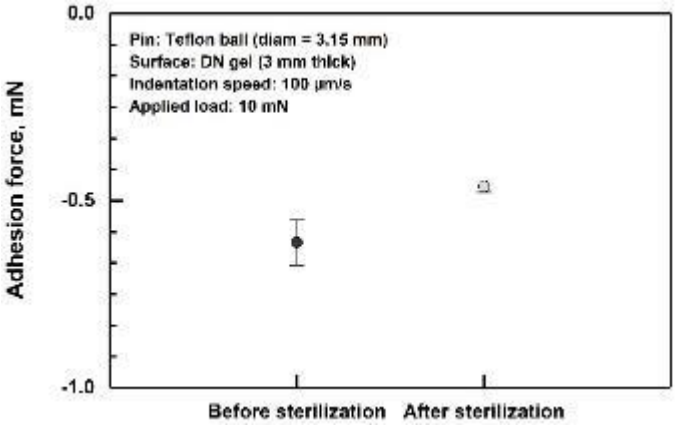

Fig. 6-21 – Error bar of adhesion force, defined by indentation test of DN gel before and after sterilization

6.2.3.2. Culture medium

First of all, right cells need to be selected for the cell growth experimentation. In our case, the promising use of DN gel is for cartilage regeneration [19], [31], [32]. Cells used should be chondrocytes, indeed chondrocytes are capable of synthetize an extracellular matrix essentially composed of type II collagen and cartilage proteoglycan (PG) [33]. As explain before chondrocytes cannot be sampling easily, thus cells used in our case are human Mesenchymental Stem Cells (hMSC). With a chondrogenic differentiation basal, the cells are expected to differentiate into chondrocytes.

However, the swollen medium is extremely important for the cell's survival. Basically, DN gel is swollen by pure water. Indeed, the whole creation of DN gel is based on pure water. Moreover, the pure water avoids any external infection and is the most neutral liquid for the DN gel composition. But the pure water did not allow the cells to adhere to the surface. As experimented in chapter 3, the adhesion on the DN gel is extremely changing depending on the water composition. Proportionally to the water evaporation, the adhesion force on DN gel becomes important. Then, the presence of water clearly reduces the cells adhesion capacity. Also, by changing the chemical swelling the DN gel, it has been possible for cells to not be completely rejected. The culture medium is essential for cells survival.

6.2.4. Culture results

6.2.4.1. Cell culture and observation technics

6.2.4.1.1. Cell Culture

For the culture of cells human bone marrow-derived mesenchymal stem cells (hMSC) were obtained commercially from Lonza (Basel, Switzerland). Before seeding on hydrogels, cells at passage 5 were expanded in a T75-flask for a week in a growth medium (MSCGM, Prod. No. PT-3001, Lonza) at 37°C in a humidified atmosphere containing 5% CO2. Growth medium was changed twice a week. Cells were seeded at 10000 cells/cm² on different types of hydrogels for 24 h for actin cytoskeleton staining.

6.2.4.1.2. Fluorescent Cell Labeling

Seeded cells on hydrogels were fixed in 4% paraformaldehyde for 30 min. Permeabilization was performed with 0.1% Triton X-100 in phosphate-buffered saline (PBS) for 3 min. Samples were incubated with rhodamine-conjugated phalloidin diluted at 1:50 in PBS, at 37 °C for 1.5 h. Afterwards, nuclei labeling was performed with 1 µ/mL DAPI (4′,6-diamidino-2-phenylindole) diluted in PBS at 37 °C for 20 min. Washes were performed using PBS between each step of the experiment. Specimens were observed by confocal microscopy (ZEISS LSM 800 Airyscan, Oberkochen, Germany).

6.2.4.2. Medium swell into the DN gel

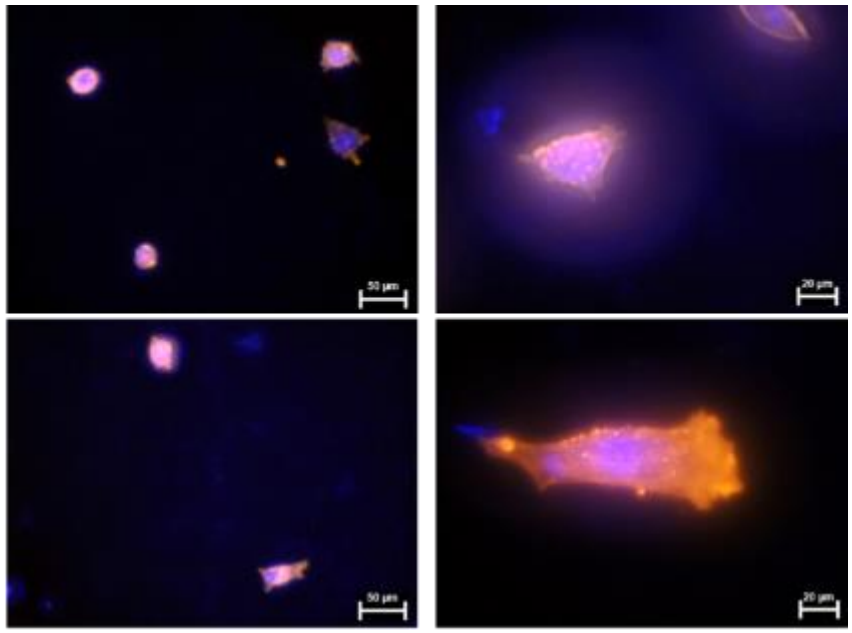

(a) On DN gel (X20) (b) On DN gel (X40)

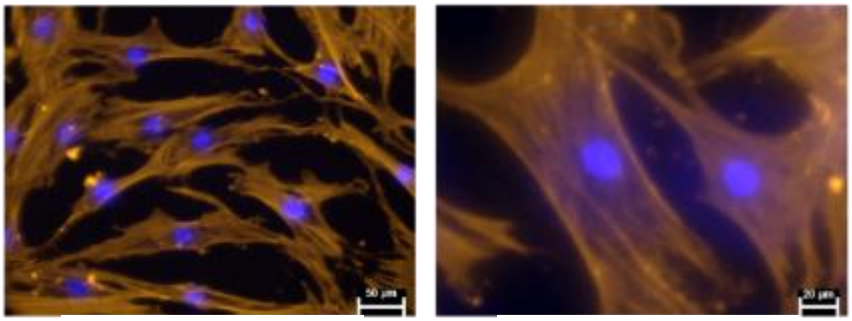

(c) On Petri dish (X20) (d) On Petri dish (X40)

Fig. 6-22 - Cell culture on DN gel and on Petri dish on day 3, (a) on DN gel, X20, (b) on DN gel X40, (c) on Plastic Petri dish X20, (d) on Plastic Petri dish X40

Hydrogel is previously sterilized and immersed into the cell culture medium for 24 hours. This step allows to swell the DN gel with the medium instead of water. It is much more favorable for the cells as explained in the previous part. The seeding process consists of a wide number. By using DN gel swallowed by water, cells did not adhere to the surface. Indeed, the surface of DN gel is highly "slippery" as stated in the following chapters by its super-low friction coefficient capacity. By comparing the seeding on DN gel with a conventional one on plastic box, by analysis the cells morphologies and number, I can see the fibrous expansion in the conventional case but not for DN gel case. In the Fig. 6-22 fluorescence observation of the cells, 3 days after seeding, highlighted in purple, nucleons and in orange, actins. This method is essential to estimate the shape of the cell. Indeed, the main drawback about the chondrocytes cells is its differentiation of the culture does not become three dimensional there is a differentiation problem. On the DN gel surface, there is only a few cells, but their shape is different because the actins seem less spread on the surface. This is a difficult factor for the survival of cells. Only a few remains, but the shape cells obtain after three days are proper shape (cf. Fig. 6-22 (a), (b)). However, on the Petri plastic dish case, cells are still numerous because they adhered well. Basically, their shape can be seen thanks to the fluorescence, actins are largely spread. Cells have a linear fixation. Then probably a dedifferentiation can occurs following this issue (cf. Fig. 6-22 (c), (d)).

Cells are clearly rounder and do not adhere much in the case of DN gel substrate. Thus, there are much less cells because a bad adhesion will be led to the death of the cell. For a same number of seeding the number of living cells on Petri dish is higher. However, the quality is more important than quantity in this case. Furthermore, the adhesion of cell can be improved by several technics as explain here after. The quality of cells seems better on DN gel substrate.

6.2.4.3. Influence of Elastic modulus of the substrate

More and more the culture cells on different substrates are investigated. Indeed, the cytoskeleton development of the cell is essential for its differentiation. Then, it has been found that the elastic modulus of the substrate on which the cells adhere greatly influence its differentiation. Cells cultured are influence by the stiffness of their substrate as demonstrated in this study [34]. This reaction is because of the response of the integrin receptors that activate different action from the cell's cytoskeleton. Then, morphologies of cells are changing with the stiffness environment change. Also, the advantage of flexible surface are the speed of migration of cells and protrusion/retraction activities.

It has been found that the morphology of the cell is rounder with a softer surface. Indeed, by increasing the stiffness of the substrate material the cells will spread their cytoskeleton. However, this observations are dependent on the type of cells used [35].

Then, in order to understand this dependence, three types of DN gel were made. The UV exposure changing the properties of DN gel it was possible to change their elastic modulus. After fabrication process, Elastic modulus property was check out by indentation measurement. Reduced elastic modulus were: 0.02 MPa, 0.06 MPa and 0.9 MPa. Conventional fabrication of DN gel give material with 0.7±0.2 MPa of elasticity.

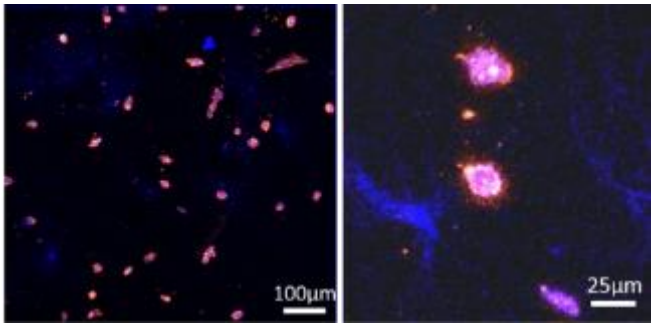

(a) 0.02 MPa

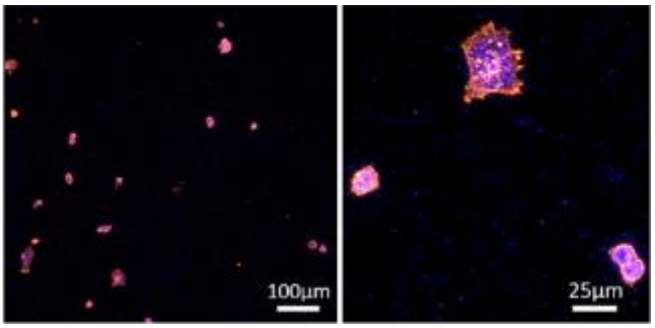

(b) 0.06 MPa

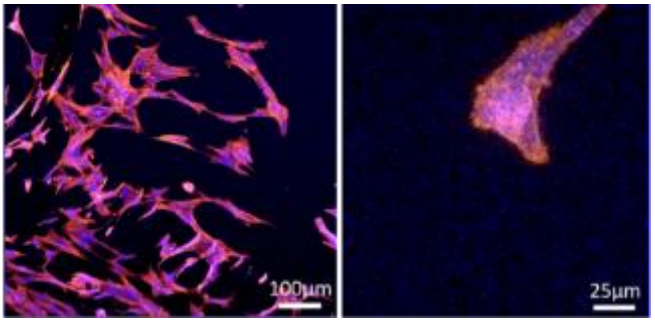

(c) 0.9 MPa

Fig. 6-23 - Cells seeding on DN gel of (a) 0.02 MPa, (b) 0.06 MPa and (c) 0.9 MPa

As exposed on the pictures Fig. 6-23, the elastic modulus of the substrate is essential for the evolution of the cell. Indeed, cells will show a rounder shape onto softer materials. At the opposite, a harder substrate allows the cells to attach and to extend their cytoskeleton. This behavior is beneficial to maintain cells alive. Cells colonized the surface and start to develop. Thus, as understood before, for a cartilage regenerations cells needs to have a round shape. However, when their actin does not attach to the surface by extended their cytoskeleton, cells hardly survive. In that case, the purpose here is to find the right equilibrium among these parameters in order to have the most suitable surface for cartilage regeneration. Then, the elastic modulus of the surface has a great importance.

6.2.4.4. Cell culture on textured DN gel

6.2.4.4.1. Parameters of dot texture

A texture was created by laser process on the DN gel surface. The size of the texture was chosen depending on the size of the cells. One key point to improve the cell adhesion and stability on the substrate is application of a texture. Indeed, more and more studies are getting interested by the texture effect on the culture of cells [11].

In our case a single dot type of texture was made by laser process:

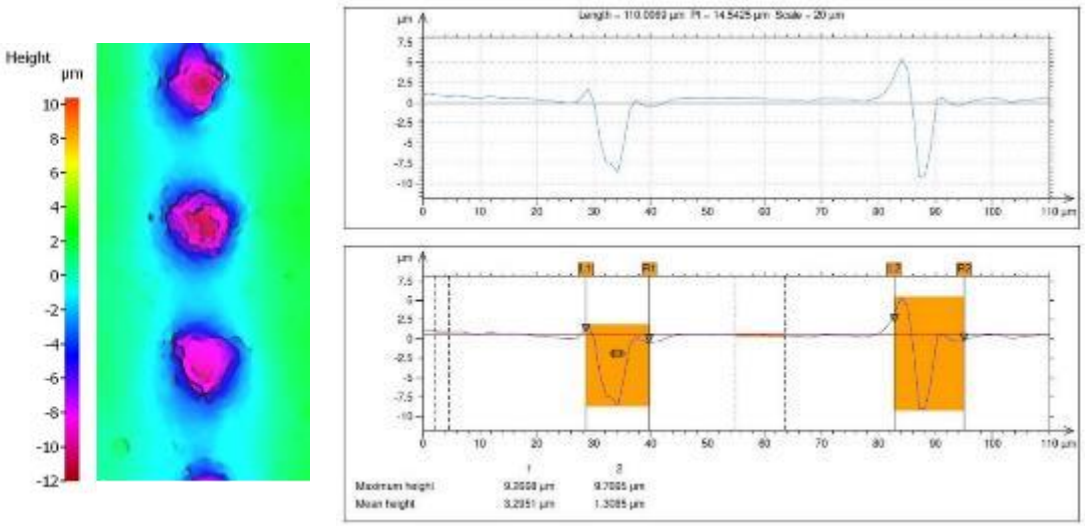

(a) Optical 3D image (b) Measurement analysis

Fig. 6-24 - (a) Dots texture made by laser (b) measurement of dots depth and diameter

By managing the laser impulse, the depth of the texture is finally about 10 µm depth. Holes are 10 µm diameter, texture is spaced 40 µm each other, then the whole surface is textured (cf. Fig. 6-24). The size of the texture was determined from the cell size. In order to create a place to stay and improve their surviving. Indeed, a chondrocyte cell size is about 10 µm [36].

6.2.4.4.2. Results

After, several experimentations, the surface texture of the material seems to have a key role in the cell's adhesion and quality. Indeed, cells mostly stayed in the scratches induce by the tweezers.

From several studies it has been proved the texture has an essential role on the cell's proliferation and differentiation. In this study [11] the texture shape influence have been investigated. Indeed, the characteristic of the texture is influent and change the shape of the cell (more or less circular) and the alignment of the cells. Also, the size of the texture is essential and will have an influence at different scale.

24 hours after, cells are rounder on a DN gel textured than on a plastic Petri dish. Therefore, cells migrate little by little to the holes. Then, the cytoskeleton is not so stretched compared to plastic Petri dish.

Then, by applying a dot texture the capacity of DN gel as a support for cartilage regeneration is greatly improved. The cell quality is better thanks to the DN gel elasticity and avoid the dedifferentiation of the cell. The texture allows cells to take place on the surface and proliferate (cf. Fig. 6-25).

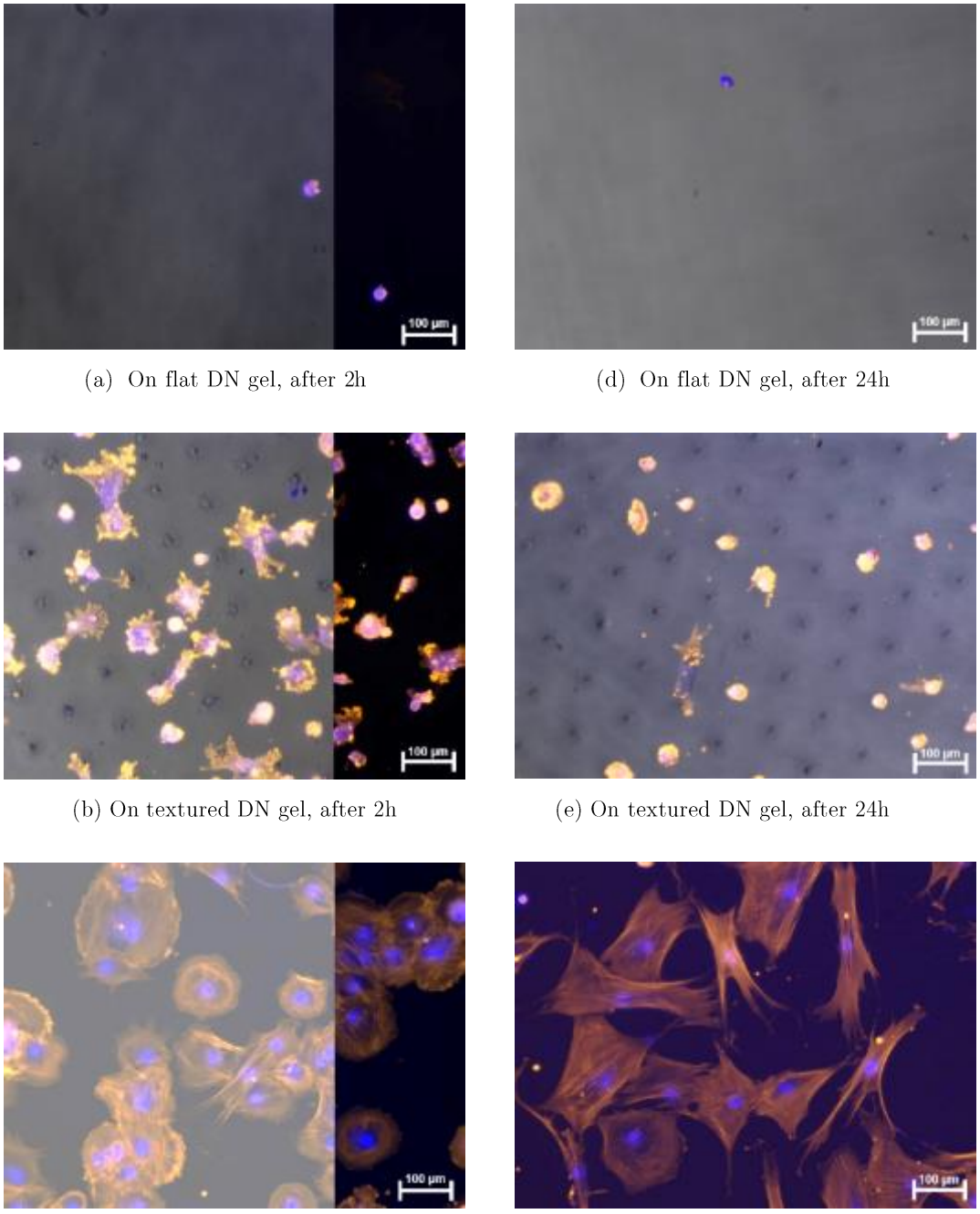

(a) On flat DN gel, after 2h

(d) On flat DN gel, after 24h

(b) On textured DN gel, after 2h

(e) On textured DN gel, after 24h

(c) On Petri dish, after 2h

(f) On Petri dish, after 24h

Fig. 6-25 - Comparison of cells shape 2 hours after seeding (a) on flat DN gel, (b) on textured DN gel, (c) on Plastic Petri dish and 24 hours after seeding (d) on flat DN gel, (e) on textured DN gel, (f) on Plastic Petri dish

6.3. Chapter conclusions

In the first part, the introduction of a texture on the DN gel favorably decreased the friction coefficient and change the trend of the Stribeck curve of the material using the same DN gel film thickness.

Also, the wear of a textured DN gel surface after friction is drastically reduced compared to a not textured material. The homogeneity of the surface can probably be influent in the smooth friction and low wear.

However, one drawback on this texture application, even if the process was the same, the texture cannot be totally controlled in term of size and shape. Instead of a laser texture application, here the abrasive paper texture is less precise and can bring some incertitude to the measurement. Moreover, it can also let some particle of abrasive paper at the interface that can affect the friction coefficient.

In the second part, the DN gel capacity as a biomaterial was investigated. Indeed, by biomimicry approach, the cartilage is clearly the natural tissue the closer to the DN gel material. Then, the purpose is to show up the capacity of DN gel to do the same role as cartilage. By firstly comparing static mechanical properties of the DN gel with the cartilage same properties, by indentation and relaxation tests. DN gel can be considered as the same group as cartilage because of their close visco-elastic properties. Then, by a simple observation of the DN gel with a new technic to avoid water evaporation under SEM, a striking similarity with cartilage has been noticed.

Besides, based on previous studies using DN gel as a support, directly implanted in the default articulation, for self-cartilage regeneration. Cells culture on DN gel have been performed. As it was already known, the capacity of DN gel for support was better than other material. The study here, focused on changed properties to improve the culture cell quality. The elastic modulus of the material was found to influence the cytoskeleton spreading of the cell. Then, a dot texture surface modification drastically improved the quality of the culture compared to classical technics.

By these founding, the DN gel as support for cartilage self-regeneration can be improve by changing their chemical composition to influence the elastic modulus combine with a change of their surface state to improve the survival of cells. More tests, including the change of the texture (bigger texture to sustain group of cells) are being experimented to improve the chondrocyte regeneration.

This DN gel can thus be integrated into the body as a support for regeneration, in this case (before cartilage regrowth) or in other application the DN gel will be

subject to high and repetitive friction. Either, because of its location in joint articulation or in other mechanical application, the DN gel is destined to be use under friction.

6.4. Bibliography

[1] X. Wang, K. Adachi, K. Otsuka, and K. Kato, "Optimization of the surface texture for silicon carbide sliding in water," *Applied Surface Science*, vol. 253, no. 3, pp. 1282–1286, Nov. 2006.

[2] X. Wang, K. Kato, K. Adachi, and K. Aizawa, "The effect of laser texturing of SiC surface on the critical load for the transition of water lubrication mode from hydrodynamic to mixed," *Tribology International*, vol. 34, no. 10, pp. 703–711, Oct. 2001.

[3] X. Wang, K. Kato, K. Adachi, and K. Aizawa, "Loads carrying capacity map for the surface texture design of SiC thrust bearing sliding in water," *Tribology International*, vol. 36, no. 3, pp. 189–197, Mar. 2003.

[4] U. Pettersson and S. Jacobson, "Influence of surface texture on boundary lubricated sliding contacts," *Tribology International*, vol. 36, no. 11, pp. 857–864, Nov. 2003.

[5] J. Bico, U. Thiele, and D. Quéré, "Wetting of textured surfaces," *Colloids and Surfaces A: Physicochemical and Engineering Aspects*, vol. 206, no. 1–3, pp. 41–46, 2002.

[6] X. Liu, H. Nanao, T. Li, and S. Mori, "A study on the friction properties of PAAc hydrogel under low loads in air and water," *Wear*, vol. 257, no. 7–8, pp. 665–670, 2004.

[7] N. Kitamura, M. Yokota, T. Kurokawa, J. P. Gong, and K. Yasuda, "In vivo cartilage regeneration induced by a double-network hydrogel: Evaluation of a novel therapeutic strategy for femoral articular cartilage defects in a sheep model," *Journal of Biomedical Materials Research Part A*, vol. 104, no. 9, pp. 2159–2165, Sep. 2016.

[8] K. Arakaki *et al.*, "Artificial cartilage made from a novel double-network hydrogel: In vivo effects on the normal cartilage and ex vivo evaluation of the friction property," *Journal of Biomedical Materials Research Part A*, no. 3, 2009.

[9] K. Yasuda *et al.*, "A Novel Double-Network Hydrogel Induces Spontaneous Articular Cartilage Regeneration in vivo in a Large Osteochondral Defect," *Macromolecular Bioscience*, vol. 9, no. 4, pp. 307–316, Apr. 2009.

[10] C. Azuma *et al.*, "Biodegradation of high-toughness double network

hydrogels as potential materials for artificial cartilage," *Journal of Biomedical Materials Research Part A*, vol. 81A, no. 2, pp. 373–380, May 2007.

[11] V. Dumas *et al.*, "Multiscale grooved titanium processed with femtosecond laser influences mesenchymal stem cell morphology, adhesion, and matrix organization," *Journal of Biomedical Materials Research Part A*, vol. 100A, no. 11, pp. 3108–3116, Nov. 2012.

[12] F. Platon, P. Fournier, and S. Rouxel, "Tribological behaviour of DLC coatings compared to different materials used in hip joint prostheses," *Wear*, vol. 250, no. 1–12, pp. 227–236, Oct. 2001.

[13] K. Chen, X. Yang, D. Zhang, L. Xu, X. Zhang, and Q. Wang, "Biotribology behavior and fluid load support of PVA/HA composite hydrogel as artificial cartilage," *Wear*, vol. 376–377, pp. 329–336, Apr. 2017.

[14] A. K. Means, C. S. Shrode, L. V. Whitney, D. A. Ehrhardt, and M. A. Grunlan, "Double Network Hydrogels that Mimic the Modulus, Strength, and Lubricity of Cartilage," *Biomacromolecules*, vol. 20, no. 5, pp. 2034–2042, 2019.

[15] J. Desrochers, M. W. Amrein, and J. R. Matyas, "Viscoelasticity of the articular cartilage surface in early osteoarthritis," *Osteoarthritis and Cartilage*, vol. 20, no. 5, pp. 413–421, 2012.

[16] L. Cacopardo, N. Guazzelli, R. Nossa, G. Mattei, and A. Ahluwalia, "Engineering hydrogel viscoelasticity," *Journal of the Mechanical Behavior of Biomedical Materials*, vol. 89, no. September 2018, pp. 162–167, 2019.

[17] S. L. Graindorge and G. W. Stachowiak, "Changes occurring in the surface morphology of articular cartilage during wear," *Wear*, vol. 241, no. 2, pp. 143–150, 2000.

[18] Y. Takaku *et al.*, "A thin polymer membrane, nano-suit, enhancing survival across the continuum between air and high vacuum," *Proceedings of the National Academy of Sciences*, vol. 110, no. 19, pp. 7631–7635, 2013.

[19] M. Brittberg, A. Lindahl, A. Nilsson, C. Ohlsson, O. Isaksson, and L. Peterson, "Treatment of Deep Cartilage Defects in the Knee with Autologous Chondrocyte Transplantation," *New England Journal of Medicine*, vol. 331, no. 14, pp. 889–895, Oct. 1994.

[20] G. D. Smith *et al.*, "Autologous Chondrocyte Implantation and

Osteochondral Cylinder Transplantation in Cartilage Repair of the Knee Joint," *The Journal of Bone and Joint Surgery-American Volume*, vol. 85, no. 12, pp. 2487–2488, Dec. 2003.

[21] N. Mohan, P. V. Mohanan, A. Sabareeswaran, and P. Nair, "Chitosan-hyaluronic acid hydrogel for cartilage repair," *International Journal of Biological Macromolecules*, vol. 104, pp. 1936–1945, 2017.

[22] A. P. Newman, "Articular Cartilage Repair," *The American Journal of Sports Medicine*, vol. 26, no. 2, pp. 309–324, Mar. 1998.

[23] J. A. . Buckwalter and H. J. Mankin, "Articular Cartilage. Part II: Degeneration and Osteoarthrosis, Repair, Regeneration, and Transplantation," vol. 79, no. 4, London: Springer London, 1997, p. 612.

[24] F. Mallein-Gerin and M. van der Rest, "La culture de chondrocytes : outil d'analyse de la différenciation et de l'organisation moléculaire du cartilage," *Médecine/Sciences*, vol. 12, no. 10, p. 1087, 1996.

[25] P. Schwinté, L. Keller, S. Eap, D. Mainard, and N. Benkirane-Jessel, "Osteoarticular Regenerative Nanomedicine : Advances and Drawbacks in Articular Cartilage Regeneration Implants," *Austin Journal of Nanomedicine & Nanotechnology*, vol. 2, no. 4, p. 1025, 2014.

[26] T. Noguchi *et al.*, "Poly(vinyl alcohol) hydrogel as an artificial articular cartilage: Evaluation of biocompatibility," *Journal of Applied Biomaterials*, vol. 2, no. 2, pp. 101–107, 1991.

[27] F. V. Sciarretta, "5 to 8 years follow-up of knee chondral defects treated by PVA-H hydrogel implants," *European Review for Medical and Pharmacological Sciences*, vol. 17, no. 22, pp. 3031–3038, 2013.

[28] K. Yasuda *et al.*, "Biomechanical properties of high-toughness double network hydrogels," *Biomaterials*, vol. 26, no. 21, pp. 4468–4475, Jul. 2005.

[29] T. Fukui *et al.*, "Intra-articular administration of hyaluronic acid increases the volume of the hyaline cartilage regenerated in a large osteochondral defect by implantation of a double-network gel," *Journal of Materials Science: Materials in Medicine*, vol. 25, no. 4, pp. 1173–1182, 2014.

[30] M. Ogawa *et al.*, "Poly(2-acrylamido-2-methylpropanesulfonic acid) gel induces articular cartilage regeneration in vivo: Comparisons of the induction ability between single- and double-network gels," *Journal of Biomedical Materials Research - Part A*, vol. 100 A, no. 9, pp. 2244–2251,

2012.

[31] K. Arakaki *et al.*, "Joint immobilization inhibits spontaneous hyaline cartilage regeneration induced by a novel double-network gel implantation," *Journal of Materials Science: Materials in Medicine*, vol. 22, no. 2, pp. 417–425, Feb. 2011.

[32] N. Kitamura *et al.*, "Induction of Spontaneous Hyaline Cartilage Regeneration Using a Double-Network Gel," *The American Journal of Sports Medicine*, vol. 39, no. 6, pp. 1160–1169, Jun. 2011.

[33] E. J. Miller, "Biochemical characteristics and biological significance of the genetically-distinct collagens," *Molecular and Cellular Biochemistry*, vol. 13, no. 3, pp. 165–192, 1976.

[34] R. J. Pelham and Y. -l. Wang, "Cell locomotion and focal adhesions are regulated by substrate flexibility," *Proceedings of the National Academy of Sciences*, vol. 94, no. 25, pp. 13661–13665, Dec. 1997.

[35] T. Yeung *et al.*, "Effects of substrate stiffness on cell morphology, cytoskeletal structure, and adhesion," *Cell Motility and the Cytoskeleton*, vol. 60, no. 1, pp. 24–34, 2005.

[36] P. G. Bush and A. C. Hall, "The volume and morphology of chondrocytes within non-degenerate and degenerate human articular cartilage," *Osteoarthritis and Cartilage*, vol. 11, no. 4, pp. 242–251, 2003.

Chapter 7 – General conclusions

In this study, the DN gel PAMPS/PDMAAm have been widely investigated. There were three main goals:

- **To clarify the potential of DN gel as a tribological material**

From the chapter 2, the DN gel friction potential has been widely studied, it is now possible to dress the Hersey number condition to results in a friction region I, a transition or friction region II. These regions are true regardless of the DN gel film thickness.

By using, for the first time, a unique configuration of DN gel as a covering film in a SiC ball – SiC disc couple of friction, typical friction coefficient tendencies with run-in periods were highlighted in friction region II. In the chapter 3, by using different DN gel film thickness, a super low friction can be reach by two different run-in process: friction mode 2, with a sudden decrease and friction mode 3 with a longer first decrease and a second decrease at the end.

From the wear analysis of the chapter 4, the DN gel after friction, wear tracks were depending on the friction mode applied. Indeed, a friction mode 2 results in a few wear and dispersed scratches whereas a friction mode 3 results in a micrometer linear wear scare.

- **To clarify the double run-in process to reach a super low friction coefficient using a DN gel film**.

Based on the results of chapter 2 and 3, analyzing the friction coefficient of the DN gel combined with the results of chapter 4 which determined the resulted wear. The chapter 5 stated mechanisms occurring on the DN gel interface depending on the friction mode.

Indeed, from the tendency of the friction mode 2 with a sudden decrease, a short run-in, and a few wear scratches observe on the surface after friction, the formation of a thick water film at the interface is probable. This behavior is likely corresponding to a hydrodynamic lubrication. This friction mode 2 mainly happens using a 6 mm thick DN gel. The contact stiffness of the system is softer than by using thinner DN gel. The viscoelasticity of a thick DN gel is favorable for the creation of thick water film interface.

Next is the friction mode 3 with the double run-in behavior. First run-in is longer than for the friction mode 2, also a second decrease is observed after a long distance friction. Here, based on the wear observed after friction and the images during the *in-situ* friction test it is assumed that the damage layer created during the first run-in period becomes profitable and led to a second decrease. In fact, the sparse layer created by the friction allows the DN gel to consist of more water at its top layer due to a density change caused by structure change. Thus, a thin film of water is form and led to a super low friction coefficient by a hydrodynamic lubrication. The thinner DN gel of 1.5 mm thick mostly presents this friction mode, based on the system contact stiffness, it surely is stiff enough to create the ideal damage layer on the surface of DN gel.

By understanding this phenomenon, a pre-textured DN gel can be imagine. This is presented in the first part of the chapter 6. Indeed, the DN gel was voluntarily damaged to mimic the first run-in occurring during friction mode 3. A thin grain emery paper was used to obtain a micrometer scale texture. Finally, it was possible to reduce the friction by using the pre-textured DN gel. The run-in period has been shortened and the final friction coefficient has been reduced.

- **To understand its interaction with chondrocytes and improve it**

From the literature background the DN gel is extremely promising for direct cartilage implantation. However, the chondrocytes development is strictly linked with the mechanical and surface properties of the support material. Thus, by managing these properties it was possible to manage the cells quality.

Indeed, a higher elastic modulus of DN gel induces a better adhesion of the cells but with a stretching cytoskeleton. Also, a textured DN gel allows the chondrocytes to keep growing on the surface while keeping their phenotype. Finally, as the DN gel already proved its capacity for support cartilage self-regeneration in small defects, this study brings keys to improve this ability by mechanics and surface properties control.

By the PhD. Work, the range of use of this DN gel was established. A better understanding of its behavior with cells and during friction was bring. And the importance of run-in during friction have been clarified.

In the chapter 1, the main purpose was to establish a complete background about Double Network hydrogels. First by exploring the simple hydrogel composition and friction capacities it led to introduction of DN gel. This stiffer and more resistant material does not have its tribological properties well explored and this is what I aim to do. Inspiring for other soft materials rubbing on hard surfaces, a friction and wear background could be drawn and the influent parameters on it are defined. Finally, a wide background about cartilage was establish, first to have a biomimicry approach, by observing the structure of the material it may be possible to reach same favorable tribological properties. Second, in order to understand that innovative solution is needed for cartilage issue. Also, this introduction exposed how largely the DN gel is used for artificial cartilage and how this work can contribute to improve the direct implantation as a support for cartilage self-regeneration.

In the chapter 2, the purpose was to deeply understand the friction occurring using a DN gel material. First, the basic properties of DN gel material were measured, from that the water content of DN gel is understood to be crucial on its properties. Then, the ideal combination of material for friction was determined. And a run-in period has been understood to be a key point about the DN gel friction property. The stress deformation of DN gel is a favorable parameter and enable to reach lower friction coefficient than SiC friction pair for similar applied loads. Finally, in this chapter, the friction regions of the DN gel were determined based on the applied pressure and sliding speeds condition:

Friction region I:	$H_s < 5 \cdot 10^{-11}$,
Transition:	$5 \cdot 10^{-11} < H_s < 1.5 \cdot 10^{-10}$,
Friction region II:	$1.5 \cdot 10^{-10} < H_s$.

In the chapter 3, from the same configuration, by using DN gel as a film on the SiC ball, the influence of the DN gel film thickness on the friction properties was highlighted. Three DN gel film thickness is investigated. Their friction coefficient is measured and compared. Finally, three mode of friction are defined:

Among the friction region I, independently of the thickness used a stable friction coefficient was measured: friction mode 1

In the transition, mainly friction mode 2 are founded, that is traduced by a sudden decrease of the friction coefficient and a single run-in period.

In the friction region II, the friction mode 3 is found, especially by using thin DN gel, this mode is a double decrease of friction coefficient leading to an extremely low final value. The first run-in process is longer than friction mode 2.

Finally, our interest focuses on the friction region II, where the DN gel can reach extremely low friction coefficient. In this region, the 1.5 mm thick DN mainly presents friction mode 3 while 6 mm thick DN gel mainly presents friction mode 2. Also, the contact stiffness of the system used the SiC ball and the three different thickness DN gel film, clearly show a negative dependence of the stiffness to the DN gel thickness. The contact pressure and the viscosity loss of the DN gel is dependent of the DN gel thickness, this dependence has an impact on the friction coefficient.

In the chapter 4, the DN gel adhesion on SiC disc was checked. After applying the different conditions to obtain the three friction modes, the adhesion of DN gel particle seems linked to the friction mode. Friction mode 1 high particles of DN gel are stick to the surface, friction mode 2 almost no DN gel particles and friction mode 3 highlighted fusion particles to the SiC surface. Then, several methods of observation were used on the DN gel material. Due to its transparency and water content it was complex to find the ideal technic. However, by the T-butanol substitution technic it was possible to observe the wear after friction on the DN gel without covering the roughness and without letting the water evaporate. By applying different friction conditions, it was possible to obtain friction mode 1, 2 and 3. The wear on DN gel was observed after these frictions and a dependence to the friction mode was found. Indeed, a friction mode 1 will presents severe scale like scar in the direction of friction. After friction mode 2, almost no wear is visible, scratches are widely spread. Finally, the friction mode 3 results in a light wear about micrometer linear scare in the friction direction.

In the chapter 5, the mechanisms of friction were analyzed by the understanding of the sacrificial bond process due to tensile stress, the creation of damage layer was understood. Indeed, from literature the DN gel is known to create a sparse layer due to tensile stress a polymer network breaks its link and

in the other one the second polymer network broke its sacrificial bond without totally separate. Thus, a high water content DN gel is introduce on the top surface. This hypothesis is validated by the *in-situ* observation technic using color water and DN gel to understand the interface. During friction mode 1, the DN gel is in a close contact with the disc. For the friction mode 2 a thick water film is discerned. However, the friction mode 3 shows a complex process, by a first adhesion of the material to the surface, creating the sparse layer, then enabling the attraction of water and leading to the creation of a thin water film at the interface.

Finally, the chapter 6 was split in two parts:

The first one is deducted from these previous observations and a pre-textured DN gel was tested. Indeed, by applying an initial texture on the DN gel surface using a thin (2000) emery paper a micrometer scale damage layer was created on the DN gel surface. Then, by comparison with a same DN gel without the texture introduction a favorable change of the friction mode is noticed for same experimental conditions. Also, the run-in period was shrunk with the introduction of texture friction mode 3 occurs. Finally, the pre-texture could replace the first run-in period during the friction mode 3 of the pristine DN gel.

The second part focused on the capacity of DN gel for chondrocytes growth support. The influence of the DN gel stiffness was understood by using three different elastic moduli of hydrogel. The cells clearly spread out their cytoskeleton in case of stiffer material. Then, the surface properties were changed to avoid the dedifferentiation of the chondrocytes. By doing so cells could grow in a dot texture without losing their phenotypes.

Acknowledgements

This Double Degree program was cooperatively led between and the Laboratory of Tribology and Systems Dynamics (LTDS) at Ecole Centrale de Lyon and the Adachi and Kanda Laboratory, in the Department of Mechanical Systems Engineering at Tohoku University. I want to express my gratitude to the person I met during this incredible opportunity.

First, I would deeply thank all my supervisors. For supervising my work in LTDS in Ecole Centrale de Lyon, and for giving me the opportunity to be enrolled in this wonderful project, I want to thank Prof. Hassan Zahouani for his support and for the opportunity he gave me to be enrolled in the DD program. Then, I also thank Prof. Phillipe Kapsa for its co-supervision and for its time with collaborative laboratory discussion.

I express a high gratitude for professors in Tohoku University for their welcoming in their laboratory and team. First my thanks go to my supervisor in Japan, Prof. Koshi Adachi for his hospitality and its generous support during my stay, also and mainly for deep discussions about my PhD work. Also, I want to particularly thank Prof. Koki Kanda, because he helps me all along my stay in Japan for many administrative duties, especially for the scholarship requirement. He taught me how to make the DN gel and worked with me on the better understanding of this material.

I also want to express my gratitude to every students I meet in Japan and France. First, Dr. Coralie Thieulin and Dr. Abdenaceur Abdouni for giving me the motivation to be enrolled in a Ph.D. Mr. Amaury Guillermin, Ms. Meriem Ayadh and Ms. Vilayvone Saisnith, for sharing the office, lunch and fun times with me before my departure to Japan. I also especially thank each student of the Adachi and Kanda Laboratory for their warm welcoming and the excellent time spent together. They also helped me to deeply discover Japan and Japanese culture. I send special thanks to Ms. Runa Suzuki for her helps in many administrative tasks and for being my friend, and Mr. Kento Ihara for his huge kindness and its interest in French culture. Finally, I have a deep thought to Dr. Yuta Muramoto, my co double degree student and my friend along my whole doctoral life in France and in Japan, for the fun and emotional time spent in our respective country, it was a pleasure to share this wonderful experience.

I realize and I am grateful for the immense opportunity that has been given to me to work in a collaboration between France and Japan. It brings a different

point of view and openness. Traveling for a year, allowed me to discover a whole new culture which I really enjoyed learning. I lived incredible experiences. Coming back to France I think a lot about cultural way from Japan and I try to use it here.

Finally, I want to thank my family very much, in particular my husband who followed me to the other side of the planet in this wonderful experience which was to live in Japan. He always believed in me and gave me a lot of confidence in my work.

This study was financially supported by Manutech SISE in France, the IDEX Lyon and Otsuka Toshimi Foundation in Japan, I want to particularly thank these financial supports which was greatly helpful for my life in Japan.